universität wien

MASTERARBEIT / MASTER'S THESIS

Titel der Masterarbeit / Title of the Master's Thesis

„Microbial Endocrinology:
Impact of BPA and Estrogen on Bacteria-to-Bacteria Communication."

verfasst von / submitted by

Mary Hildeghard Ward

angestrebter akademischer Grad / in partial fulfilment of the requirements for the degree of

Master of Science (MSc)

Wien, 2021/Vienna, 2021

Studienkennzahl lt. Studienblatt / degree programme code as it appears on the student record sheet:	UA 066 830
Studienrichtung lt. Studienblatt / degree programme as it appears on the student record sheet:	Masterstudium Molekulare Mikrobiologie, Mikrobielle Ökologie und Immunbiologie
Betreut von / Supervisor:	Univ. - Prof. Dr. David Berry PhD

CONTENTS

LIST OF TABLES AND FIGURES:

1. ABSTRACT

Reproduktionsrate und Sterberate sind wichtige Faktoren für den Erfolg von Arten in einer Gemeinschaft. Sowohl die Reproduktions- als auch die Sterberate können durch Drift oder Selektionsdruck aus der Umwelt verursacht werden. Frühere In-vivo- und In-vitro-Studien haben gezeigt, dass die Exposition gegenüber Bisphenol A (BPA) die Diversität der Mikrobiom-Gemeinschaft und den funktionalen Phänotyp des Wirts beeinflusst. Diese Studien modellierten die Dynamik der Mikrobiota in einem Bioreaktor oder in tierischen Wirten für 10 oder mehr Tage und die meisten bemerkten eine Abnahme im Phylum Firmicutes. Ein kürzlich durchgeführtes In-vivo-Experiment zeigte, dass das durch Autoinducer-2 (AI-2) vermittelte Quorum Sensing die Firmicutes nach Streptomycin-Belastung spezifisch anreichert. AI-2-Signalisierung ist ein wichtiger Regulator des Bakterienwachstums und ist in Firmicutes im Vergleich zu Bacteroidetes, den beiden primären Phyla des Darms, signifikant häufiger anzutreffen. Es wurde gezeigt, dass 17β-Estradiol, E2, das AHL-vermittelte Quorum Sensing hemmt (Beury-Cirou A 2013).

In dieser Arbeit wurde der Einfluss von BPA und E2 auf die AI-2-Erkennung und die bakterielle Physiologie untersucht. Es wurden unterschiedliche Auswirkungen von E2 und BPA auf das Wachstum verschiedener *E. coli*-Stämme, *V. harveyi* und *Enterococcus faecalis* zwischen den getesteten Spezies und Stämmen beobachtet. Auffälligerweise wurde eine 6-fache Steigerung des Wachstums von *V. harveyi* beobachtet, wenn es mit 100nM E2 im Vergleich zu keiner Behandlung inkubiert wurde, und es wurde ein linearer Trend relativ zur E2-Konzentration beobachtet. Signifikantes Quenching wurde sowohl für BPA als auch für E2 bei physiologisch relevanten Konzentrationen mit einem *V. harveyi* Biosensor beobachtet. Die Dosis-Wirkungs-Aktivität der Biolumineszenz-Ausgabe von *V. harveyi* als Reaktion auf synthetisches AI-2, E. coli-Stämme, 13 Darmstämme und Fäkalien von gesunden männlichen und weiblichen Menschen wurde ebenfalls bewertet. Von den 13 analysierten Darmisolaten enthielten die meisten putatives genomisches *luxS*, das konditionierte Medien produzierte, die Biolumineszenz in *V. harveyi* induzierten. Wichtig ist, dass fäkale Gülle von männlichen, aber nicht von weiblichen gesunden Freiwilligen Biolumineszenz in *V. harveyi* induzierte. Die Dynamik der fäkalen Mikrobiota und die AI-2-Produktion in einer Batch-Fermentation wurden ebenfalls untersucht. Im Gegensatz zu früheren Studien behielten BPA-exponierte Fermente eine höhere Diversität der Observed-, Shannon- und Chao1-Metriken als die Kontrolle bei; die Unterschiede in der Gemeinschaftsstruktur zwischen der 25uM-BPA-Behandlung und der Kontrolle waren jedoch nicht signifikant. In Übereinstimmung mit Tierstudien wurde eine höhere Abundanz von Bacteroides sp. im BPA-exponierten Ferment im Vergleich zum Kontrollferment beobachtet, mit einer signifikanten Anreicherung von Bacteroides uniformis und Allistipes.

Bisher beschränkten sich die Studien darauf, wie E2 und BPA die Gesundheit über körpereigene Mechanismen beeinflussen. Diese Beobachtungen unterstützen einen neuartigen Mechanismus, bei dem die BPA-Exposition den Phänotyp der Darmmikrobiota, möglicherweise die Zusammensetzung der Gemeinschaft, beeinflussen und durch die AI-2-Störung zu einem Holobionten-Phänotyp führen könnte. In der Tat könnte es eine angeborene Rolle für E2 bei der Regulierung des Mikrobiota-Phänotyps und möglicherweise der Zusammensetzung der Gemeinschaft geben. Zukünftige Untersuchungen zur Erforschung der Darmmikrobiota als Vermittler endokriner Störungen könnten zu neuartigen Behandlungen für derzeit schwer behandelbare Syndrome führen, die mit Mikrobiota- und Hormondysregulationen verbunden sind.

1. ABSTRACT

Reproduction rate and death are important factors in species success in a community. Both reproduction and death rate can be caused by drift or selective pressures from the environment. Previous *in vivo* and *in vitro* studies have shown that Bisphenol A (BPA) exposure impacts microbiome community diversity and functional phenotype of the host. These studies modeled microbiota dynamics in a bioreactor or in animal hosts for 10 or more days and most remarked on a decrease in the Phylum Firmicutes. A recent *in vivo* experiment demonstrated that quorum sensing mediated by Autoinducer-2 (AI-2) specifically enriched Firmicutes after streptomycin challenge. AI-2 signaling is an important regulator of bacterial growth and is significantly more prevalent in Firmicutes compared to Bacteroidetes, the two primary phyla of the gut. 17β-estradiol, E2, has been shown to inhibit AHL-mediated quorum sensing (Beury-Cirou A 2013).

In this work, the impact of BPA and E2 on AI-2 detection and bacterial physiology was explored. Differential effects of E2 and BPA on growth of various *E. coli* strains, *V. harveyi* and *Enterococcus faecalis* were observed between species and strains tested. Strikingly, a 6 fold increase in growth of *V. harveyi* was observed when incubated with 100nM E2 compared to no treatment and a linear trend was observed relative to E2 concentration. Significant quenching was observed for both BPA and E2 at physiologically relevant concentrations using a *V. harveyi* biosensor. The dose-response activity of *V. harveyi* bioluminescence output in response to synthetic AI-2, *E. coli* strains, 13 gut strains and feces from healthy male and female humans was also evaluated. Of the 13 gut isolates analyzed, most contained putative genomic *luxS* produced conditioned media that induced bioluminescence in *V. harveyi*. Importantly, fecal slurry from male but not the female healthy volunteer induced bioluminescence in *V. harveyi*. Fecal microbiota dynamics and AI-2 production in a batch fermentation were also explored. In contrast to previous studies, BPA exposed ferments maintained higher diversity of Observed, Shannon, and Chao1 metrics than the Control; however, differences in community structure between 25uM BPA treatment and Control were not significant. In agreement with animal studies, higher abundance of *Bacteroides* sp was observed in BPA exposure compared to the Control ferment, with significant enrichment of *Bacteroides uniformis* and *Allistipes.*

Until now, studies have been limited to how E2 and BPA impact health via mechanisms of the body. These observations support a novel mechanism in which BPA exposure could influence gut microbiota phenotype, possible community composition, and result in a holobiont phenotype through AI-2 disruption. Indeed there could be an innate role for E2 in regulation of microbiota phenotypes and possibly community composition. Future investigations to explore the gut microbiota as a mediator of endocrine disruption could lead to novel treatments to currently intractable syndromes associated with microbiota and hormone dysregulation.

2. INTRODUCTION

2.1 The microbiome and dysbiosis.

The gut microbiome is composed of the sum of all extrachromosomal material found in the gut. The largest portion is derived from bacteria. Over 90% of whom belong to two phyla, namely Bacteroidetes and Firmicutes (Arumugam M et. al 2011). Gut microbiota contributes both to the wellbeing and to the disease status of the host (Laukens D 2016, Markle et. al. 2013). The first colonizers of the human gut are “inherited” matrilineally in the case of vaginal birth; however, analysis of the meconium and fecal samples of infants demonstrate that the first communities fluctuate significantly and differ from the community which is persistent after two years of life (Evans JM 2013). Despite the randomness of colonization during the first two years of life, gut microbiomes of adults largely converge to have a similar phyllic distribution of bacteria (Rinninella E 2019). Deterministic factors such as nutrients, environmental filters (including the immune system), and competition drive the emergence of similar microbiome compositions between individuals (Savage DC 1972). While community convergence among adults is observed at high taxonomic resolution, variation between individuals and persistence of different enterotypes suggests a role host specific factors which are intrinsic in stability of an individual’s microbiome (Arumugam M et. al 2011). Variation in diet (Arumugam M et. al 2011), host genetics (Org E 2016, Kovacs A et al. 2011), health status (Vayssier-Taussat et al. 2014), age (Mueller S 2006, de la Cuesta-Zuluaga J et. al. 2019, Yatsunenko T 2012) and sex (Shin JH 2019, Flores R et al. 2012, Fuhrman BJ 2014) have been shown to contribute to interindividual differences in the gut microbiome. Due to these factors and daily variations in community composition in an individual overtime, a defined normal microbiome composition has yet to be established (Human Microbiome Project Consortium 2012).

Despite this observation, many studies suggest a key functional role in human health fully covered in cited reviews, including specific microbial metabolites such as Short Chain Fatty Acids (SCFA)(Ríos-Covián D et. al 2016) and vitamins (LeBlanc JG et. al 2013), modulation of the host immune system (Belkaid Y 2014) and hormone homeostasis (Baker JM 2017). Hence, characterization of microbiota composition has come under intense focus. Dysregulation of the gut microbiome, referred to as dysbiosis, is the state in which the community of microbes changes to a composition that is no longer in homeostasis with the host (Petersen C 2014). In dysbiosis, a change in community membership has been correlated to immune (Belkaid Y 2014), metabolic (Li X et. al. 2017) and hormone dysregulation (Kwa M et. al 2016). Several heuristics based on composition have emerged from the literature to characterize this state and include: reduced alpha diversity, an increase in the proportion of Proteobacteria, and a change in the ratio of the predominant phyla where the ratio of Firmicutes to Bacteroidetes is reduced (Carding S 2015, Shin NR 2015). Given interindividual differences and the redundancy of

functional potential of the microbiome, a better working definition based on microbiota activity rather than community composition may prove more useful to characterize a dysbiotic state (Carding S 2015, Brüssow H 2020). Building on Koch's postulates, several studies have demonstrated that transfer of microbiota from one animal may confer the same phenotype to the naive recipient: in metabolic syndrome (Vrieze A et. al. 2012, Ridaura VK et. al 2013, Liou A.P 2013, Koren O 2012), hormone dysregulation (Markle J et. al 2013, Eriksson H 1969, Shimizu K 1998), inflammation (Kaliannan K 2018), Polycystic ovary syndrome (Guo Y et. al. 2016) and hypertension (Li J et. al. 2017). Recent studies have emerged that link exposure to synthetic chemicals, xenobiotics, including pharmaceuticals, pesticides, sweeteners and industrial chemicals to a change in the composition of the microbiome to one of a diseased phenotype. Recently, Bisphenol A (BPA) has been linked to microbiome dysregulation. Strikingly, diseases linked to exposure to BPA are the same those correlated with microbiome dysregulation, see previous citations. Indeed, currently intractable syndromes such as metabolic disorders, autoinflammatory diseases, and diseases related to estrogen dysregulation have been studied in rats and broad correlation studies of BPA exposure. Unfortunately, although correlations studies have demonstrated a link between exposure of BPA in a human population with disease, animal studies and *in vitro* studies of host tissues have failed to reproduce a mechanism to link exposure to disease. These recent studies suggest a novel mechanism in which BPA causes disease via microbiota modulation and reasons for which disease outcome based on exposure is variable between individuals.

2.2 Endocrine Disruptor Bisphenol A

2.2.1 BPA chemistry, uses, and exposure.

BPA, 2,2-bis(4-hydroxyphenyl) propane, is one of the most synthesized chemicals in the world and is widely used in the manufacturing of polycarbonate resins. These resins are used predominantly in food and beverage storage applications and measurable BPA contamination can be found in soil, air and tributaries that collect run-off. Although BPA is ubiquitously abundant in the environment, primary human exposure is thought to be through a diet that includes tinned food with an inner can-coating, fish (where fish at higher trophic levels containing a higher concentration of BPA), and beverages stored in plastic bottles (vom Saal FS 2014, Vandenberg L 2009). This compound consists of two phenolic rings linked by a methyl bridge which, in turn, is attached to two functional methyl groups, see Figure 3. Its activity is due to the presence of hydroxyl groups; however due to the phenol groups, BPA is highly stable, persists in the environment, can bioaccumulate and is rapidly absorbed in´to the body upon regular exposure (Genuis S 2012). BPA is chemically similar to DES, diethylstilbestrol, a synthetic estrogen, which also contains two phenol rings and where the the central methyl moieties have been substituted for by ethyl groups, see Figure 3 for comparison to BPA (Corrales 2015, Almeida S 2018). Only the unconjugated BPA species, or "free" BPA, exhibits

estrogenic behaviour. Excretion of metabolized serum compounds occurs through the bile or urine and low-molecular-weight compounds (<325 kDa), such as BPA, are more often observed in urine than in bile (Claus S 2016). Within 6 hours of exposure in adults, a glucuronide moiety is conjugated to BPA in the liver and this metabolite is then excreted almost completely in the urine (Völkel W 2002). In neonates to 3 years of age, metabolism and excretion of chemicals is through the bile, as renal excretion develops. In addition, glucuronidation activity is significantly less in this age range (Anderson GD 2002). This suggests that gut microbiota of small children could be exposed to BPA via bile excretion.

Exposure to BPA has been linked to obesity, metabolic disorders, inflammation, infertility, cancer, neurological disorders from perinatal exposure, decrease in testosterone and GnRH in men, polycystic ovarian syndrome (Wang J 2013, Bertoli S 2015, Huang Y 2017, Huo X 2015, Konieczna A, 2015, Seachrist DD 2015,Roen L 2015, Schulster M 2016). In human populations, exposure has been measured at mean value of of 2 to 4 ng mL−1 of unconjugated BPA detected in adult and foetal serum and correlates to well below the “safe” exposure level of 50 ug/kg/day set by the Environmental Protection Agency of the United States (Bertoli S 2015, US EPA 2010). It is important to note that the presence of unconjugated BPA in the blood suggests high daily exposure to BPA, although exposure routes vary by geography and occupation (Bertoli S 2015). The United States and Europe have the highest recorded levels of BPA in environmental samples and in samples of human cohorts (Corrales J 2015, Lang IA 2008). Analysis of concurrent BPA levels and disease data collected by the Center for Disease Control in the United States demonstrated several trends: i, 93% of the cohort (n = 2,517) tested in 2003 had measurable amounts of BPA in their urine; ii, that higher levels of BPA are correlated with at greater risk for heart disease, Type 2 diabetes, and increases in liver enzyme activity; and iii, the threshold values of BPA measured which was correlated with disease were much lower than predicted by previous toxicology studies (Lang IA 2008). This analysis proposes most of the population is exposed to BPA on a daily basis and that the threshold for negative impact on health outcomes may be much lower in cases of chronic exposure.

2.2.2 Controversy over BPA exposure and disease

A controversy has sparked concerning the relevance of the low dose animal studies to human health due to differences in BPA metabolism in rodents compared to humans and how toxicity is determined. General toxicology predicts harm based on a linear dosing model, where threshold harm is based on acute exposure and the harm is assumed to follow a linear curve. Levels considered safe for adults are based on the rapid metabolism of BPA (Völkel W 2002), low serum levels of BPA observed and weak estrogen receptor avidity of BPA, 1:2000 (Bertoli S 2015). Researchers in the field of endocrinology have argued that signal molecules of the endocrine system do not follow a linear dose curve. Rather these molecules have the most profound effects on the system at very low and very high thresholds. Indeed, for the diseases correlated with BPA exposure in human populations, the effect is proposed to occur after long term exposure that results in an epigenetic restructuring (Vandenberg LN 2009, Sharma RP 2015). Even within the field of endocrinology, however, the lowest threshold of significant effect

in a rodent model was 10 times greater than that to which humans are typically exposed (vom Saal FS 2014, US EPA 2010). Variation in exposure routes, uncontrolled contamination of BPA in serum sample containers used by the Food and Drug Administration of the USA (FDA) tissue specific responses, and failure to observe an impact of BPA on limited timescales have all been reasons why results have failed to be reproduced between studies (Vandenberg L 2009, EFSA 2016, Qin X-Y 2012, Völkel W 2002). Lastly, most studies are conducted in rodent models whose metabolism of BPA is much slower, 2-3 days compared to 6 hours in humans; therefore, positive results found are not directly comparable to humans exposure to BPA (Kamrin MA 2004). Circumstantial evidence concerning BPA exposure and human disease fuels this fierce debate (Corrales J 2015).

2.2.3 BPA and gut microbiota community composition.

Recently several published studies demonstrated that exposure to BPA results in a shift in community members in the gut microbiota of mice, rabbits, dogs and zebrafish (Reddivari L 2017, Lai KP 2016, Javurek AB, 2016, Malaisé Y 2016, Koestel et al. 2017, Liu Y. et. al 2016). BPA exposure was correlated with an enrichment of taxa associated with dysbiosis and disease, with a few exceptions. The shifts observed in mammals resemble pre-diabetic and obese microbiome communities and communities that are correlated to inflammatory phenotypes (Reddivari L 2017, Lai KP 2016, Javurek AB, 2016, Malaisé Y 2016). Only one study observed a significant change in Alpha diversity with BPA administration (Lai KP 2016). Early life exposure can be more drastic in effect, as this is the window period in which the microbiome community dynamics are formed, when the intestinal barrier epithelium is immature, and when liver metabolic activity is reduced compared to adults (Rodríguez JM 2015, Ma B 2018, Ginsberg G 2009). In one study, rabbits were perinatally exposed to 200 ug/kg/day via dams for 15 days of gestation and 7 days of nursing. Researchers noted reduction in microbiome diversity in the treated group and enrichment of SCFA producers. They also observed an increase in serum lipopolysaccharides (LPS) and proinflammatory cytokines in the F1 generation. Both parameters are preclinical symptoms of an inflammatory phenotype and Irritable Bowel Syndrome (Reddivari L 2017). In another murine perinatal exposure study, researchers followed the F1 generation to postnatal day (PND) 170. Perinatal exposure was via dams from gestation day 15 to weaning of pups (PND 21) with dams exposed to 50 µg/kg/day body weight of BPA of two animal cohorts. In both cohorts, researchers noted at PND35 glucose intolerance and at PND45 hepatic inflammation in male offspring and increased IL-17 and TNF-α levels, pro-inflammatory cytokines. Lastly, significant decrease in Firmicutes, specifically Clostridia, and a significant increase in Bacteroides was observed. This study also suggested that the change in gut microbiome was related to the reduction in insulin sensitivity in the animals tested (Malaisé Y 2017).

Direct exposure in adult male mice for 10 weeks to BPA treated water (120 ug/mL) also resulted in a microbiome shift. The community shift was similar to mice in the same study who were fed a high fat diet (HFD). HFDs are correlated to inflammation and considered diabetogenic. Again the shift was typified by decrease in Firmicutes and Clostridia. In addition, a decrease in diversity in the gut microbiota was observed. These microbiota alterations parallel the microbial structure observed in diabetes patients (Lai KP 2016). In a side-by-side comparison of mice exposed to 50mg/kg of feed weight of BPA or estradiol 0.1ppB, 0.1 ug/L, supplemented water, researchers observed a comparable shift in the microbiome between the two treatments (Javurek A et. al 2016). This suggests that the mechanistic action of BPA and estradiol may be the same. In another *in vivo* study, BPA exposure resulted in a dysbiotic change in microbial metabolites and aggravated dextran sulfate sodium induced colitis in mice (DeLuca JA 2018). Lastly, a zebrafish model demonstrated that the gut microbiome mediates low dose effects of BPA exposure not observed in germ-free fish (Tal T et al. 2016). No speculation was provided by the authors of these *in vivo* studies as to the mechanistic action in which BPA impacts gut microbiota composition. While the magnitude in microbiota community shift varied from study to study, taxa belonging to Firmicutes were disproportionately impacted in treatment with either BPA or E2 compared to controls, see Table 1 for a summary.

Table 1:Microbiota Changes on BPA Treatment or Incubation

Microbiota Changes on BPA Treatment or Incubation			
Study	Conditions	Model	Change in Bacteria
Lai KP et. al. 2010	BPA treated water (120 ug/mL)	adult male CD-1 mice	Decreased Shannon diversity, **decrease in Firmicutes**, Clostridia spp., *Lactobacillus intestinalis*, *Clostridium viride*, *Eubacterium dolichum*, and *Coprococcus,* **increase Proteobacteria** (*Epsilonproteobacteria*), *Helicobacter ganmani*
Javurek A et. al. 2016	50mg/kg of feed weight of BPA, perinatal to weaning of dams	California field mouse (*Peromyscus californicus*)	Parental: **increased** Mogibacteriaceae, *Sutterella* spp, and Clostridiales, Mollicutes Prevotellaceae. F1: **increased** Mogibacteriaceae, Bifidobacterium, Akkermansia, Methanobrevibacter, Sutterella.
Malaise et.al. 2017	perinatal exposure of dams to BPA (50 µg/kg body weight/day) in corn oil, orally	C3H/HeN mice	Trend of **decreased Firmicutes** and **increased Bacteroidetes**. Significant **increased** *Enterobacterium hallii*, Bacteroides, and **decrease** Bifidobacterium
Reddivari L et. al. 2017	perinatal exposure of dams 200ug of BPA/kg of body weight/day orally from gestation day 15 through postnatal day 7.	Dutch-Belted rabbits	**Decreased Firmicutes**, Oscillospira and Ruminococcaceae. Significantly different beta diversity, UniFrac
Koestel et al., 2017	two brands of commercial canned dog food, compared to dry chow, where serum BPA was monitored	gonadectomized male and female dogs (*Canis familiaris*)	**decreased *Bacteroides*** spp., *Streptophyta*, Erysipelotrichaceae, and *Flexispira* spp. and **increased** *B. ovatus*, *Prevotella* spp., *Ruminococcus* spp., and *Cetobacterium somerae*
Liu Y. et. al 2016	5 weeks to BPA (200 or 2,000 µg/L)	adult male zebrafish (*Danio rerio*)	**Increased** Shannon and Chao1 diversity, i**ncreased** phylum CKC4, decreased Proteobacteria, namely *Acinetobacter*, *Aquabacter*, *Bosea* and *Xanthobacter*

Differences in molarity and perinatal versus direct exposure make these studies difficult to compare. In addition, defined mechanisms of BPA are confounded by this chemical's impact on the expression of estrogen regulated processes including immune response, inflammation and gut epithelial integrity (DeLuca JA 2018, Malaise 2018). Changes in gut microbiota composition may be a secondary outcome to primary reorganization of host tissue (Rosenfeld CS 2017). BPA has also been shown to increase intestinal permeability and this effect is exacerbated in females (DeLuca JA 2018, Braniste V 2010). Intestinal permeability results in higher O2 concentrations in the gut which would select for facultative anaerobes, such as Enterobacterales. Enrichment of this taxonomic Order is correlated to disease and dysbiosis (Zeng MY 2017).

2.2.4 Evidence of direct impact of BPA on microbiota

Disambiguation of BPA's impact on host and bacteria requires *in vitro* investigations of BPA on microbiota. Only one study, to my knowledge, by Wang et. al (2018), examined the impact of BPA incubation in an *in vitro* gut microbiota model. Interestingly, some of the trends observed *in vitro* contradict those observed *in vivo*. Wang et al examined BPA exposure in a SHIME model of the gastrointestinal tract, to monitor BPA bioavailability and degradation products over a 10 day fecal ferment as well as a shift in bacterial communities. SHIME, Simulator of the Human Intestinal Microbial Ecosystem, mimics each compartment of the gastrointestinal tract to elucidate kinetic processes of chemical metabolism and absorption by gastrointestinal tract, with the unique feature of including the role of gut microbes in this process. In this experiment, 100nM, 1uM, and 10uM amended nutritional media was fed to the stomach vessel 3 times per day over 10 days. The fecal sample of a young healthy man was used to innoculate the last three vessels in this five vessel system, modeling the ascending, transverse and descending colon. Vessels were protected from light and maintained at constant pH, temperature, and oxygen concentration. Interestingly, while lower concentrations of BPA were correlated to reduced diversity, higher concentrations of BPA resulted in increased diversity. Specific enrichment in organisms with BPA degrading activity, such as *Lactobacillus, Acidovorax, Stenotrophomonas, Megasphaera, Microbacterium and Alcaligenes* were observed. Significant changes were noted at the level of order. Of note, exposure of HepG2 cells to filtered extracts of BPA treated ferments increased expression of estrogen receptor α, β ,and γ; These changes exceeded the receptor changes observed with exposure to BPA alone and are attributed to the increased estrogenic activity of BPA metabolites (Wang et. al 2018).

BPA possible bacteriostatic and bactericidal properties could result in bacterial community shifts observed in animal studies. Several studies have demonstrated that phenolic compounds, similar to BPA, cause oxidative stress in bacteria due to non-lytic membrane damage and that Gram negative bacteria are more resilient to this stress. This could explain a shift at the community level observed in antibiotic or BPA induced dysbiosis (Zaborowska M 2020, Thompson 2015). In another study of xenobiotics, Digoxin, Digitoxin, Nizatidine, Ethanol,

Phenacetin, Sulfasalazine, researchers observed a change in gene expression and human fecal microbial community physiology *in vitro* in as little as 4 hour batch fermentation; however, community composition remained stable (Maurice CF 2013). BPA has been investigated as an antimicrobial agent directly. This study quantified the Zone of Inhibition caused by BPA (219uM to 2.19 mM) of four isolates, *Staphylococcus aureus, Bacillus subtilis*, *Proteus vulgaris* and *Escherichia coli*, using a disc diffusion assay. The zone of inhibition BPA at was dose dependent was comparable to streptomycin at a concentration of 2.19 mM BPA. Inhibition was observed at the lowest concentration tested, and sensitivities were similar between isolates (Rasheed A 2013).

The pharmacokinetics of BPA has been thoroughly tested in its toxicity to mammalian cell lines and in *in vivo* animal models. As BPA is an agonist of estrogen receptors, it is possible that BPA may mimic functions regulated by estrogen in the host and in the bacterial community. Recently, the relationship between estrogens and gut microbiota composition has come under study. Estrogens' various roles in the host and how these functions impact gut microbiota composition are discussed in the following paragraphs. Similarity in response of gut microbiota to estrogens and BPA in human and animal studies would suggest a specific mechanism action which may be highly conserved across host species.

2.3 Evidence of Relationship Between Sex and Gut Microbiome Composition.

2.3.1 Human observational studies.

Investigation into host factors which contribute to gut microbiota composition have been conducted in recent years to better understand the relationship between the host, microbiota and disease. Recently, several researchers have looked into the relationship between sex and microbiome composition in healthy human adults. In a European cross-sectional study, flow cytometry-based *in situ* hybridization was used to determine the correlation between location, age or sex and gut microbiota composition. While age differences were found to be significantly correlated in some geographic regions, only sex related enrichment in males in the *Bacteroides-Prevotella* group*,* specifically *Bacteroides vulgatus,* was found to correlate with sex in all geogrpahic regoins sampled (Mueller S et al. 2006). Further investigations correlated systemic estrogens and specific estrogen metabolites measured in the urine and/or feces to gut microbiota compositions. Flores et al. (2012) compared systemic estrogens in urine and feces to microbiota composition, β-glucuronidase and β-glucosidase activities, and fecal microbiota composition of 51 epidemiologists composed of men and post and premenopausal women. Positive correlation of systemic estrogens and most estrogen metabolites were found to significantly correlate to abundance of genera of the phylum Firmicutes including, non-*Clostridiales* and taxa from the family *Ruminococcaceae*; however, no correlation

between estrogens or their metabolites were found in premenopausal women likely due to samples being taken at various points in the menstruation cycle (Flores et al 2012). Of note, estrone was the primary factor in driving these correlations. Slightly different methods found similar results to Flores et. al. In this study, positive correlations between the ratio of parent estrogens to estrogen metabolites and enrichment of taxa belonging to Clostridiales and Rumminococcus in postmenopausal women were observed (Fuhrman BJ, et al. 2014). In addition, the ratio of parent estrogens to estrogen metabolites was negatively correlated to the genus *Bacteroides*. One study of men and women ages 25-65 stratified participants based on serum concentrations of testosterone and estradiol, respectively (Shin JH 2019). While no significant difference was observed between gut microbiota diversity in men, significantly higher diversity was observed in the highest serum testosterone group relative to the medium and low tertiles. Higher serum estradiol concentrations was also significantly correlated to increased alpha diversity and evenness (Shannon and Simpson indices). With respect to estradiol specifically, Firmicute-Bacteroidetes ratio was inversely related to serum estradiol concentration and phylum Proteobacteria was also negatively correlated with serum estradiol. In contrast to the previous studies, no significant difference was observed in Rumminoccae or Clostridiales with increasing estradiol (Shin JH 2019). In a study comparing sex, meonopause-status and serum steroid concnetration, Mayneris-Perxachs J et al. (2020) observed significant beta-diversity difference in pre-monopausal women compared to men or post-menopausal women. In addition, steroid synthesis and degradation pathways were significantly upregulated in gut microbiota of premenopausal women and this correlated to higher serum progesterone. Interestingly, obesity status eliminated the differences observed between groups.

Serum estradiol concentrations increase over the gestational period and peak at the third trimester during pregnancy. Stool of pregnant women were monitored in several studies observing the changes in fecal microbiota communities in relation to serum estrogen levels. (Edwards SM 2017, Nuriel-Ohayon M 2016). By sequencing the bacterial 16S variable region of fecal samples from the first and third trimesters, one study compared relative health status, Body Mass Index (BMI) and gestational period to microbiota composition. Of the 91 participants, most microbiota diverged significantly from study onset. In contrast to the Shin et. al. 2019 study, an overall increase in Proteobacteria and Actinobacteria, and reduced richness was observed over gestation in which estradiol levels increased significantly (Koren O 2012). Development of gestational diabetes and BMI did not correlate to the differences observed in beta-diversity, unweighted UniFrac Distances. Of note, authors report that differences in beta-diversity distribution could be attributed to an increase in Firmicutes and a depletion Bacteroidetes, between the first and third trimesters. Enrichment in Firmicutes and Proteobacteria is also commonly observed in obese pateints (Koren O 2012). Another study compared how BMI influenced gut microbiota in overweight pregnant women (n=18) and to normal weight controls (n=36) using qPCR and Fluorescent in Situ Hybridization (FISH) at the first and third trimester. *Clostridium, Bacteroides*, and *Staphylococcus* groups and *Akkermansia muciniphila* were significantly enriched for both groups when comparing first and third trimesters, although bacterial load only significantly increased for the normal weight group (Collado MC 2008). Lastly, a third study observed no significant difference in

bacterial diversity of four body sites tested (feces, vagina, saliva and tooth/gum) using a linear mixed-effects (LME) model to regress alpha diversity measures against gestational time in 40 pregnant women sampled weekly. Both alpha diversity (Shannon Index) and beta diversity (Unifrac) were considered (DiGiulio DB 2015).

2.3.2 Animal studies.

When studying humans, significant confounding factors can result in contradicting data (Shin JH 2019). Of particular difficulty is the variation in diet and geography in the human population which attribute the most to individual diversity of gut microbiota (Kovacs A 2011). Animal studies have further elucidated the relationship between estradiol and gut microbiome composition, as researchers can control for confounding factors in host population's behaviour and physiology. Two studies compared the gut microbiota composition in mice relative to genotypes and sex. The first compared a congenic mouse population whose genetic polymorphisms reflect the frequency observed in human populations (Kovacs A 2011). In contrast to many studies in this field, Kovacs et. al. used ARISA, automated ribosomal intergenic spacer analysis, which is more sensitive to species and strain level differences than 16S DNA fingerprinting used in the previously mentioned experiments. Greater similarity was observed in the distribution of species, by Jaccard Similarities, when comparing groups based on genotype rather than similarity by sex accross genotypes. Further, Org et. al 2016 compared 689 mice from 89 inbred strains using 16S DNA fingerprinting. Mice strains varied in the magnitude of community composition difference between sex by strain, where some sex differences were more drastic in some strains compared to others. Hence, genotype could influence the magnitude of sex influence on gut micrbiota composition. Linear discriminant analysis elucidated that *Allobaculum, Anaeroplasma*, and *Erwinia* were enriched in males*,* while *SMB53* from family *Clostridiaceae* and 3 members of family *Lachnospiraceae* were enriched in females*., specifically Dorea, Coprococcus and Ruminococcus.* Further analysis of gonadectomized mice of 3 strains demonstrated that diet dependent response in gut microbiota was sex dependent, although trends in microbiota composition were confined to the mouse strain.

Ovariectomized mice and male mice were used to evaluate specific effects of estradiol absences and absolute concentration on gut microbiota. In one study, gut microbiomes and related phenotypes of ovariectomized mice and male mice given water amended with 4000 ng E2/mL were compared to untreated mice (Kaliannan K et. al 2018). Gut microbiota of mice clustered by male/ovariectomized and female/ovariectomized+E2/male+E2 when comparing Bray Curtis distance. In addition, E2 treatment was significantly correlated with lower Proteobacteria abundance, decreased Firmicute-Bacteroidetes ratio, and increased *Akkermansia* abundance. It is interesting to note that this study demonstrated that metabolic syndrome observed in the nontreated group male could be transferred to a naive female mouse via fecal microbiome transfer. Further, the presence of estrogen or antibiotic treatment changed the gut microbiota composition and reversed the transferred disease phenotype. It was also shown, by comparing E2 treated with untreated ovariectomized mice, that gut microbiome mediates the preventive effect of estrogen development of low grade inflammation and a buildup of endotoxins associated with the onset of metabolic syndromes (Kaliannan K 2018). In agreement with these findings, a study elucidating the impact of estrogen on Male Wistar rats exposed to microgravity found that a protective effect of injected estradiol benzoate to microgravity induced Proteobacteria overgrowth (Yang, Y 2018).

Table 2: Microbiota Changes with Estrogen

Microbiota Changes with Estrogen			
Study	Conditions/Sample	Population/Model	Change in Bacteria
Flores et. al. 2012	urine (estrogens) and feces (16S)	25 men, 7 postmenopausal women, and 19 premenopausal women	In men and postmenopausal women urinary estrogens very strongly and directly associated with **increased richness** and alpha diversity, and **Clostridia** taxa. No trend could be determined for the premenopausal women.
Fuhrman et. al. 2014	urine (estrogens and their metabolites) and feces (16S)	60 post-menopausal women	**Increased diversity, *Clostridiales*** and ***Ruminococcus*** with estrogen concentration, and **decreased Bacteroides**
Shin JH et al. 2019	serum testosterone in men and estradiol in women and feces (16S)	57 men and women stratified by hormone level	**Increased** relative abundance of **Bacteroidaceae** and **Veillonellaceae**, **decrease Rikenellaceae**, **Porphyromonadaceae**, **Odoribacteraceae** and **Lachnospiraceae** with estrogen concentration. High estrogen women have more **Firmicutes** than **Bacteroides**.
Karen O et al. 2012	feces first and third trimester, and postpartum (16s)	91 pregnant women of varying pre-pregnancy BMIs	Changes between the first and third trimester were highly individual. Generally **increase** in **Proteobacteria** and **Actinobacteria,** and **reduced Clostridiales** and **richness.**
Org E, et al. 2016	cecum and fecal samples (16s); males and ovariectomized females dosed 5 mg pellet of 5a-dihydrot-estosterone 90 day release.	89 different adult inbred strains of mice, n = 689; ovariectomy and E2 replacement with C57BL/6J, C3H/HeJ, and DBA/2J mice	**Lachnospiraceae *(Dorea, Coprococcus*** and ***Ruminococcus***) were more abundant in female mice. In E2 replacement, prevented shift in microbes seen in untreated ovariectomized females. Differences in bile acid production by sex noted.
Kaliannan K, et. al. 2018	feces (16s); males and ovariectomized females dosed via water 4000 ng E2/mL water for 2 week	C57BL/6 mice, male, female, and ovariectomized.	Estrogen treatment **lowered *Proteobacteria*** abundance, **decreased Firmicute/Bacteroidetes** ratio and changed intestinal alkaline phosphatase expression.

2.3.3 Endogenous Metabolism and Signaling of Estrogens.

Estrogens are ubiquitous signalling molecules in the mammalian body and regulate a multitude of factors that could induce microbiota community change. Estrogens are synthesized endogenously from C18 steroids in mammals: 17β-estradiol (E2), estrone (E1), and estriol (E3), where E2 is found in the highest concentration relative to the other estrogens, in cycling females (Gruber, C M.D 2002). C18 steroids are formed in steroidogenic cells via oxidation activity of cytochrome P450 of mitochondria. P450 monooxygenase activity aromatizes the reduced cholesterol to form estrone and estradiol precursors androstenedione and testosterone, respectively. Sequential enzymatic and spontaneous hydroxylation results in the formation of the final estrogens. Estradiol is primarily synthesized in the gonadal tissue of both sexes while the main site of estrone and estriol synthesis is in the liver (Gruber, C M.D 2002). Extra-gonadal estradiol synthesis lacks C19 steroid precursor anabolism found in gonadal tissue for the full biosynthetic pathway of hormones. Localized estrogen synthesis from serum C19 precursors is widely distributed in the brain, adipose tissue, bones and gastrointestinal tract (Stocco C 2012, Barakat R 2016). Estrogens are mostly found bound reversibly to sex-hormone binding globulin or, to less of an extent, ablumin in the serum. The mechanism of action of estrogens occurs through direct interaction with nuclear estrogen receptor α (ERα) and estrogen receptor β (ERβ), indirect activation of these receptors via a phosphorylation cascade, or through a cell-membrane associated estrogen receptor, referred to as the classic pathway and alternative pathway, respectively. Of note, membrane associated estrogen receptor activation is rapid, transcriptionally independent, and mediates the short-term, rapid production and activity of insulin in pancreatic beta cells (Gruber, C M.D 2002).

While E2 excretion is regulated by the hypothalamus and pituitary, the activity of various estrogens is modulated by the liver, small intestine, kidney, placenta, uterus, adrenal gland, biliary epithelium, gut, prostate, ovary, and breast tissue. These tissues have microsomal UDP-glucuronosyltransferase and cytosolic sulfotransferases that conjugate UDP-glucuronic acid or sulfate to estrogens (Raftogianis R et. al 2000). Resulting modifications reduce affinity of estrogens for ERα and ERβ and increase their chemical polarity. Further, these modifications facilitate the elimination of estrogens via urine and bile. Discovery of glucuronidase and steroid sulfotransferase in steroid tropic tissues and observations of prolonged half lives of modified estrogens compared to parents species, suggests that conjugation facilitates hormone homeostasis by increasing availability of estrogens and not only elimination (Raftogianis R et. al 2000). Indeed, conjugated estrogens are metabolized by several families of enzymes that are broadly expressed in host tissues and by gut microbiota and include: Hydroxysteroid dehydrogenases (HSDs), β-glucuronidase, β-glucosidase and sulfatases (Kisiela M 2012, Baker JM 2017, Kwa M 2016, Ginsberg G 2009, McIntosh FM 2012, Flores, R 2012, Velmurugan 2017). Hydrolysis of UDP-glucuronic and sulfate can result in reabsorption of estrogens and contribute to increased enterohepatic circulation of these hormones (Gruber, C M.D 2002).

2.3.4 Estrogens' activity in gut tissue.

In addition estrogens play an important role in gut epithelial tissue integrity, bile production, and local gut immune response. Intestinal epithelium integrity is positively correlated to estrogen levels through the upregulation of tight junction proteins and indirectly through modulation of inflammatory cytokines (van der Giessen J 2019). Two mouse studies examining the role of exogenous estradiol administration and inhibition of androgens in male mice resulted in improved resilience to gut injury (Baker 2016). Sex differences in bile composition between male and female and sham overectomized and overectomized female mice has been observed (Org E 2012). Bile acid composition is correlated to healthy (Kemis JH 2019) and dysbiotic (Wang Y 2019) gut microbiota composition. In addition, sex differences were observed in intestinal alkaline phosphatase (IAP) production in female mice, mice treated with E2, and in duobdenal *ex vivo* incubations with E2 (Kaliannan K 2018). IAP is an antimicrobial peptide known to influence the composition of intestinal gut microbiota and specifically targets LPS-related and Gram-negative microbial groups (Kaliannan K 2018). This result may explain the downregulation of *Escherichia coli, E. coli.* under estrogen treatment in rats (Yang, Y 2018). Lastly, expression of estrogen-inducible protein lactoferrin could impact microbiota composition by sequestration of iron (Newbold RR et. al. 1992).

Estrogen also modulates immune system function of the gut (Oakley OR 2016, Merkel SM 2001, Barakat R 2016), the intestinal mucous layer (Diebel M 2015), gut transit time (Mayer EA 2014), and epithelial cell turnover (Oakley OR 2016, Nakatsu C 2014). All lymphoid tissue expressess ERα and β which repress expression of multiple NFκβ-driven cytokines and inhibit inflammation (Garcia-Reyero N 2018, Barakat R 2016). In addition, estrogens exert an anti-inflammatory effect by suppressing B- and T-lymphopoiesis and the induction of Th2

anti-inflammatory cytokines such as IL-10, IL-4, and TGF (Barakat R 2016). In contrast, estrogens act as an adjuvant of glucocorticoid mediated inflammation and increase pro-inflammatory cytokines IL-6, IL-8, TNFα, and activator protein 1 more than activity of glucocorticoids alone (Garcia-Reyero N 2018, Blasco-Baque V 2013, Straub RH. 2007). Estrogen synthesis in the gut is concentrated in the Peyer's Patches (PP) and mesenteric lymph nodes. Oakley et. al. (2016) observed that local aromatization in these tissues accounted for higher local E2 levels than in the gonads of the same animal in a murine model. PP's are the site of acquired antigen-specific intestinal IgA response in the Gut Associated Lymph Tissue (GALT). PP Cy19 aromatase expression is the highest within the distributed GALT. Estrogenic compounds suppress immune function through targeted apoptosis and inhibition of immune cell proliferation in the GALT (Barakat R 2016). Estrogens modulate local Toll-like receptor response, cytokine expression, and production of immunoglobulins. For example, immune attenuating response E2 is mediated by ER β which modulates the expression Toll-like receptor 4 on the cellular membrane (Oakley OR 2016). Toll-like receptor 4 mediates the inflammatory response in the presence of endotoxin lipopolysaccharide (LPS) (Merkel SM 2001). For example, female mice with ablated ER β exhibit inflammatory phenotypes (Oakley OR 2016). In addition, ovariectomized female mice exhibited a stronger inflammatory response to LPS, which was not observed in intact female mice. Normal inflammatory response was also restored by estrogen administration (Merkel SM 2001). In addition, estrogen also regulates epithelial cell turnover through ERα and β in the crypts such that ER β signaling inhibits epithelial cell proliferation (Oakley OR 2016). Gut microbiota composition is correlated to the distribution ER β in intestinal tissue (Menon R 2013) and it is possible that compositional changes may be related to Toll-like receptor 4 expression and downstream immune signalling regulated by localized estrogen concentration (Oakley OR 2016). Lately, estradiol is a key regulator of metabolism by regulating saity through modulation of leptin and lipoprotein lipase expression, cannabinoid receptor antagonism, and regulation of the spatial deposition of adipose tissue and its metabolism (Eyster KM 2016, Mayes JS 2004, Barakat R 2016).

Despite global differences in estrogen between sexes, estrogen concentration and activity of aromatase in the gut is thought to be monomorphic (Oakley OR 2016). Greater exposure to estrogen in the gut could occur if systematic estrogen metabolism is impaired or altered by the enzymatic activity of microbiota and result in longer periods of enterohepatic cycling. Exogenous estrogens, like BPA, could interact with enzymes and receptors differently to their endogenous orthologues and could result in a dyshomeostasis via aberrant modulation of IgA expression. From IgA expression, to bile acid expression and final antimicrobial peptides, like intestinal alkaline phosphatase, show possible mechanisms for a host mediated relationship between estrogen and gut microbiota composition. More interestingly, evidence exists that estrogens have a direct impact on bacteria and may clarify a host independent mechanism of action.

2.3.5 Evidence of direct impact of estrogen, E2, on microbiota.

While estrogen regulated host factors have potential to influence gut microbiota composition, estrogens also have a direct effect on microbes and can improve symbiont fitness. For example, short term incubation of *Pseudomonas aeruginosa* with estrogen induction of reactive oxygen species and longer term incubation resulted in the dysregulation of virulence gene *mucA* in a cystic fibrosis disease model (Chotirmall S 2012). In addition, *in vitro* studies have demonstrated that E2 induces bacterial growth. For example, *Prevotella intermedius* takes up E2 and progesterone, which enhances its growth (Neuman H, 2015). Kornman KS, et al. (1982) observed enhanced growth of *Bacteroides melaninogenicus* and *Bacteroides gingivalis*, where estradiol served as a substitute for vitamin K. Interestingly, estrogen inhibits vitamin K utilization of vitamin K in *Prevotella intermedia sensu lato* (Fteita D 2014). Researchers speculated that this species prefers estrogen to vitamin K. *Vibrio fetus var. venerealis* growth is induced in the presence of estradiol; however this induction was inhibited with the addition of progesterone at equal or excessive stoichiometric molarity (Walsh 1973). Hence, *Vibrio* growth induction pathway is likely different from *Prevotella*. Observations suggest *Vibrio* and *E. coli* have receptors that are specific to host hormones progesterone and estrogen, not just cholesterol derivatives and that these molecules act as ligands which regulate bacterial metabolism.

In contrast, estrogens' impact has also been observed to be deleterious to growth and bacteria-to-bacteria communication. Growth of *E. coli* deficient in the multiple-drug efflux steroid efflux pumps can be suppressed by estrogens. The substrate for these efflux pumps includes bile acids and steroid hormones. Interestingly, Elkins et. al. (2006) observed that estrogen uptake activity of these efflux pumps was impacted by progesterone amendment, but not with exogenous bile acids and hydrocortisone (Elkins CA 2006). Evidence also suggests direct impact on interkingdom communication via estrogen signaling. In microbes endemic to the oral cavity, E2 disrupts biofilm formation in *B. gingivalis* (Kornman KS 1982) but induces biofilm formation in 3 *Prevotella* species (Fteita D 2018). Indeed, Beury-Cirou A (2013) demonstrated that E2 disrupts quorum sensing and supraphysiological concentrations. The impact of E2 on bacterial monocultures shows the differential response between species and strains of bacteria. This differential response which results in growth, growth inhibition, and interference with quorum sensing (QS) suggests that E2 exposure in the gut could influence gut microbiota composition. Disruption of quorum sensing possibly represents a robust mechanism of regulating gut microbiota behavior and composition. As quorum sensing is often used as a mechanism to coordinate expression of virulence genes, existence of a general disruptor of this signal in the gut would prove evolutionarily advantageous. The forthcoming discussion of quorum sensing, gives context as to the impact quorum sensing disruption could have on bacterial behavior, colonization, and community composition in the gut.

2.4 Quorum Sensing

To compete for niche space, like the human gut, bacteria have evolved communication systems to coordinate complex intra and interspecies behavior, generally referred to as Quorum Sensing (Thompson J et. al 2015). Quorum Sensing (QS) allows for the coordination of gene expression across a population of bacterial cells and relies on the production and detection of extracellular signals. In bacteria, signal molecules are metabolically inexpensive to synthesize, typically constitutively expressed and can be autoregulated in response to the concentration of the same signal (compared to paracrine and autocrine type signaling of metazoans). Similar to animal hormonal signaling, the dose response to QS signals is often not linear, where there is a threshold below which and above which the response is repressed (Rickard AH 2006). QS regulates genes in a population dependent manner, where higher densities of cells increase efficacy of an often costly behaviour, but provide a competitive advantage en mass (Abisado R 2018). In general, QS signals diffuse or are exported into the environment. The signal molecule binds to a cognate receptor and induces a signal transduction cascade or is simply imported into the cell. Typically a change in gene expression occurs once a threshold of the signal is met. Examples of such coordinated behaviours include biofilm formation, toxin secretion, competence, Type 6 secretion systems, bacteriocins, sporulation, adhesion, antibiotic synthesis and motility and can be important factors in niche colonization (Abisado R 2018, Thompson J 2016). Bacteria synthesizing the signal actively remove it from the extracellular space via translocation or degradation (Abisado R 2018, Praneenararat T 2012).

2.4.1 Types of quorum sensing systems in bacteria.

Three systems of QS gene regulation are known in the gut microbiome and are grouped by Gram-negative acyl-homoserine lactone (AHL)-mediated, also called AI-1, Gram-positive peptide-mediated, and interspecies signaling mediated by Autoinducer-2 (AI-2). Many Proteobacteria are known to contain *luxI* or *luxM* which synthesize AHLs from *S*-adenosylmethionine (SAM) and an acylated acyl carrier protein (ACP) from the fatty acid biosynthesis pathway (Swearingen MC 2013, Abisado R 2018). The fatty acyl side chains can vary in length and oxidation and this variation accounts for the observed intraspecific specificity. While enteric pathogens like *Yersinia enterocolitica* and *Salmonella* contain LuxR- and LuxI-type proteins, common gut bacteria of the genera *Escherichia*, *Klebsiella*, and *Enterobacter* lack any known AHL synthase in their genomes (Swearingen MC 2013). AHL is freely diffusible across the cell membrane and interacts with transcription factor LuxR (Swearingen MC 2013, Miller M 2001). Although AHL signaling has traditionally been thought of as an intraspecies communication system, it is well known that QS receptors exist in bacteria without the cognate signalling molecule synthase, providing a mechanism for “eavesdropping” on competitors (Swearingen MC 2013). Gram-positive bacteria synthesize oligopeptides as QS signals (AIP). The signal peptide is secreted via a dedicated ATP-binding cassette (ABC) transporter and

requires the use of an adaptive two-component response. In this case, a membrane bound receptor kinase detects the signal, followed by activation of the response regulator via phosphorylation (Miller M 2001). Over 300 AIPs have been identified (Wynendaele E, 2013*)* and seven have been characterized from *Enterobacteria faecalis,* alone (Verbeke F 2017).

Unlike AIP and AHL family of QS molecules, AI-2 detection and production is not species specific and it is synthesized and detected by both Gram positive and negative bacteria species in the gut (Pereira CS 2012). LIke AHLs, AI-2 is a byproduct of the synthesis of S-adenosyl-L-methionine, SAM, a major methyl donor in the cell and recycling of methionine in the Activated Methyl Cycle (Redanz 2012, Sun J 2004). In bacteria, SAM is a methionine substrate involved in methionine or cysteine biosynthesis. Hence, SAM synthesis could be a proxy for basic metabolic activity of a cell to other cells to indicate high metabolic activity and high population density via secretion of HSLs and AI-2 (Pereira CS 2012). Hence, AI-2 signalling is related to metabolic activity. This signalling could communicate good conditions for growth or induce persistence due to absence during starvation. Given the prevalence of AI-2 signalling in the gut, this signaling molecule has come under investigation as a target for gut microbiome engineering (Foo JL et. al 2017). S-ribosylhomocysteine lyase or AI-2 synthase, *luxS*, acts on S-ribosylhomocysteine (SRH), detoxing the cell from this toxic intermediate and producing DPD, 4,5-dihydroxy-2,3-pentadione, the precursor to AI-2. Further reactions act on DPD form specific signaling molecules which all reside under the umbrella term AI-2 (Rezzonico, F 2008, Grandclément C 2016). While the synthase, *luxS,* is highly conserved across taxa, little homology has been found between receptors for AI-2 and few cognates have been identified through sequence homology (Winans SC , Torcato IM 2019). This suggests a great breath of species specific responses to AI-2 based on binding affinities and pathways (Torcato IM 2019).

AI-2 is detected either due to passive diffusion into the cytoplasm, like AHL, or a two component signal transduction pathway, similar to AIP. Two contrasting detection systems, that of *Vibrio harveyi* and *E. coli*, have been well characterized. In *E. coli*, and several other enteric pathogens, AI-2 binds to membrane bound LsrB, which is complexed with an ABC transporter system and cytoplasmic kinase, LsrK. Hence, AI-2 is actively transported into the cell and is then subsequently phosphorylated to Phospho-AI-2. Phospho-AI-2 is an antagonist for DNA bound repressor LsrR. Phosphorylation also blocks passive diffusion of sequestered AI-2 across the membrane, sequestering the signal. Association of Phospho-AI-2 with LsrR results in the dissociation of this protein from the DNA and expression of AI-2 regulated genes which include increased expression of *luxS* and the ABC-transport system in a positive feedback loop. In contrast to the active transport of AI-2 by *E.coli*, AI-2 passively enters the periplasmic space of *Vibrio* and binds to membrane kinase LuxP. Binding of AI-2 with LuxP causes a dimerization with another membrane bound protein LuxQ. Dimerization results in a phosphorylation cascade which blocks the degradation of *luxR* mRNA in an Hfq, sRNA, and sigma 54 dependent manner. Absence of DNA-binding transcriptional activator, LuxR, results in reduced expression of the AI-2 regulated Lux Operon (Xavier and Bassler 2005, Vendeville A 2005). Heterogeneity of the cognate receptor, differential membrane diffusibility, local AI-2 concentration attenuation or

enhancement, and coupling with species-specific QS systems results in a fine tuned strategic response to a general AI-2 message (Torcato IM 2019). See Figure 1 which depicts the contrasting detection pathways of *E. coli* and *V. harveyi*.

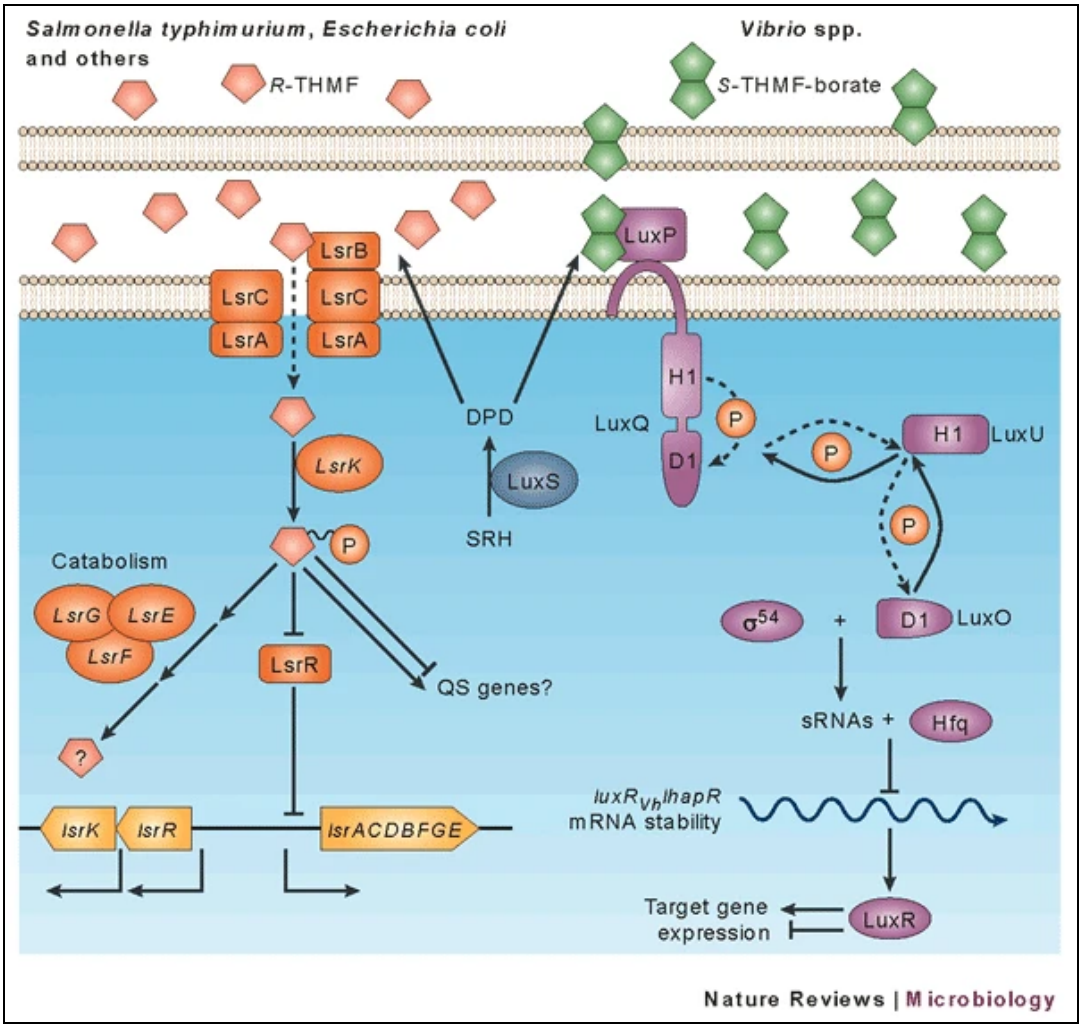

Figure 1: Depiction of well characterized AI-2 signal transduction pathways in *Escherichia coli* and *Vibrio* sp. Notably, *E. coli* uses active transport of AI-2 and phosphorylated-AI-2 blocks the transcriptional repressor, LsrR. *Vibrio* sp., on the other hand, uses a phosphorylation cascade, where AI-2 remains in the periplasmic space in association with LuxP. The phosphorylation cascade results in the transcription of regulatory sRNA and Hfq mediated induction of transcriptional regulator LuxR translation. Both models passively diffuse AI-2 into the environment. AI-2 is in two forms, R-THMF and S-THMF-borate, both of which induce bioluminescence in *V. harveyi.* Image from Vendeville, A., Winzer, K., Heurlier, K., Tang, C. M., & Hardie, K. R. (2005). *Making "sense" of metabolism: autoinducer-2, LUXS and pathogenic bacteria. Nature Reviews Microbiology, 3(5), 383–396.* doi:10.1038/nrmicro1146 .

2.4.2 Autoinducer-2 in the gut.

Synchronized production and secretion of virulence factors, biofilm formation, adhesion, and changes in motility are important phenotypes expressed by bacteria colonizing the gut (Pereira 2012, Buck BL 2009, Rickard AH 2006). In the gut, AI-2 regulation of these genes coordinate colonization (Christiaen SE 2014, Pereira 2012, Ismail A 2016). AI-2 is a virulence factor for many well known enteric pathogens, such as *Salmonella enterica* Serovar *Typhimurium*, *Clostridium difficile,* and *Escherichia coli (Enterohemorrhagic E. coli)* has been well characterized (Choi J 2007, Lee A 2005, Bansal T 2008, Kim Y 2008). In contrast to other enteric pathogens, *Vibrio cholera* secretes virulence factors and induces biofilm production in response to low levels of AI-2, while at higher concentrations these behaviours are inhibited (Higgins D et. al. 2009). In these examples, AI-2 signaling mediates virolence in addition to microbiome restructuring. Less obviously, AI-2 signalling can have the opposite effect, as putative AI-2 expression has also been detected widely in the genomes of commensal gut microbiota samples and isolates and it is disproportionately distributed among the dominant phyla of microbiota in the gut (Rao RM 2016, Sun J 2004, Thompson 2015, Lukás F 2008, Torcato IM 2019).

Further, it has been demonstrated in co-colonization of mice, that AI-2 expression by *Ruminococcus obeum* reduces virulence of *Vibrio cholera* independently of *V. cholera*'s native AI-2 signalling pathway (Hsiao A et. al. 2014). Another research group showed that AI-2 regulated iron-uptake gene was necessary for *Bifidobacterium breve* UCC2003 to confer resistance to *Salmonella* in a *Caenorhabditis elegans* model (Christiaen SEA et. al. 2014). In addition, many commensals, such as species from genera *Bifidobacterium*, *Lactobacillus*, *Rumminococcus*, *Eubacteria*, and *Roseburia*, considered beneficial flora, contain *luxS* in their genome and may use signaling to compete (Krzyżek P. 2019). Lastly, treatment by isogenic *E. coli* expressing AI-2 or lacking *luxS*, restored the microbiome community of mice after streptomycin induced dysbiosis in the AI-2 expression group (Thompson J et. al. 2015). Interestingly, this niche composed of 90% Firmicutes and Bacteroidetes, putative *luxS* is detected in 83.33% and 16.83% respectively, which supports the differential impact when AI-2 signaling between these two phyla (Thompson J 2015). This is particularly interesting since the antibiotic used, streptomycin, selectively targets Firmicutes over Bacteroidetes.

Studies of gut microbiome succession events observed changes in the predominant phyla from Firmicutes to Bacteroidetes upon change in mucin permeability in the colon. Permeability of mucin in the colon allows for bacteria to access gut epithelial tissue and interaction of host and bacteria directly (Johansson M.E.V 2015). The mammalian host also makes an AI-2 mimic on damage by dextran sulfate sodium (DSS). The AI-2 mimic is detected by the same signal transduction pathway as its bacterial analogue (Ismail A et. al. 2016). Since gut microbiome composition is correlated with recovery of gut epithelium post damage, researchers proposed that the AI-2 mimic may help select for community structures that support healing of the intestinal epithelium (Ismail A 2016). Establishment of Firmicutes in the gut could

be regulated by host and bacterial AI-2 signaling pathway, as seen in Ismail A et. al. study as both DSS exposure and exposure to bacteria increased host expression of the AI-2 mimic *in vitro*. Niche forming foundations afforded by AI-2 expression and detection demonstrate how host microbe interactions utilize this QS signaling system.

Taken together, this suggests a complex role of AI-2 signaling in the gut, both protective against invasion of pathogens and supportive of their virulence, recovery from antibiotic induced dysbiosis and microbiota supported healing in the gut. In organ systems, disruption of endogenous cellular communication systems occurs in cases of mutations in signal reception, signal synthesis, or due to exposure to exogenous signals, such as environmental contaminants (Berridge MJ 2012). Hence, disruption of bacteria-bacteria communication and host-bacteria communication by exogenous chemicals or host gene dysregulation could interfere with initial colonization events of the microbiome and recovery of homeostasis post perturbation.

2.5 Quorum Quenching

Quorum quenching, (QQ), is defined as the disruption of detection or synthesis of a quorum sensing molecule (Grandclément C 2016). QQ molecules and enzymes work endogenously as autoregulators of QS and exogenously as a counter strike against another species' quorum sensing systems. This allows for fine tuned response locally to the signal and a complex gene regulation based on absolute ranges of the QS signal. QQ has been explored as an antibiotic alternative, as many pathogens use AI-2 signaling to induce virulence genes with important implications in agriculture and health (Praneenararat T 2012). Various methods have been used to identify QQ molecules. *In silico* methods have been applied widely and are used to model possible docking sites of proteins associated with a quorum sensing network. Predicted molecules are then screened with an engineered biosensor or endogenous reporting system. In addition, chemical synthesis and then modification of the endogenous quorum sensing molecules has been used to screen for QQ molecules in a top down approach (Praneenararat T 2012). Evaluation of the QQ candidate as an antagonist rather than an agonist requires a benchtop model, where a biological sensor is paired with molecular techniques to demonstrate phenotypic and molecular components of inhibition. Biosensors which contain a colorimetric reporter gene or anti-toxin screens for larger libraries are commonly used. Some endogenous reporters can be exploited to measure magnitude of QQ such as the motility of *Yersinia enterocolitica*, pyocyanin and pyoverdin production in *P. aeruginosa*, and bioluminescence in *V. harveyi* (Grandclément C 2016, Li M 2008). Possible molecular targets include proteins that regulate translocation of AI-2, like LsrK (*E. coli*), phosphorylation of AI-2, again like LsrK (*E. coli*) or LuxP/Q in *Vibrio*, bind AI-2 repressor, like LsrR (*E. coli*) or interact with Hfq, like in *Vibrio*.

The first global AI-2 QQ molecule characterized was a furone from sea algae *Delisea pulchra.* Furones are a five-membered heteroaromatic ring containing an oxygen atom (Husain A 2019). Interestingly, furones have been shown to disrupt expression of known AI-2 regulated genes and the synthesis of AI-2 in both Gram negative and Gram positive bacteria. In *E. coli* and species with similar QS systems, furones have been shown to covalently bind to LuxS, preventing AI-2 synthesis. In *V. harveyi*, furones have been shown to affect binding of transcription factor LuxR (Grandclément C 2016). Most QQ molecules discovered are chemically similar to the QS molecule or substrates for its synthesis and interact with the synthase, the receptor protein, or the response regulator; however, it is feasible that QQ molecule could interfere with QS molecule uptake via interaction with LsrK (*E. coli)*. Recently, QQ molecules from animals have been identified, including long-chain fatty acids linoleic acid, oleic acid, palmitic acid, and stearic acid inhibit AI-2-based QS in *V. harveyi* at 0.1mM and above (Widmer et al. 2007). Evolved or stochastic cross-affinity of certain molecules for AI-2 receptors exist. How bacteria and the host adapt to these changes continues to be of important interest to research.

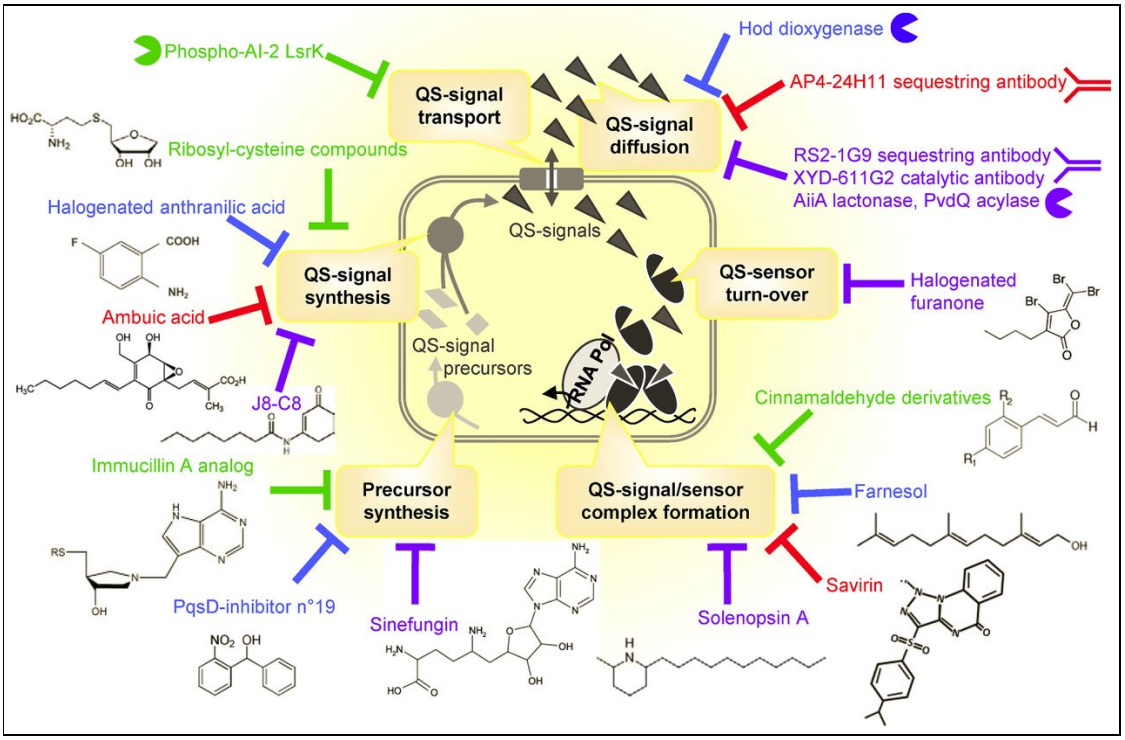

Figure 2.. QQ targets in the AHL, AI-2, PQS and AIP QS pathways. The different QS steps targeted by QQ actors are indicated in the black boxes. The color of the stop lines indicates which QS-signal pathway is affected and AI-2 (green colour). Image and description from Grandclément C, Tannières M, Moréra S, Dessaux Y,Faure D, Quorum quenching: role in nature and applied developments, *FEMS Microbiology Reviews*, Volume 40, Issue 1, January 2016, Pages 86–116

2.5.1 BPA and E2 as quorum quenching molecules.

As suggested by Fteita et. al (2018) and Korman et al (1982) bacteria QS could be disrupted by host hormonal signaling. Indeed, E2 has been demonstrated to disrupt QS signalling *in vitro* biosensor model (Beury-Cirou A 2013). Quorum sensing signal, AI-2, is both a metabolite and transcriptional regulator in gut bacteria (Pereira CS 2013). As mentioned previously, AI-2 signalling capability is skewed dramatically towards Firmicutes in the gut microbiome (Thompson J 2015). This distribution mirrors the disproportional impact BPA and E2 have on gut microbiome communities in mammal models, see Table 1 and Table 2. Thompson et al. (2015) demonstrated that AI-2 induces proliferation of bacterial cells capable of AI-2 detection, specifically Firmicutes. In mammal models exposed to BPA, depletion Firmicute populations, and enrichment Bacteroidetes, who predominantly lack *luxS*, was consistently observed (Malaisé Y 2016, Reddivari L 2017, Lai KP 2016). *In vitro* experiments have shown that AI-2 signaling is impacted by glucose availability, where lower levels of glucose and higher levels of cAMP reduce expression of AI-2 in *E. coli* (Pereira CS 2013). In mice exposed to BPA, their resulting microbiomes resembled mice fed a high fat diet, a diet by definition low in glucose (Lai KP 2016). In another study, brominated BPA which spontaneously forms in plumbing at room temperature, has been demonstrated to disrupt biofilms (Li C 2015). Biofilm formation is often regulated via a QS mechanism (Pereira CS 2013, Grandclément C et al. 2016, Praneenararat T et al. 2012, Li M et al. 2008). While results from isolates and *in vivo* studies suggest that E2 may influence bacteria physiology directly and impact microbiome composition, the literature available to date is limited and no studies have yet analyzed the direct impact of E2 exposure on fecal gut microbiota.

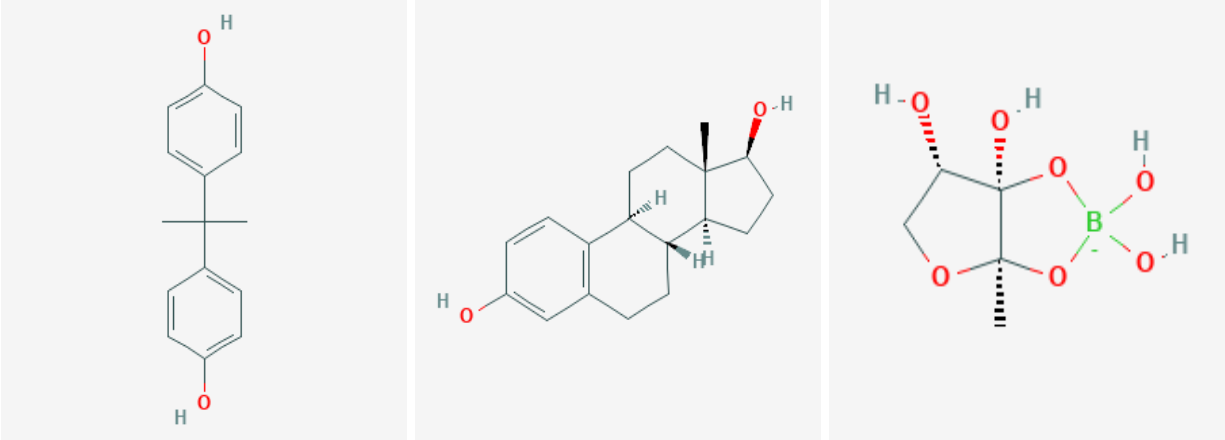

Bisphenol A **Estradiol** **THMF- Borate (AI-2)**

Figure 3. 2D image of Bisphenol A, Estradiol and AI-2. All images sourced from https://pubchem.ncbi.nlm.nih.gov/compound/

2.6 *Vibrio harveyi* as a Biosensor.

.

To investigate E2 and BPA as possible QQ molecules, biosensor *V. harveyi* was used. The Bassler Lab first identified borated-tetrahydrofurane, S-THMF-borate, AI-2, through purification of the receptor protein LuxP from *V. harveyi* in complex with the QS signal molecule (Chen X.2002). It was soon discovered that *V. harveyi* response was not specific to borated furnone (Xavier KB, Bassler BL 2005). Exposure of *V. harveyi* to THMF-borate, and other molecules derived from DPD, resulted in the induction of light emitting reaction through expression of *luxCDABE* in a dose dependent manner. After this observation, *V. harveyi* has been used to identify putative AI-2 signals from other species (Mok KC 2003, Xavier KB, Bassler BL 2005). Hence, this pathway has been exploited for high throughput screening of putative AI-2 expression systems. Like other species, AI-2 detection is just one of several QS pathways in *V. harvey*i which regulate light production. For specific detection of AI-2, strain *Vibrio harveyi* TL26 is a knock out for the synthesis pathways that induce light production by this species and has been used as a model to test for induction or inhibition of *luxCDABE* in an AI-2 dependent manner (Thompson 2015, Ismail A 2016). *V. harveyi* has been used to screen candidate QQ molecules through measuring the expression of bioluminescence (Widmer et al. 2007). In this study, *V. harvey* TL26 was used to detect AI-2 production in various gut isolates and human fecal samples and to detect Quorum Quenching by BPA and E2.

3. OBJECTIVES

The goal of this work was to elucidate if the impact of direct exposure of bacteria to BPA or E2 and if this impact could confer a predictable community shift. Differential growth due to toxin tolerance or induction of reproduction could be a selective advantage. Coordinated multicellular behavior, which is regulated by quorum sensing, is advantageous for growth. Hence the impact of E2 and/or BPA on AI-2 detection and production was the core focus. Lastly, I explored if the observations in monoculture are captured in *ex vivo* complex fecal communities.

1. Screen the effects of BPA and E2 on growth in *V. harveyi*, *E. coli* strains and, *E. faecalis* on growth kinetics.

2. Screen for production of AI-2 in gut microbiota strains and human male and female fecal microbiota with biosensor V. harveyi.

3. Measure degree of BPA and E2-induced disruption of AI-2 detection with biosensor V. harveyi

4. Analyze differential AI-2 production and community composition of fecal ferments incubated with and without BPA amendment.

4. METHODS

4.1 Screening of physiological effects of BPA and E2 on the growth of *V. harveyi*, *E. coli* K-12 strains and *E. faecalis*.

Strains:

Various strains of *E. coli* derived from *E. coli* K-12, MG1655 and BW25133, were assessed. Both wild type and mutants deficient in genes related to AI-2 signalling were compared. *E. coli* MG1655 strains used were wild-type, *E. coli* MG1655_WT , *E. coli* MG1655_ΔlsrK, and *E. coli* MG1655_ΔlsrRΔluxS. ΔlsrRΔluxS knockout removes the repression of AI-2 regulated operon and the synthesis of AI-2. *E. coli* MG1655_ΔlsrK a knockout of *lsrK* prevents *E. coli* from internalizing AI-2. *E. coli* BW25133 strains used were, *E. coli* BW25133_WT, *E. coli* BW25133_ΔlsrR, *E. coli* BW25133_ΔluxS. *E. coli* BW25133_ΔlsrR strain allows for unregulated expression of *lsrK* and *luxS* (Δ*lsrR*). *E. coli* BW25133_ΔluxS is deficient in AI-2 synthesis. In addition, *V. harveyi* AI-2 reporter strain TL26 (ΔluxN ΔluxS ΔcqsS) which is disabled for detection of autoinducers of bioluminescence, CAH-1 and AI-1, but not AI-2 and deficient in AI-2 synthesis. All *E. coli* MG1655 strains and *V. harveyi* TL26 were validated and supplied generously by Professor Xavier of Instituto Gulbenkian de Ciência, Portugal. *E. coli* BW25133 are from the Keio collection. All *E. coli* BW25133 strains are (Δ(araD-araB)567, ΔlacZ4787(::rrnB-3), λ^-, rph-1, Δ(rhaD-rhaB)568, hsdR514) with specific mutations in ΔluxS768::kan, ΔlsrR733::kan where endogenous gene is replaced by kanamycin resistance gene. These isolates were generously provided by Dr. Armin Resch Universität Wien. *Enterococcus faecalis* was isolated from the mouse gut in our lab and has 100% sequence homology to *Enterococcus faecalis* strain NBRC 100480. Stains were grown in the appropriate media. Briefly LB for *E. coli* strains, 5 grams yeast extract, 10 grams NaCl, and 10g tryptone per liter. LM for V. harveyi, contains 5 grams yeast extract, 20 grams NaCl, and 10g peptone per liter. And for *E. faecalis,* RCM, contains yeast extract 13 g, peptone 10g, glucose 5 g, soluble starch (Maiz) 1 g, NaCl 5 g, sodium Acetate 3 g, and cysteine hydrochloride 0.5g per liter. Strains were grown in 5 mL fresh media, LB(*E. coli* strains), LM (*V. harveyi*) overnight at 30C, 300 rpm or RCM (*E. faecalis*) at 37C overnight.

Experimental Conditions BPA and E2 on growth of *V. harvey* and Various Strains of *E. coli*:

Bacteria were grown overnight under the appropriate conditions and were then diluted 100x (approximately OD600 0.03) in fresh media the following day and aliquoted, in triplicate for each treatment. Growth curves were monitored over 5-8 hours using a plate reader using

OD650 or OD600,, with Versamax Microplate Reader, by Molecular Devices. Measurements for OD600 were made on a Infinite 200pro (Tecan Trading AG, Switzerland. due to visa issues and lab access. All treatments were matched to vehicle control: 1-5% DMSO, 1% Ethanol or Aqueous preparations in LM, LB, or RCM media. For BPA solvated in DMSO, *E. coli* MG1655 or *V. harveyi* was incubated with 25 mM BPA with 5% DMSO, 5% DMSO, 10 mM BPA with DMSO(1%), 10 mM BPA with 1% DMSO, 5 mM with 1% DMSO, 2.5 mM with 1%DMSO, 1.25 mM with 1% DMSO, 1 mM with 1% DMSO, 1 mM BPA, 100 uM BPA, 10 uM BPA, 1 uM BPA, 100 nM BPA, 10 nM BPA, or 1nM BPA. OD650 was taken every hour for 6-8 hours. Concentrations of BPA higher than 1mM resulted in skewed absorbance numbers OD650 measures. BPA solvated in DMSO. 1:100 dilution of overnight culture was incubated with the various treatments and OD 650 was taken every 0.5 hours. At the final time point, wells with the same treatment and bacteria were pooled (1uL/well/in one mL fresh media). 10 uL of this was plated and the ImL and the plates were incubated overnight at 30C. Final OD650 and colony counts were compared. 1uL aliquots were pooled from each group to inoculate 1mL fresh media to detect bactericidal and bacteriostatic effect post incubation. In addition, BPA concentrations higher than 1mM, a serial dilution of each pool was evaluated in a petri plate assay for actual viable cell counts. 1M BPA stock was solvated in DMSO, autoclaved, and stored at room temperature. Aqueous (aq) BPA stock was prepared by solvating 200uM BPA in the appropriate media and autoclaved. Media stored at room temperature and made fresh monthly. Concentrations ranging from 100uM - 1mM BPA are the concentrations used in animal studies, while human exposure from diet is 1nM -100nM of BPA (vom Saal F 204).

The tolerance of strains to 17B-Estradiol (E2), Sigma E2758, was also compared *V. harveyi* was grown overnight at 28C in LM, then diluted 1:100 in fresh LM for the detection assay. *E. coli* K-12 derivatives; BW25133 (WT, Δ*lsrR*, Δ*luxS*) and MG1655 (Δ*lsrK*) were grown overnight at 28C. OD600 was taken and bacteria were diluted (0.3/OD600 * 200 uL in 10 mL fresh LB). Diluted strains were then grown in the presence of 100 nM, 75nM, 50nM, 25nM, 10nM, 5nM, 1nM, 0 nM E2. Growth was monitored with a Infinite 200pro (Tecan Trading AG, Switzerland) every hour for 5 hours. Plate incubated at 37C with shaking with final OD600 reported. Treatment groups were compared to vehicle, 100% Ethanol, 1% final well concentration, further referred to as “No Treatment”. 1mM stock of solvated in 90% Ethanol was prepared and stored at 4C.

4.2 Detection of AI-2 with biosensor *V. harveyi*.

Strains:

Clostridium innocuum from DSMZ, *Ruminococcus lactaris, Bacteroides caccae, Bacteroides uniformis, Bacteroides ovatus, Bacteroides volgatus, Bacteroides thetaiotaomicron, Parabacteroides goldsteinii* strain JCM 13446, *Lactobacillus reuteri, Enterococcus faecalis, Bacteroides eggarti, Bacteroides sterosis* were selected for the putative presence or absence of *luxS* in their genome. Strains were cultured from glycerol stock in 5mL Brain and heart infused media (BHI) or RCM media in an anaerobic tent at 37C for 24 hours or 48 hours. Escherischia

coli MG1655_Δ*lsrK* was used as a positive control and was cultured at 28C overnight in Lysogeny Broth, LB; (10g NaCl, 10g Peptone, 5g Yeast Extract per liter). Conditioned media was filter sterilized with a hydrophilic 0.20 uM filter, Chromafil (Macherey-Nagel, Germany). *Vibrio harveyi* strain TL26 was used as a biosensor to detect the relative concentrations of AI-2. 10% Conditioned media was used to induce *V. harveyi* in a background of fresh LM. *V. harveyi* was grown overnight at 28C in LM, then diluted 1:100 in fresh LM for the detection assay.

AI-2 Detection Assay:

The methods used are revised from the current gold standard developed by Bassler BL et al. (1993) and validated in many systems (Rajamani S and Sayre R. 2018), including human saliva and feces (Raut N 2013). I validated *V. harveyi* TL26 responds to synthetic AI-2, aqueous from Carbosynth and compared it to AI-2 synthesized by *E. coli* MG1655. The aim here was to determine if there are differences in growth and bioluminescence induced by synthetic vs. *E. coli* synthesized AI-2. Briefly, all strains were grown overnight in 5mL fresh media at 30C and 300 rpm, while in London, otherwise grown without shaking. *V. harveyi* were diluted 100x in fresh media. AI-2 synthesizing *E. coli* media was filter sterilized. *V. harveyi* was incubated with 10 uL of various concentrations of AI-2 (2.5 uM - 160 uM) diluted in LM or dilutions of conditioned media from *E. coli* MG1655_Δ*lsrK* , or *E. coli* MG1655_Δ*lsrS*Δ*lsrR* conditioned media (1x, 0.5x, 0.25x). Both luminosity and OD650 were taken every 30 minutes for 4 hours. Luminosity values were normalized to cell density, luminosity/OD650 or OD600. Density measurements were taken on a Versamax Microplate Reader, by Molecular Devices. Luminosity measurements were taken on FLUOstar Omega, by BMG Labtech using on-platform settings for luminosity or Infinite 200pro (Tecan Trading AG, Switzerland). It was noted that AI-2 had no impact on the growth of *V. harveyi*, which is contrary to reports that observed a possible growth reduction of 30% of induced cultures compared to a non-induced. Secondly, *E. coli* MG1655__Δ*lsrK* induced faster proliferation in all three *E. coli* K-12 strains tested compared to synthetic and AI-2, but no change in growth was noted in *V. harveyi*. There was not enough time to assess the molar output of AI-2 by *E. coli* during this phase of the project; therefore, only synthetic AI-2 was used in later experiments.

Conditioned media of gut strains were filter sterilized media, 0.2 micron, was added to 180 uL, 10%, of 1:100 diluted *V. harveyi* in a 96 well plate. 10% of BHI, RCM, or LB media used to grow isolates was used as a negative control. 200uL reactions were halved by aliquoting 100uL to a black 96 well plate from the clear polystyrene plate in which the reactions were mixed. OD600 and luminosity measurements were taken every hour for 5 hours on an Infinite 200pro (Tecan Trading AG, Switzerland). Luminosity was calculated by normalizing the luminosity measure to the OD600 (“luminosity”=Luminosity/OD600). All reactions were completed in triplicate. Treatments were matched with media or vehicle control concentrations. Bacteria were anaerobically cultured from 100uL of glycerol stock at 37 C without shaking for 24 hours. At 24 hours, cultures were filter sterilized using a 0.2 uM filter and AI-2 production was determined using the *V. harveyi* biosensor.

For fecal extract (healthy female volunteer) and fecal ferment (healthy male volunteer), fecal samples were collected under ethics approval by a medical professionals in Vienna, Austria (healthy female patient) and Cork, Ireland (healthy male volunteer). The female's fecal extracts were from the same patient, premenopausal, at the high and low peaks of estrogen cycling. Viennese samples were collected and immediately frozen for later analysis. Frozen samples were thawed and a sample was diluted, 100mg fecal sample to 1mL LM broth and filter sterilized with 0.20 uM filter. Extracted samples were used to inoculate fresh V. harveyi cultures for a final well concentration of 10%. Samples were diluted additionally for 50%, 25% with LM for final well concentrations of 5% and 2.5% respectively. Cork samples were diluted 2:100 weight/volume in Basal Media and fermented, see following for preparation. 10 mL aliquots were taken at 0, 4, 16/19, and 24 hours. Post centrifugation, samples were filter sterilized and diluted to 5% final well concentration in the *V. harveyi* assay.

4.3 Screening of BPA or E2 as quorum quenching molecules using biosensor *V. harveyi.*

The methods used are revised from the current gold standard developed by Bassler BL et al. (1993) and validated as a system to detect quorum quenching by (Lu, Hume and Pillai 2004; Widmer et al. 2007). Briefly, *V. harveyi* TL26 was grown in fresh media overnight at 30C. Culture was 100x diluted, approximately 0.03 OD650, in fresh media the following day aliquoted, in triplicate, on to a 96 well plate, final volume of 200uL and split with a multichannel pipette between a opaque walled and a clear walled 96 well plate, final volume 100uL.

Concentrations ranging from 1nM - 1mM BPA, aqueous or DMSO solvated, and E2 100nM, 75nM, 50nM, 25nM, 10nM, 5nM) from a 1mM stock solvated in 90% Ethanol were tested. AI-2 and putative QQ molecules, BPA and E2, were added at the same time. OD650 or OD600 and Luminosity measurements were taken hourly. Luminosity scores were normalized for cell growth, where "Luminosity" = Lumens/OD600 or 650. BPA concentrations were chosen based on the tolerance of *V. harveyi* to BPA solvated in DMSO and hypothesized levels of exposure from canned food sources. AI-2 concentrations varied to match the molarity range of putative QQ molecules. 40uM AI-2 for 50uM QQ molecule and above, 25 uM AI.2 and 1uM AI-2 were used throughout the experimental trials. From this work it appears that 25uM and above best distinguish QQ molecules by concentration and QQ qualities.

4.4 Fecal Sample Preparation, Fermentation and Sequencing Pipeline

Fecal Fermentation

For the fermentations, fresh stool sample of a young healthy man was collected by a nurse, sealed with an oxygen depleting catalyst and immediately delivered to a 37C anaerobic cabinet. The sample was collected and delivered to the cabinet within 30 minutes. Stool was homogenized with a sterile spatula. 53g of stool was mixed with 300mL reduced and autoclaved PBS with 20% glycerol in a filtration bag, manually. Filtered stool was strained into a sterile beaker and then aliquoted into 15 mL falcon tubes (6 mL per aliquot, total volume 12mL, 18 tubes total). On average each falcon tube contains 2g/12mL (17% w/v) of fecal sample for a final 1% w/v feces used as bioreactor inoculum.

Cork samples were fermented in pH and temperature stabilized 200mL bioreactor fermentations. Fecal samples were incubated with Basal Media, BM; supplemented with arabinogalactan, pectin from apple, starch from potato, xylan from corncob, inulin from dahlia tubers along with porcine mucin, vitamin K, Haemin, see supplement, and was prepared the day of experiment, see Supplement for details. Ferments were maintained at constant 37C temperature, pH 6.8, and anoxic by Applikon Bioreactor platform. One liter of BM was prepared for 4 vessels, then heated on a hot plate to dissolve fibers. 200mL basal media was aliquoted into the vessels, with the exception of the amended media, then autoclaved. After autoclave, 200uM BPA-basal media was used to inoculate treated to each oxygen depleted, pH normalized (pH 6.8), vessels after autoclave for a final volume of 200 mL. Final concentrations, 25mL BPA 200uM stock, solvated in BM, was used for 25uM BPA. 3mL of 0.8g/12mL filter sterilized L-cysteine was then added to each vessel to further reduce the media. Bioluminescent experiments compared, L-Cysteine treated, fecal inoculated BM, to Autoclaved BM with and without BPA.

Prepared fecal sample inoculum were thawed in an anaerobic cabinet, then mixed to homogenize inoculum before adding 12mL to each bioreactor, for 1% fecal mass/volume initial inoculation. 10mL aliquots are taken at T= 0,4,16/19, and 24 hours. All aliquots were centrifuged at 3000g for 30 minutes at 4C. Supernatant and pellet are stored separately at -80C for further analysis. A total of two fermentations, technical replicates, were analyzed for community composition and AI.2 production using aliquots from the same stool sample.

Genomic Extraction:

Genomic material was extracted using DNeasy Blood and Tissue Kit, Qiagen, Germany, according to manufacturer's protocol. 16S amplicons were targeted with 515F Parada and 806R Apprill according to in house thermocycling protocol. Amplicons were then normalized using

SequalPrep™ Normalization Plate Kit, 96-well, Thermo Fischer Scientific Inc. Sequencing was performed on Illumina MiSeq, Illumina USA.

Sequencing Analysis Pipeline:

Sequencing data was processed as follows. Input data was filtered for PhiX contamination with BBDuk (BBTools, Bushnell B, sourceforge.net/projects/bbmap). Demultiplexing was performed with the python package demultiplex (Laros JFJ, github.com/jfjlaros/demultiplex) allowing 1 mismatches for barcodes and 2 mismatches for linkers. Primers were verified with the python package demultiplex (Laros JFJ, github.com/jfjlaros/demultiplex)allowing 2 and 2 mismatches for forward and reverse primers, respectively.Barcodes, linkers, and primers were trimmed off using BBDuk (BBTools, Bushnell B, sourceforge.net/projects/bbmap) with 45 and 49 bases being left-trimmed for F.1/R.2 and F.2/R.1, respectively. SSU rRNA gene sequences classified using SINA version 1.6.1 (https://www.ncbi.nlm.nih.gov/pubmed/22556368) and the SILVA database SSU Ref NR 99 release 138 (https://www.ncbi.nlm.nih.gov/pubmed/23193283).

Prepared DADA2 (https://github.com/benjjneb/dada2), were further analyzed in R version 4.0.2 using packages phyloseq version, Release (3.11)(McMurdie PJ 2013) and vegan version 2.4-2. (https://github.com/vegandevs/vegan/). Statistical analysis and figures were performed useíng R version 4.0.2 and packages (). See Supplement for documentation on code used in this thesis. Links to tutorials and references that informed the statistical methods are also documented. Source data for all experiments is available including summary statistics.

Bioinformatics:

Since the AI-2 produced by *Escherichia coli* K-12 was known to induce bioluminescence in *V. harveyi*, putative AI-2 producers were selected through phylogenetic analysis of *E. coli* K-12 luxS, AI-2 synthase using EggNog 4.5.1 (http://eggnogdb.embl.de/#/app/results?seqid=P45578).

4.5 Data Analysis.

All data analysis was carried out using R version 4.0.0, ggplot2 version 3.3.3 and Rstatix version 0.6.0. Final OD600 for various growth kinetic tests was used as a proxy for cell count. Final OD600 was normalized to sterile media absorbance. In processing bioluminescence data, cell count was normalized to the media blank absorbance at OD600. Relative light units (RLU) were calculated by dividing the bioluminescent raw reading by the normalized cell count. Data is expressed as a ratio of experiment to defined control (E/C). The mean of the ratio between replicates was then compared using Kruskal Wallis to determine if a significant difference existed in the dilution series. A Wilcoxon Pairwise Rank Test was then applied to determine which dilutions significantly differed from each other. Bonferroni Correction was used to adjust p-value for multiple hypothesis testing. 16S community data was analyzed with Rstatix version

0.6.0, phyloseq version 3.12, vegan version 2.5-7 packages. Bray Curtis distance was used to compare Beta diversity. PERMANOVA was used to determine if the difference was significant. Shannon, Inverse Simpson, Chao, and Observed diversity were used to measure Alpha diversity. Data was compared by treatment, incubation time, and trial using the Mann Whitney Test. Differential diversity by treatment was analyzed with the Wilcoxon Rank Test. Rarefied sequence depth was used for all analysis pipelines. See supplement for R code.

5. ACKNOWLEDGEMENTS

I would like to thank Dr. David Berry, Universität Wien, who gave me independence and the resources to pursue this hypothesis at the start of my studies. To Dr. Jovana Mijaljovic, Universität Wien, for her feedback on results during the course of this work, my thesis, and providing fecal samples of the healthy female volunteer. To Dr. Guiseppe Ercoli, University College London, for providing me space to do my proof of principle experiments when I ran into visa trouble in Austria. To Dr. Paul O'Toole, University Cork College, for his insightful questions, the opportunity to use his groups bioreactors and FACs for the fecal ferment. To Dr. Alexandra Ntemiri, University College Cork, for providing protocols and training for the fecal fermentations. To Dr. Karina Bivar Xavier, Instituto Gulbenkian de Ciencia, for providing *Vibrio* and *E. coli* MG1655 strains, without which this thesis would not have been possible. I would also like to thank Dr. Armin Resch, Universität Wien, for providing cloning advice and *E. coli* BW1365 strains. To Dr. Federico Baltar, Universität Wien, for allowing me to use his department's Tecan plate reader, without which this research would have been halted. To Dr. Isabella Moll, Universität Wien, for providing molecular tools unavailable in my division. To Dr. Petra Petjavic, Joint Microbiome Facility, for 16S sequencing and the opportunity to experience the sequencing pipeline first hand. To Dr. Bela Hausmann, Joint Microbiome Facility, for advice on R code and sequencing analysis. To Dr. Christine Hawkes, University of Texas at Austin, who first inspired my love for microbial ecology. To Dr. Andrea Gore, University of Texas at Austin, who gave me the opportunity to get my first taste of research and the exciting field on neuroendocrinology during my Bachelors and the experience which gave the foundation for this thesis. Lastly, I would like to thank the Gut Group for support and curiosity about my hypothesis.

6. RESULTS

6.1 Differential Impact of E2 and BPA Treatment by Species and Strain.

6.1.1 *E. coli* demonstrates induced growth and resilience with BPA incubation, retardation of growth in *V. harveyi.*

Differential resistance to an environmental chemical could result in a niche favoring one community composition over another. While direct impact of BPA on bacteria has been previously tested by Rasheed et. al (2013), here I explored concentrations in the range of possible human exposure, which are the focus of this thesis. Hence, this work builds on this data using concentrations between 1nM and 1mM with 5 strains: *Vibrio harveyi* TL26 and 4 strains of *E. coli* MG1655 and *E. coli* BW1365 deficient in various genes in the AI-2 signaling pathway, see Strains in Methods. *Enterococcus faecalis*' growth was also analyzed under exposure to BPA (aqueous) at 100nM to 100uM.

Due to the poor solubility of BPA, molar concentrations of BPA higher than 1mM obscured OD650 measurements due to the resulting opacity of the amended media. After 6 hours of incubation, reaction triplicates were pooled to inoculate fresh media, 1:1000, and agar plate and incubated overnight. In this method, it was assumed that total viable cells after BPA incubation relates proportionally to the final OD650 and colony forming units(CFU) on plates after dilution and overnight incubation. No growth was interpreted as the possible bactericidal nature of BPA and less growth bacteriostatic impact of BPA treatment. Optical Density at 650nM (OD650) and colony count on plates were in agreement. Figure 4(a) shows the final OD650 of overnight cultures. It was found that the threshold tolerance for *E. coli* species was between 2.5 and 5mM BPA, E. coli_WT was more tolerant than either *E. coli* MG1655_Δ*lsrS*Δ*lsrR* or *E. coli* MG1655_Δ*lsrK* to BPA. At higher concentrations, above 1mM, *E. coli* MG1655_Δ*lsrS*Δ*lsrR* was more susceptible to BPA growth retardation than the other strains, and compared to 1% DMSO, vehicle. Since the final OD650 of all strains were comparable to growth in vehicle control, DMSO, the differential growth between strains by treatment may be attributed to differential response to BPA. BPA was found to be bactericidal for *V. harveyi* at 1mM BPA, as no growth was observed after incubating the treated cultures in fresh unamended media in liquid or plates.

Tolerance to BPA (1nM to 1mM) in aqueous conditions, BPA(aq), was compared to BPA solvated in DMSO by incubation of *V. harveyi*, *E. coli* BW25133 (WT, _Δ*lsrK,* _Δ*lsrR,* _Δ*luxS)* with BPA(aq) solvated into LM or LB, respectively. *V. harveyi* growth was significantly inhibited at 1mM, p-value = 0.012 compared to unamended LM and no growth inhibitions was observed at BPA 50uM and below. Interestingly, *V. harveyi* tolerance was one fold higher in incubations with

1% DMSO background, where BPA 1mM but not 100uM, significantly inhibited growth, p-value = 1.1e-11 see Figures (4(c) DMSO) and (4(d) BPA(aq)). Differences in response to BPA based on vehicle was also observed in *E. coli*. Interestingly, at concentrations of BPA below 100uM, the growth of *E. coli* MG1655_WT in DMSO significantly stimulated; In contrast, this was not observed in, *E. coli* BW25133_WT incubated without DMSO, where no significant effect of BPA (5uM-100uM) was observed, Figures 4(b)DMSO and 4(e)BPA(aq). Both *E. coli* BW25133_Δ*lsrR* and BW25133_Δ*luxS*, showed significant growth induction in the presence of BPA(aq) relative to no treatment. The relationship between BPA concentration and growth was positively correlated in *E. coli* BW25133_Δ*lsrR,* Figure 5(a), but negatively correlated in BW25133_Δ*luxS*, Figure 5(b). In this strain, significant growth induction was observed only at lower BPA concentrations (5uM - 25uM). No changes in growth rate were observed *E. coli* BW25133_Δ*lsrK,* see Figure 5(c). At high concentrations, ΔlsrR/ΔluxS growth was inhibited compared to WT and Δ*lsrK* at the same concentration. At lower concentrations, Δ*lsrR* or Δ*luxS* showed growth induction while WT and *lsrK* did not. It is important to note that *E.coli* BW25133 instead of *E. coli* MG1655 was used in BPA(aq).

Only one gut isolate, from mouse, *Enterococcus faecalis* was successfully cultivated and analyzed for tolerance of aqueous BPA up to 100uM. The isolate was incubated at 37C in an anaerobic tent and growth monitored over 6 hours with a plat reader. As depicted in Figure (6). BPA appears to have no influence on the growth of *E. faecalis* under these experimental conditions.

Figure 4(a-e). Final growth after 24 hours incubation of pooled BPA (1mM - 25mM) *V. harveyi* and various strains *E. coli* K-12 (4(a)) Final OD650 of *V. harveyi tl26,* and *E. coli MG1655* strains deficient in the AI-2 signaling pathway(4(b)) and final OD650 of *E. coli* MG1655_WT in 1mM-1nM BPA (DMSO) 4(c). growth of V. harveyi in 1nM to 100uM BPA. 4(d). Final OD600 of *Vibrio harveyi* TL26 with BPA (1nM-100uM) solvated in LM media. 4(e). Final OD600 of *E. coli* BW25133_ WT T5 OD600 with BPA (5nM-100uM) solvated in LB media. Box plots below are the average of triplicate over 1-4 trials (specified).

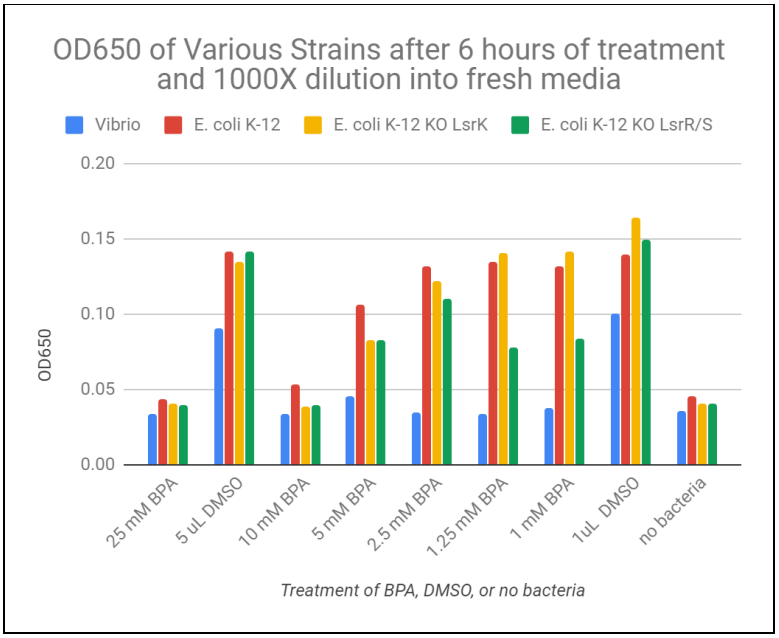

Figure 4(a). Final growth after 24hours incubation of pooled BPA (1mM - 25mM) treated *V. harveyi* and E. coli strains. Each treatment was measured once. *V. harveyi* is blue, *E.coli* MG1655_WT is red, *E.coli* MG1655__Δ*lsrK* is yellow, and E.coli MG1655__Δ*lsrRluxS* is green. Liquid media measurements agreed with counts on agar plates.

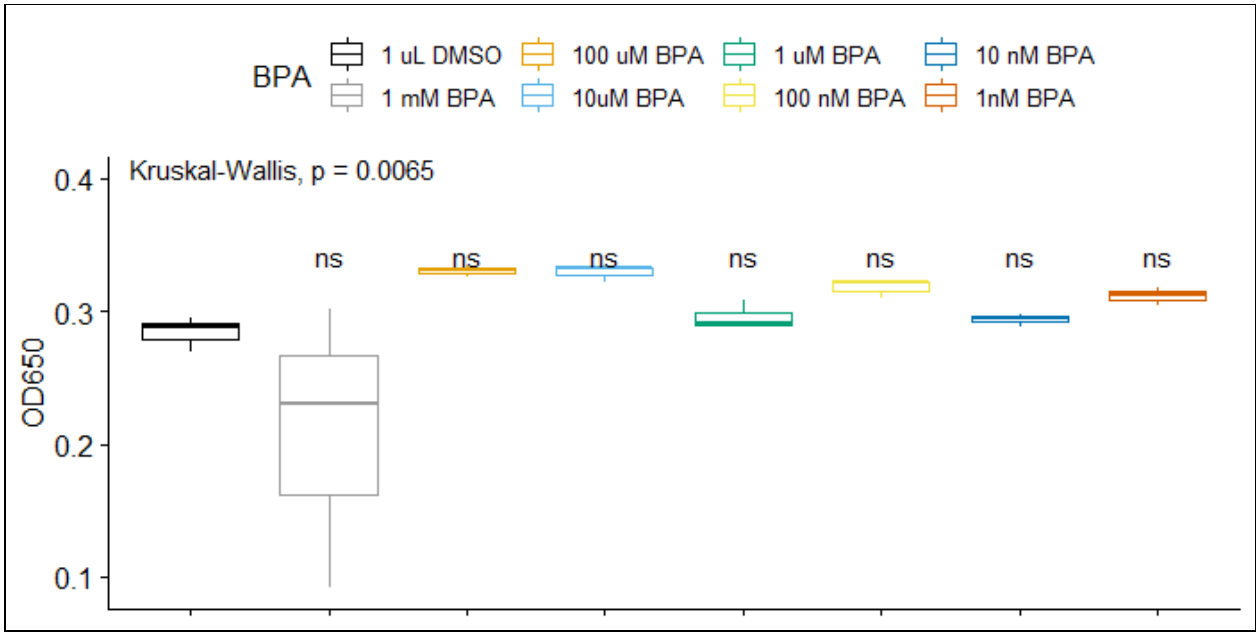

Figure 4(b) Final growth of E. coli MG1655_WT in BPA (1nM to 1mM), 1% DMSO, final well concentration. Kruskal-Wallis test compared mean final OD650 across all treatments, p-value = 0.0065. Final OD650 at 5 hours. p-values (*) ≦0.05 pairwise Wilcoxen paired test as compared to 1% DMSO solvent control. Wilcoxen paired test values corrected for multiple hypothesis testing using Bonferroni t-test adjustment. Box plots represent the standard deviation from the mean of n=3 technical replicates, one trial.

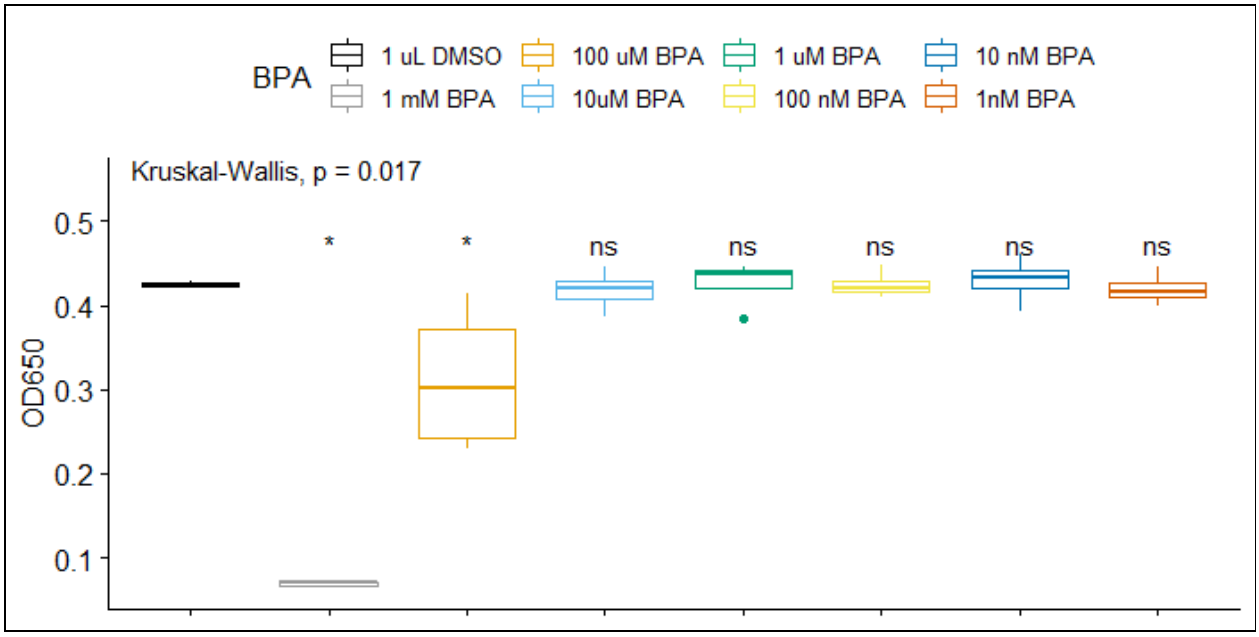

Figure 4(c). Final growth, OD650, of *V. harveyi* TL26 in BPA (1nM -1mM) BPA solvated in DMSO, 1%, 1uL DMSO, final well concentration. Kruskal-Wallis test compared mean final OD650 across all treatments, p-value = 0.017. Final OD650 at 5 hours. Only 1mM BPA showed significant effect on the growth rate of *V. harveyi* and where (*) p-value ≤ 0.05, compared to DMSO alone, black line, Wilcoxon Pairwise Test. Wilcoxon Pairwise Test values corrected for multiple hypothesis testing using Bonferroni

adjustment. 1mM BPA and not lower concentrations is bactericidal to *V. harveyi.* Box plots represent the standard deviation from the mean of n=4 technical replicates, one trial.

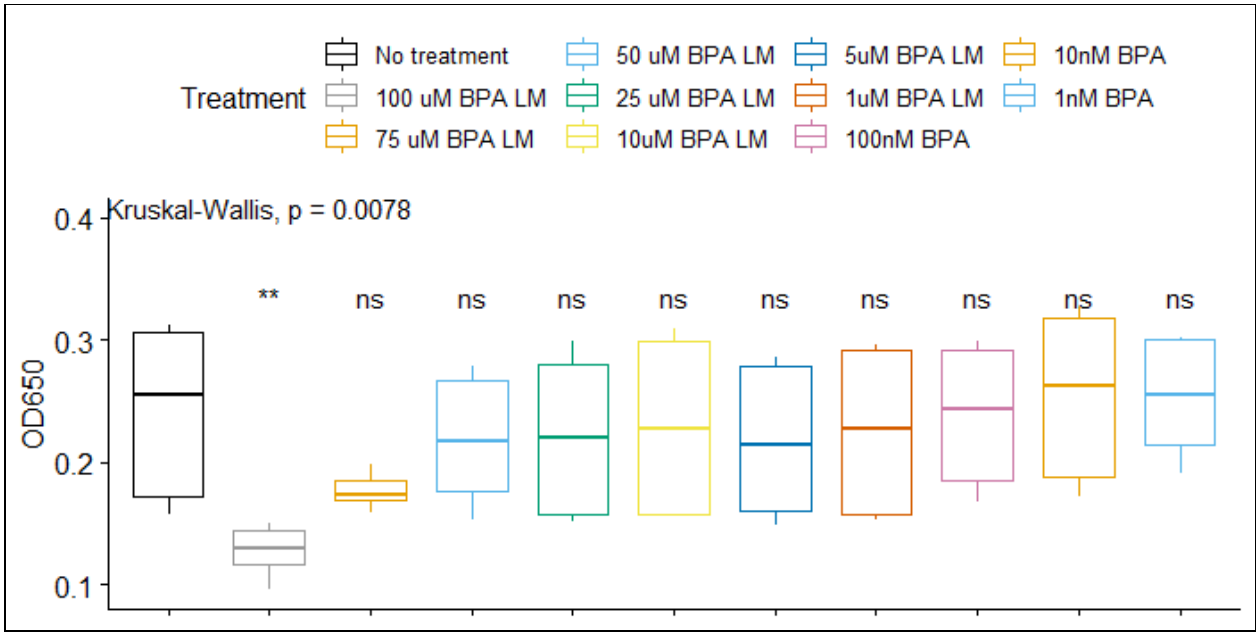

Figure 4(d) Final growth *V. harveyi* TL26, OD650, with BPA (1nM-100uM) amended media. "No Treatment" is unamended LM media. Kruskal-Wallis test compared mean final OD650 across all treatments, p-value = 0.0078. A trend towards a dose dependent response in growth inhibition is seen; however, only 100uM BPA treatment inhibits growth significantly compared to no treatment, p-value ≤ ** 0.005 . Wilcoxen values corrected for multiple hypothesis testing using Bonferroni adjustment. Box plots represent the standard deviation from the mean of n=6 technical replicates.

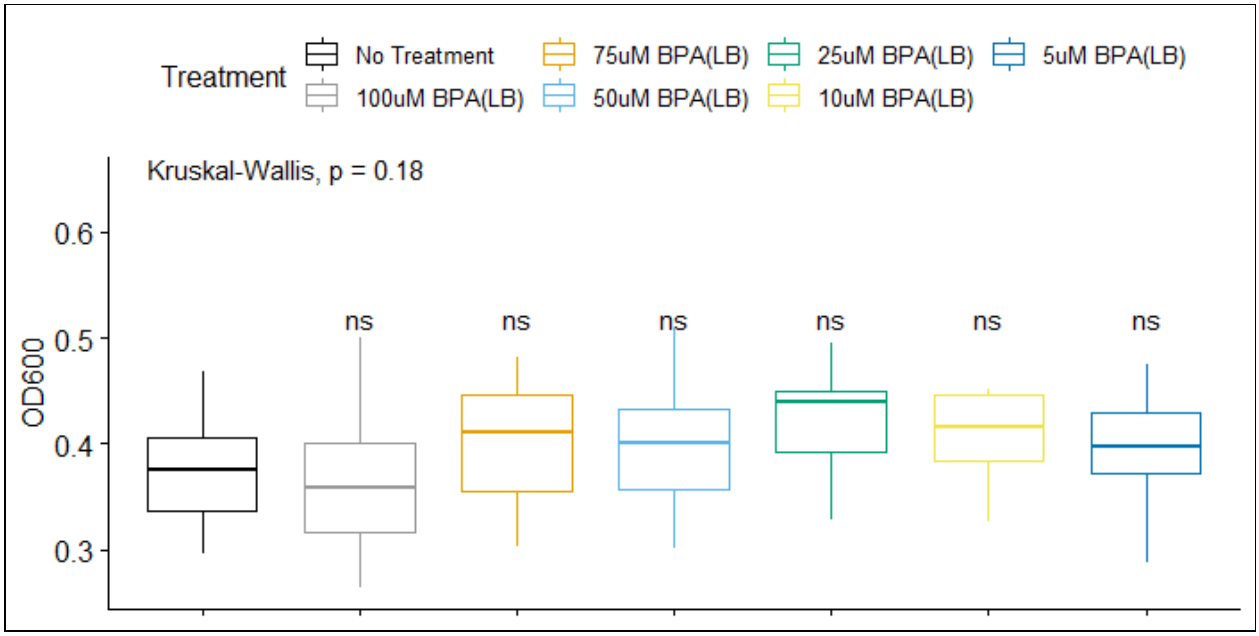

Figure 4(e) Final growth *E. coli* BW25133_WT. OD600 with BPA (5uM-100uM) amended media.. "No Treatment" is unamended LB media. Kruskal-Wallis test compared mean final OD650 across all treatments, p-value = 0.18. The significant growth induction observed when BPA is solvated in DMSO was not observed in aqueous solutions compared to no treatment, p-value > 0.05 (ns). Wilcoxon Pairwise Test values corrected for multiple hypothesis testing using Bonferroni adjustment. Box plots represent the standard deviation from the mean of 3 technical replicates, 4 biological replicates, n = 12.

Figure 5 (a-c).Three technical replicates and 4 biological replicates were analyzed for each treatment. The box plots represent the distribution over all replicates, final n = 12. Wilcoxon Pairwise Test compares each treatment to the “No Treatment”, unamended LB media. Wilcoxon values were corrected for multiple hypothesis testing using a Bonferroni adjustment. Kruskal-Wallis tested for significant difference across all treatments.

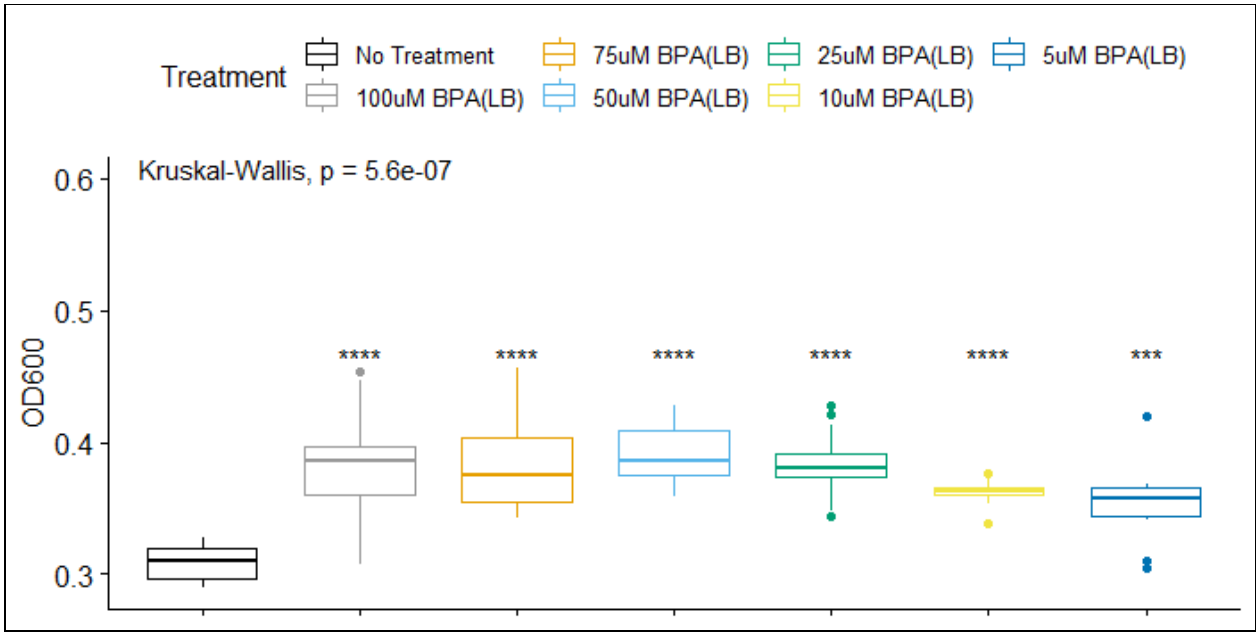

Figure 5(a). Final growth *E. coli* BW25133_Δ*lsrR* in BPA (5uM-100uM) amended media. Growth induction was observed at every concentration in the lsrR mutant. p-values≦ ****(1 e-4), ***(0.0005), in a dose-dependent manner. Box plots represent the standard deviation from the mean of 3 technical replicates, 4 biological replicates, n = 12. The Wilcoxon Pairwise test compares BPA treatment to LB only control, “No treatment”.

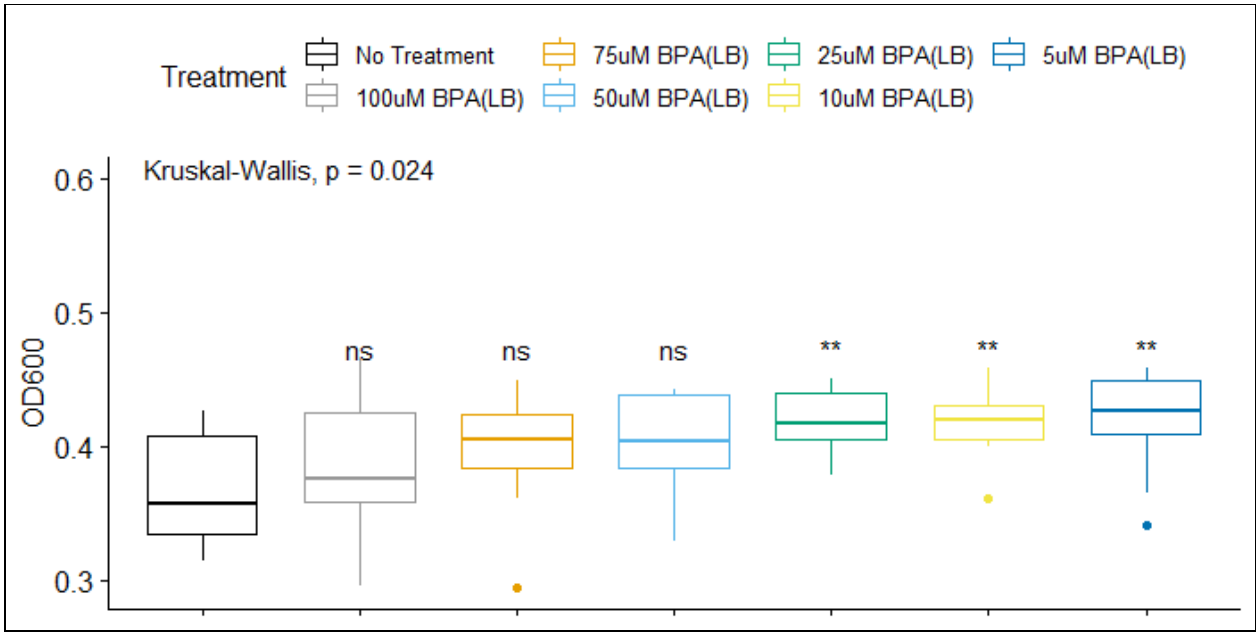

Figure 5 (b). Final growth *E. coli* BW25133_Δ*luxS* in BPA (5uM-100uM) amended media. No endogenous AI-2 expression due to luxS knockout and complete endogenous regulation due to presence of *lsrR* and *lsrK*. Box plots represent the standard deviation from the mean of 3 technical replicates, 4 biological replicates, n = 12. Wilcoxon Pairwise compares BPA treatment to LB only control, "No treatment".

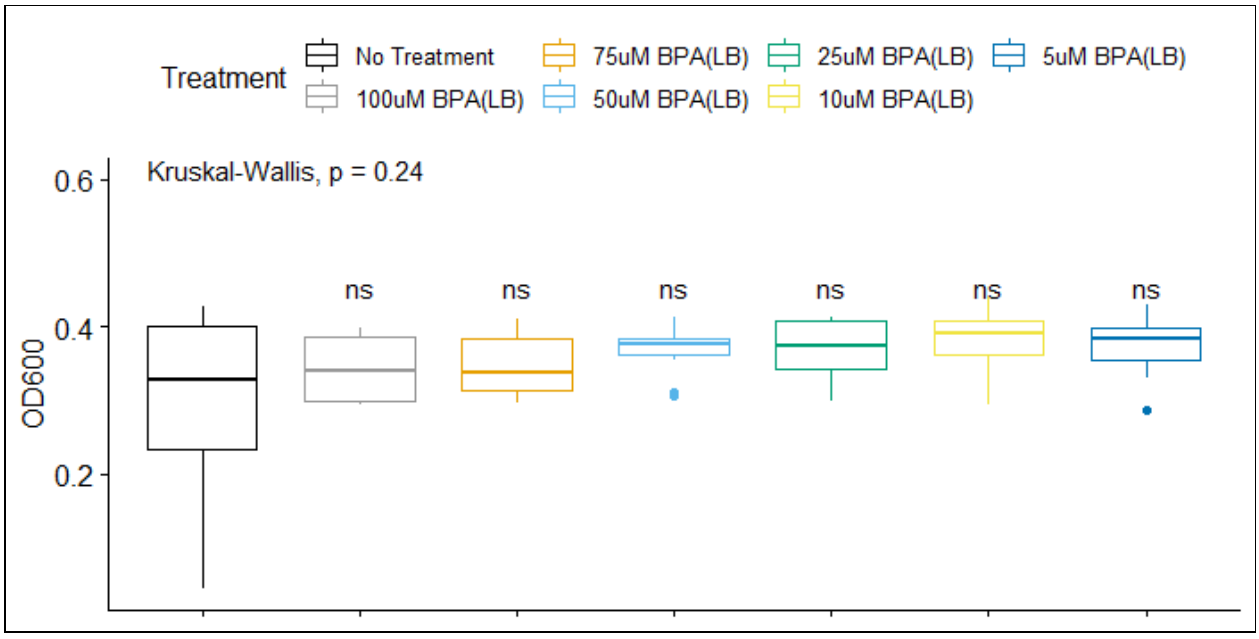

Figure 5(c). Final growth *E. coli* MG1655_Δ*luxS* in BPA (5uM-100uM) amended media. *E. coli* MG1655_Δ*lsrK,* deficient in transport plus AI-2 activation, *lsrK*, endogenous AI-2 and regulation pathway intact. AI-2 can diffuse across the membrane but has been shown to only accumulate in the media. No induction of growth was seen in this mutant, like the parent strain *E. coli* BW25133 at any treatment level compared to unamended control media p-value > 0.05 (ns). Box plots represent the standard deviation from the mean of 3 technical replicates, 4 biological replicates, n = 12. Wilcoxon Pairwise Test compares BPA treatment to LB only control, "No treatment".

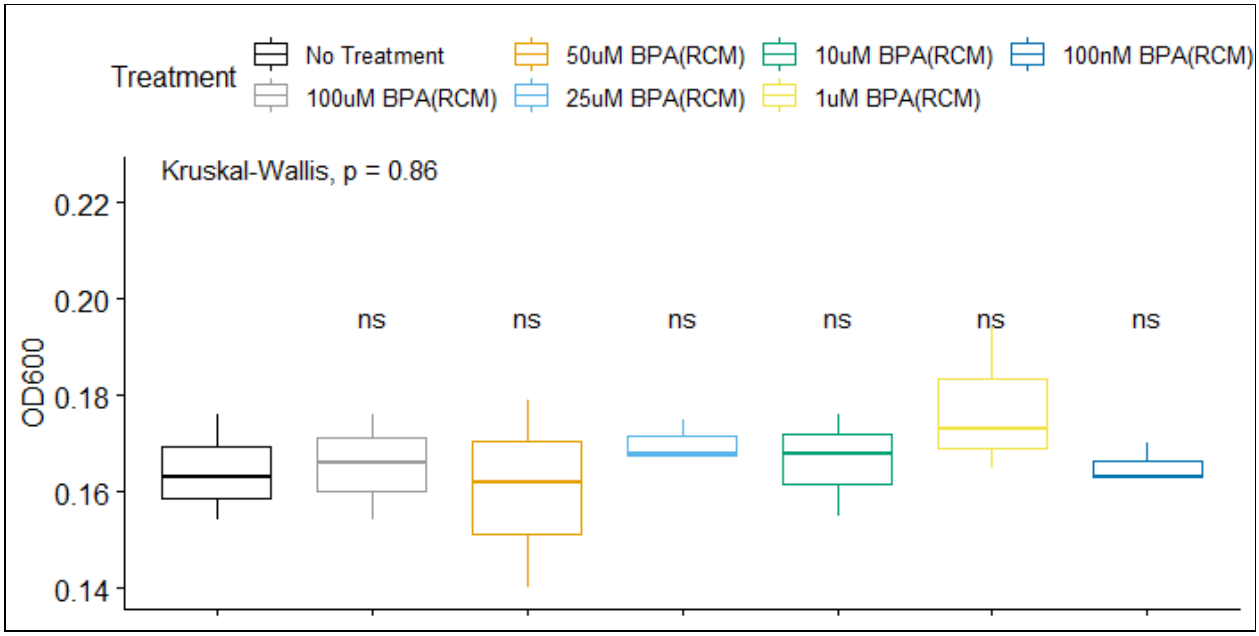

Figure 6. Final growth *E. coli* *E. faecalis* in BPA (100nM - 100uM) amended media. Graph of growth of mouse gut isolated *E. faecalis* anaerobically grown in Reinforced Clostridia Media amended with 100nM - 100uM BPA(aq) Time points were averaged over 5 measurements: n=3 for No treatment, only RCM, and BPA treatments, n = 3 for treatments (100nM-100uM BPA). Box plots represent the standard deviation from the mean of 3 or 6 technical replicates. All treatment levels were compared to unamended control media p-value > 0.05 (ns). Wilcoxon Pairwise Test compares BPA treatment to RCM only control, “No treatment”.

6.1.2 E2 effects *E. coli* growth differentially by strain

Bisphenol A is a xenobiotic which interacts with receptors responsible for estrogen signalling. Steric and chemical properties result in a 1000X lower affinity of BPA to ER**α** and ER***β*** than endogenous estrogens. If BPA has a direct impact on the physiology of bacteria as shown in the previous section, it is possible that endogenous estrogen in the gut may also result in a similar pattern on microbial growth. To investigate this question, I repeated the same assays for bactericidal and bacteriostatic effects of E2 on *V. harveyi* and various strains of *E. coli* BW25133 using endogenously relevant concentrations of E2**.** Similar to observations with BPA incubation, E2 treatment induced the growth of *E. coli* BW25133_Δ*lsrR*, but not any of the other *E. coli* strains tested, although this effect was not significant. An inverse relationship between E2 concentration and *E. coli* growth induction was observed. The growth of *E. coli* BW25133_Δ*lsrR* is correlated to E2 concentration in a non-linear dose dependent curve where a midpoint maximum growth was observed at 10-50nM, Figure 7(c). Growth induction at these concentrations was significant, p-value = 50 nM (0.0070), 10nM (0.0074). LsrR is a DNA binding protein that regulates the expression of the *lsr* operon. Interestingly, *E. coli* MG1655_Δ*lsrK* growth was inhibited at increasing E2 concentrations and was significant at 100nM E2, p-value (0.033), see Figure 7(b).

Figure 7(a-c). Final averaged growth, OD600, of *E. coli* BW25133 (WT, Δ*lsrR*, Δ*luxS*) and MG1655_Δ*lsrK* grown in the presence of 5nM-100nM E2. *E. coli* BW25133_WT Figure 7(a), *E. coli* BW25133_Δ*lsrR* Figure 7(b), Δ*luxS* (not shown), *E. coli* MG1655_Δ*lsrK*, Figure 7(c) Final OD600 was taken at 5 hours incubation.

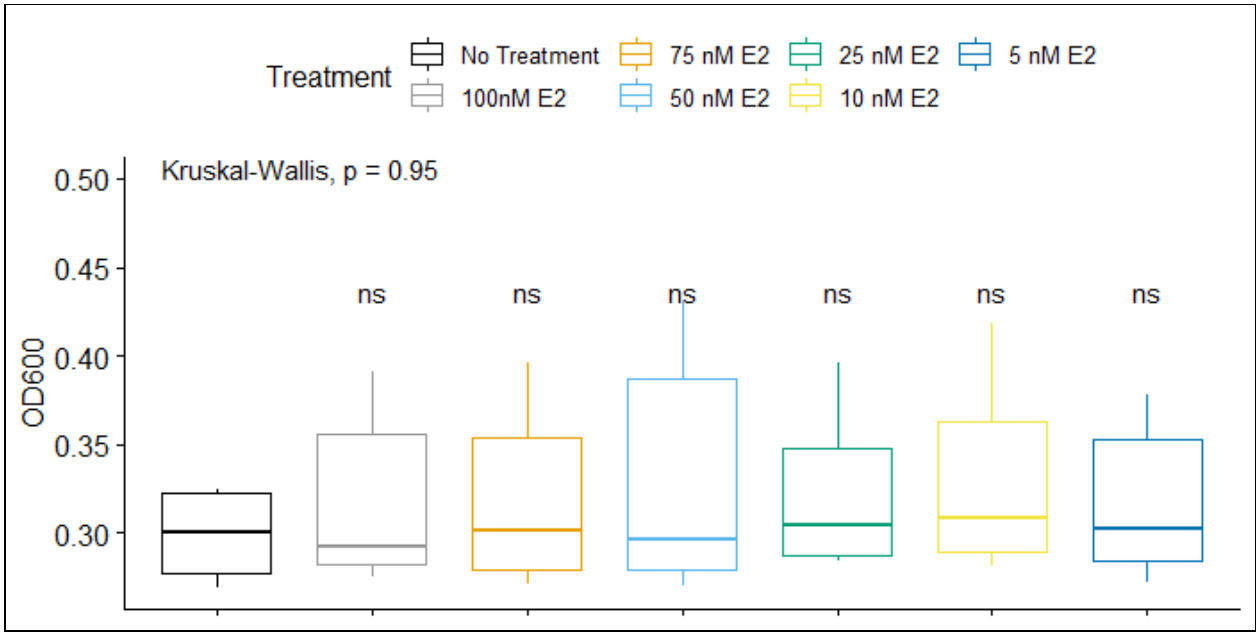

Figure 7(a). Final growth, OD600, of *E. coli* BW25133_WT in 5nM-100nM E2. Box plots represent the standard deviation from the mean of 3 technical replicates, 4 biological replicates, n = 12. All treatments were compared to unamended control media p-value > 0.05 (ns). Wilcoxon Pairwise Test compares E2 treatment to 1% Ethanol, "No Treatment".

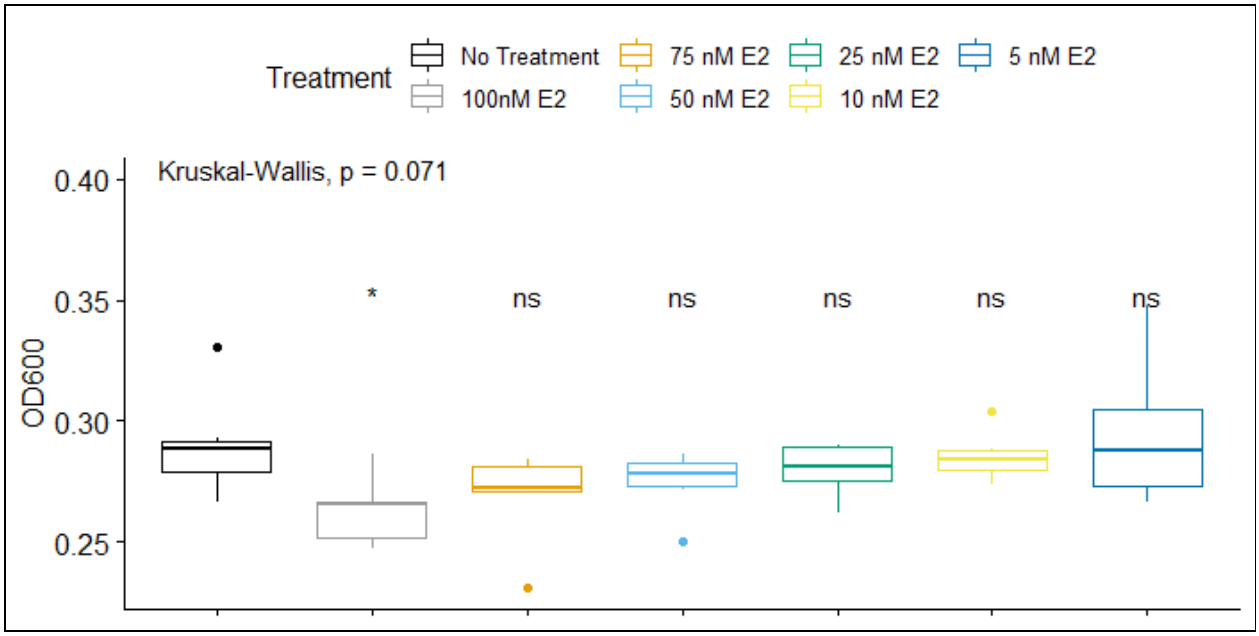

Figure 7(b) Final growth, OD600, of *E. coli* BW25133_Δ*lsrK* in 5nM-100nM E2. *E. coli* BW25133_Δ*lsrK* mutant lacks the ABC transporter and kinase of AI-2. Box plots represent the standard deviation from the mean of 3 technical replicates, 4 biological replicates, n = 12, p-value ≤ *(0.05). Wilcoxon Pairwise Test compares E2 treatment to 1% Ethanol, "No Treatment".

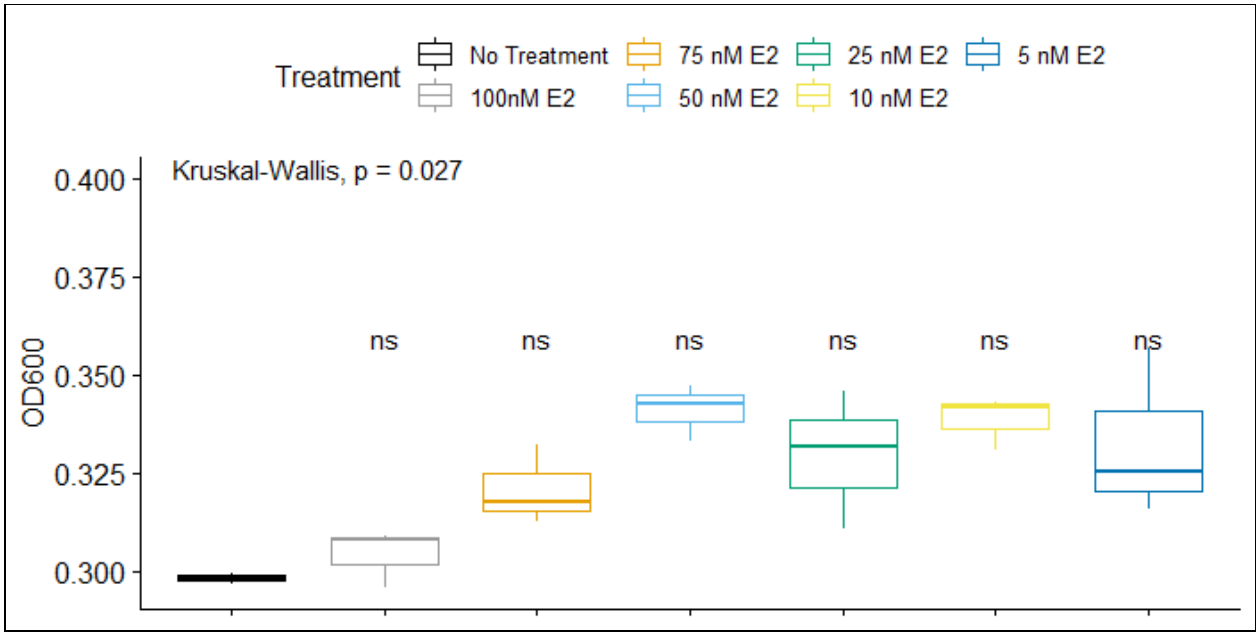

Figure 7(c) Final growth, OD600, of *E. coli* BW25133_Δ*lsrR* in 5nM-100nM E2. *E. coli* BW25133_Δ*lsrR* mutant allows for unregulated expression of the Lsr Operon. Box plots represent the standard deviation from the mean of 3 technical replicates, 4 biological replicates, n = 12, p-value > 0.05 (ns). Wilcoxon Pairwise Test compares E2 treatment to 1% Ethanol, "No Treatment".

6.1.3 E2 and feces from crest of estrogen cycling induce growth in *V. harveyi.*

A positive correlation between E2 5nM-100nM and final growth in *V. harveyi* was observed, where concentrations of as low as 10nM of E2 induced significant growth, p-value = 0.017. Pairwise Wilcoxon Test compared to 1% Ethanol control, see Figure 8(d). In addition, two fecal samples were collected at the predicted high, crest, and low, trough, points of the estrogen cycle from a young healthy female donor and presence of estrogen was quantified using LC-MS. Homogenized feces, filter sterilized, were used to inoculate *V. harveyi* at 10%, 7.5%. 5%, and 2.5% final well concentration. The sample from the predicted crest of estrogen (P1) of the estrous cycle induced an almost 2 fold growth in *V. harveyi* compared to the stool sample collected at the predicted estrogen trough. Wilcoxon Pairwise Test was performed on the final OD600 fecal extracts from both timepoints. Significant difference was found between *V. harveyi* incubated in fecal extract from peak E2 in the estrous cycle (P1), but not in treatment with fecal extract from the trough (P2), p-values =P1 10% (0.016), P1 7.5%(0.024), P1 5%(0.012), see Figure 8(c). LC-MS data of the fecal samples showed E2 concentration to be 40ng/g at the peak and was undetectable in feces at the predicted E2 trough. Given feces is mostly water, the molar concentration was approximately ~147nM. Flores et a. (2012) found similar concentrations of estradiol in feces, ~9ng/g feces. Fecal samples were subject to B-glucuronidase and unconjugated E2 concentration found in the LC-MS data could be different

before treatment. Although Flores et al. (2012) measured conjugated E2 to be ~3ng/g, or 25%. Indeed, growth of *V. harveyi* was observed in fecal samples from crest E2 of estrous and E2 amendment showed similar curves, see figures 8(a) and (b) for the growth curve comparison. Enhanced growth induction was noticeable at the first time point at one hour.

Figure 8: Growth Curves *V. harveyi* Incubated with Female Fecal Slurry (2.5-10%) or E2. (5-100nM).

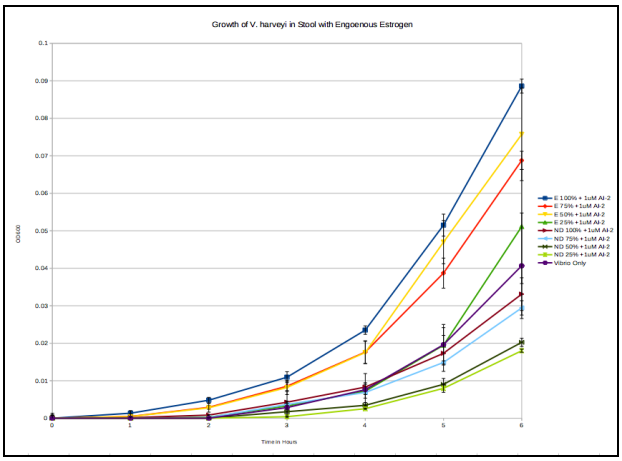

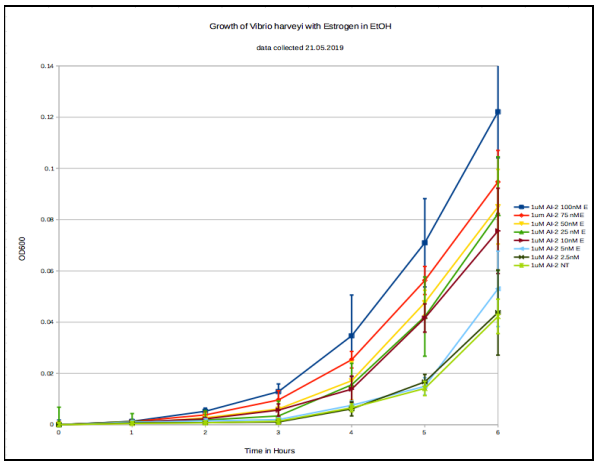

8(a) **8(b)**

FIgure 8(a) Blue, 1X Fecal Slurry Estrogen (FSE) or 100nM Estradiol; Red, 0.75X FSE or 75nM Estradiol; Yellow, 0.5X FSE or 50nM Estradiol; Green, 0.25X FSE or 25nM Estradiol; Dark Red, 1X Fecal Slurry (ND); or **8(b)** 10nM Estradiol; Light Blue, 0.75X ND or 5nM Estradiol; Dark Green, 0.5X ND or 2.5nM Estradiol; Light Green, Vibrio Only. Error bars represent one standard deviation from the mean of the technical replicates.

Figure 8(c-d) Box plots of the standard deviation of all the samples, where n = 6 for final OD600 of *V. harveyi* incubated in Fecal Extract(c) and E2(d) incubation.

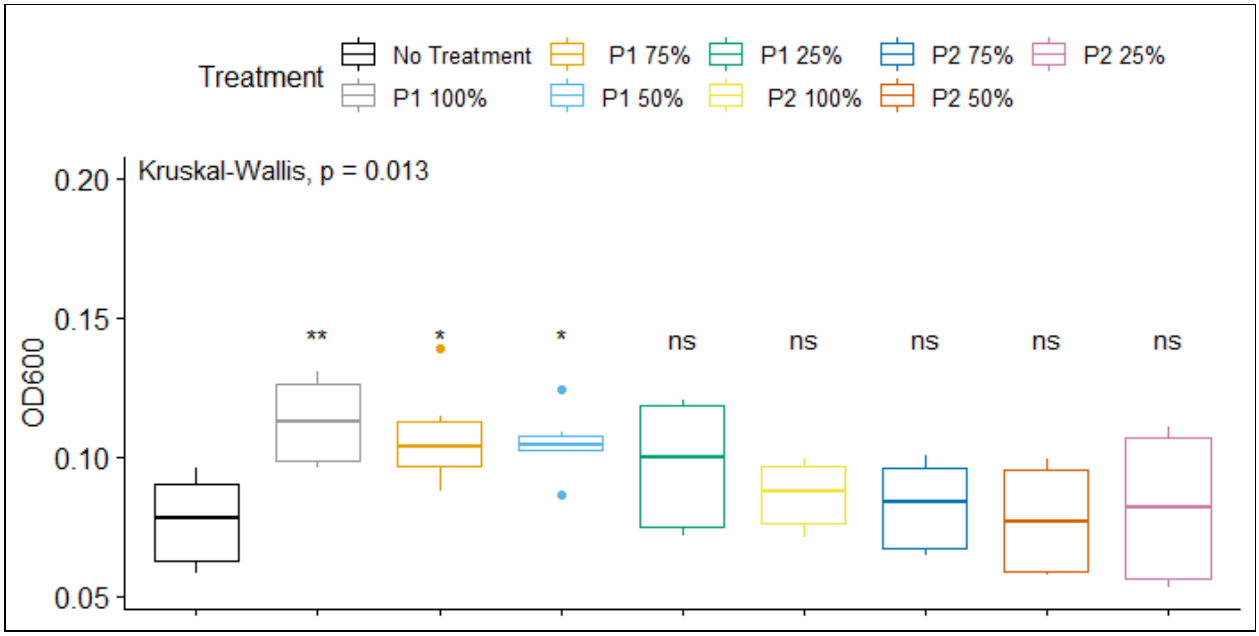

Figure 8(c). Final OD600 of *V. harveyi* incubated in 10% female fecal slurry. (P1 or 2 100%, or less. P1 samples were taken at volunteer's crest estrogen cycle. P2 samples were taken at the volunteer's estrogen trough. p-values = P1 10% (0.005**), P1 7.5%(0.020*), P1 5%(0.013*). Wilcoxon Pairwise Test compares fecal extracts to LM only, "No Treatment".

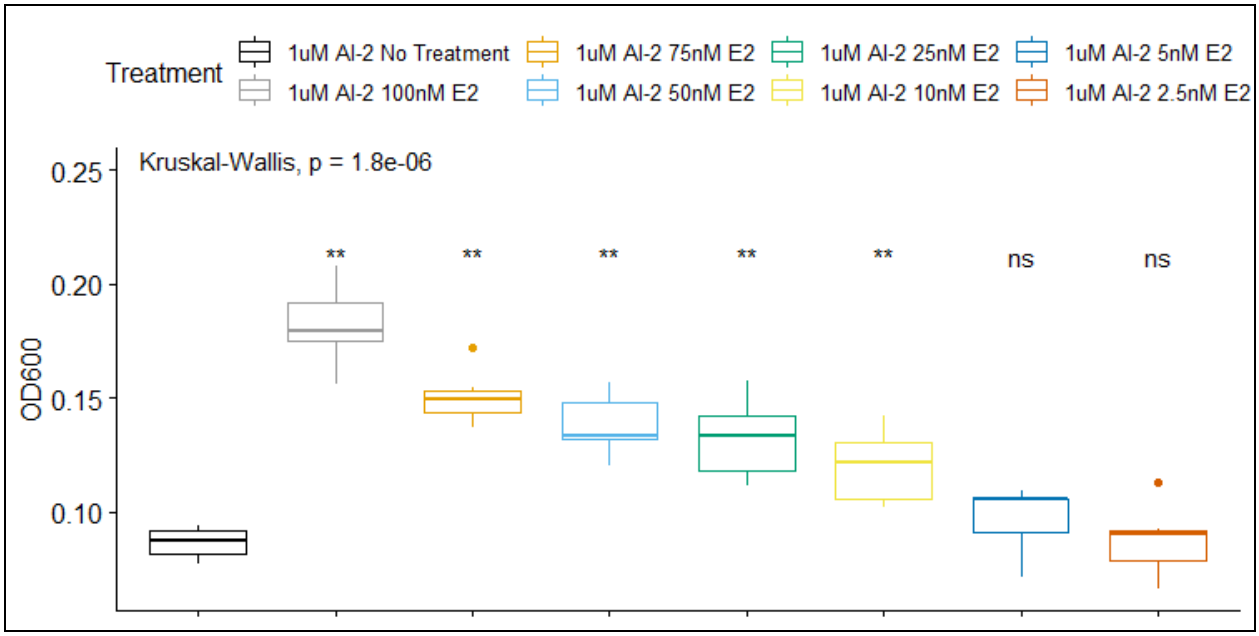

Figure 8(d). Final growth, OD600, *V. harveyi* incubated in 1% Ethanol and E2 (5nM-100nM). p-values≦ **(0.005). Wilcoxon Pairwise Test compares fecal extracts to LM only, "1uM AI-2 No Treatment". All samples were induced by 1uM AI-2.

6.2 Both Synthetic and *E. coli* synthesized AI-2 Induce Bioluminescence in *V. harveyi.*

Using the V. *harveyi* detection system, the bioluminescence production induced by synthetic AI-2 at known concentrations was compared to endogenous AI-2 synthesis by *E. coli* MG1655_Δ*lsrK*. The magnitude of luminosity did not increase proportionally to AI-2 molarity, but rather plateaued at 40 uM of AI-2. The fold difference in the highest concentration of AI-2, 160uM, was only 2.19 ± 0.10 fold higher than the bioluminescence induced by 2.5uM AI-2, see Figure 9(a). Hence, there may be a threshold of maximum induction by cell density. Compared to 2.5uM AI-2, conditioned media from the *E. coli* MG1655_Δ*lsrK* and ΔlsrR/luxS strains induced significantly less bioluminescence in *V. harveyi* (Figure 9(b.2)). To infer the molarity of AI-2 produced by *E. coli* MG1655_Δ*lsrK*, induction of bioluminescence from the 10% dilution was scaled by a factor of 10, 5% by a factor of 20, and 2.5% by a factor of 40 and compared to luminosity induced by 2.5uM synthetic AI-2(Figure 9(b.1)). All scaled measurements induce significantly more bioluminosity than 2.5uM AI-2, p-value ≤ 0.05. As expected, *E. coli* MG1655_ΔlsrR/luxS conditioned media did not induce bioluminesce in *V. harveyi.*

Figure 9(a-b). Comparison of growth(a) and induction of bioluminescence(b) by synthetic AI-2 and *E. coli* synthesized AI-2.

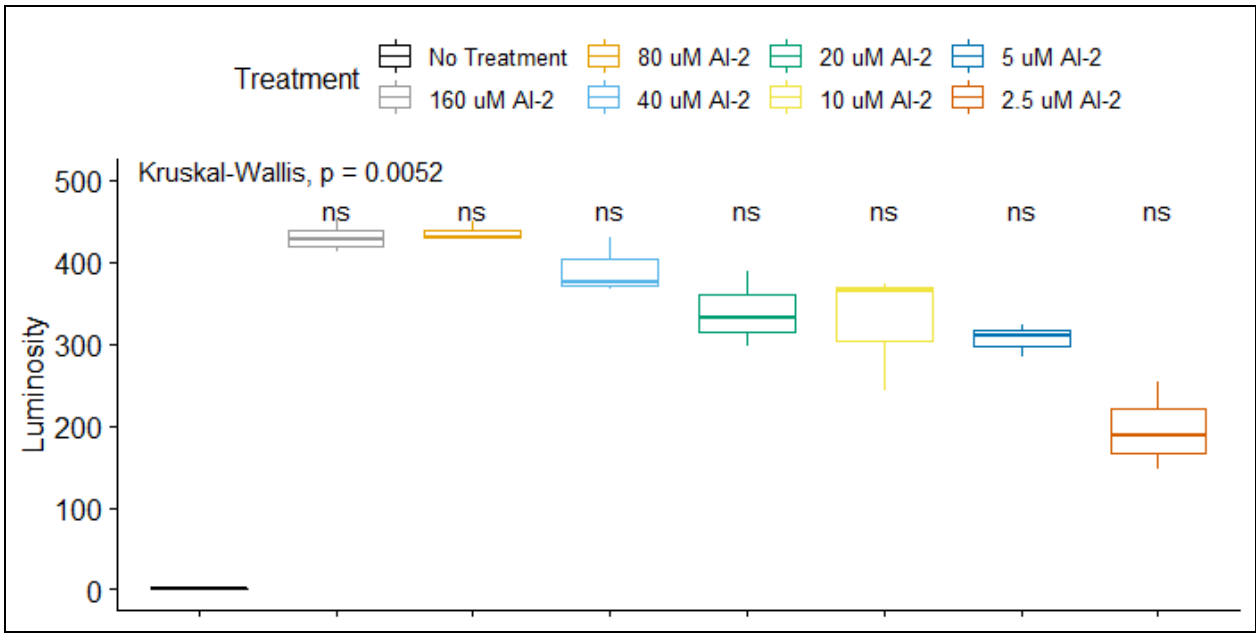

Figure 9(a). Bioluminescence induced in *V. harveyi* incubated with synthetic AI-2 (2.5uM -160uM). Box plot depicts standard deviation about the mean of 3 technical replicates (n = 3). Luminosity is a ratio between "No Treatment" and the luminosity measured in various AI-2 concetrations. Significant difference within the group, Kruskal-Wallis, p-value = 0.0052. Wilcoxon Pairwise Test for pairwise comparison of each condition to "No Treatment" where *V. harveyi* was incubated with fresh LM media. p-value > 0.05 (ns). Ratio of 160uM AI-2 to 2.5uM AI-2 is 2.2, while ratio 40uM AI-2 to 2.5uM AI-2 is 2.0.

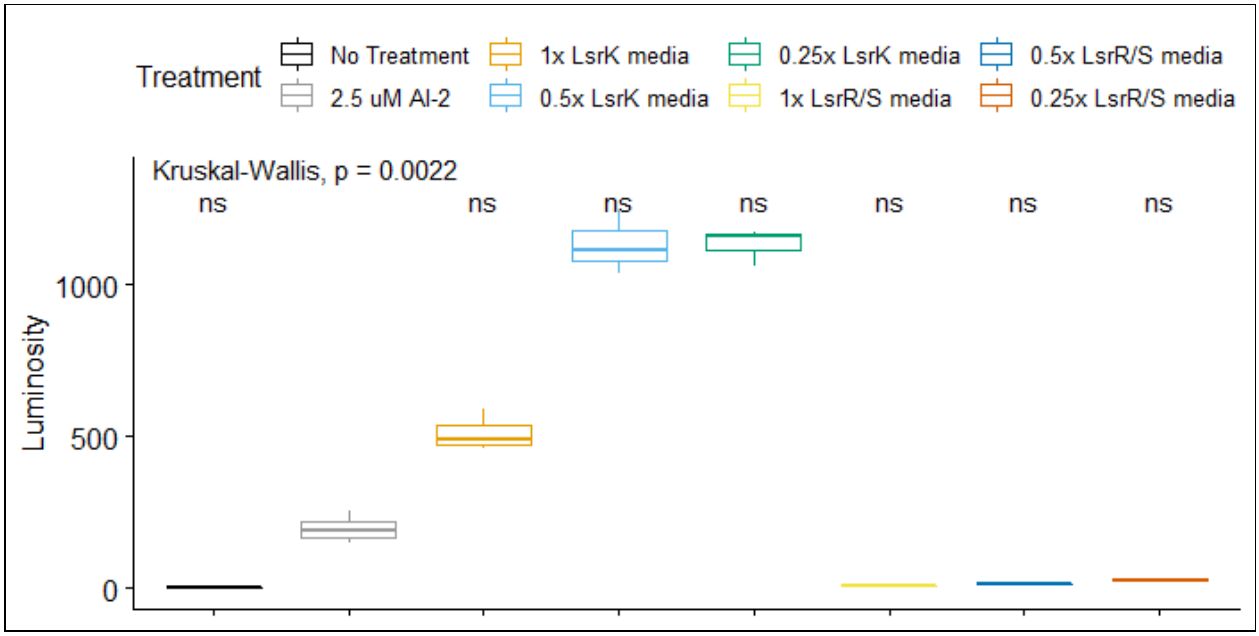

Figure 9(b.1)-scaled: Bioluminescence induced by E. coli conditioned media compared to synthetic AI-2. Strain *E. coli* MG155_Δ*lsrK* synthesizes AI-2 and *E. coli* MG155_Δ*lsrRS* does not. In this graph, bioluminosity values to estimate molarity of AI-2 in conditioned media is scaled proportionally. 1x, 0.5x and 0.25x respresent 10%, 5% and 2.5% final well concentration and were scaled by a factor of 10, 20, or 40 respectively. Both synthetic AI-2 and that synthesized by *E. coli* induced bioluminescence in *V. harveyi* TL26. Box plot depicts standard deviation about the mean of 3 technical replicates (n = 3). Significant difference within the group, Kruskall-Wallis, p-value > 0.05. Wilcoxon Pairwise Test for pairwise comparison of treatments are relative to 2.5uM AI-2. Not all Gut Strains with *luxS* make detectible AI-2.

6.3 Representative Gut Microbiota with *luxS* Induce Bioluminescence in *V. harveyi.*

Thirteen gut strains were cultured in BHI or RCM to determine if the presence of putative *luxS* homologue conferred production of AI-2 using *V. harveyi* biosensor. As expected, all isolates lacking *luxS* failed to induce bioluminescence. In order of decreasing magnitude, *R. lactaris>E. faecalis>>L. Reuteri*, *B. stercoris*, *B. eggarti* conditioned media induced bioluminescence in *V. harveyi* (see Figure 10a and 10b). Interestingly, the magnitude of bioluminescence induction was not comparable based on OD600 across bacteria tested. Instead, *L.reuteri* grew to the highest density followed by *E. faecalis*, *R. lactaris*, *B. eggarti* and *B. stercoris*. It is well known that AI-2 production occurs at different growth stages. It is also the case that at certain growth stages bacteria begin to uptake AI-2 at a faster rate than excretion. This could result in decreased induction of bioluminescence in V. harveyi (Xavier KB and Bassler BL 2005). *B. volgatus* was expected to induce bioluminescence, however, due to its poor growth in all trials, the amount of AI-2 may not have been sufficient to induce a response in *V. harveyi*. Cell density may be only one causal factor, as a significant increase in AI-2 concentration was observed in *E. coli* MG1655_Δ*lsrK* at similarly poor growth, specifically OD600 of 0.017, from previous experiments not shown here. The limit of detection of *V. harveyi* under these experimental conditions has been shown to be 400nM of synthetic AI-2 (Vilchez R 2007). This threshold, in the presence of metabolic inhibitors, or absence of a working *luxS* resulted in failed detection.

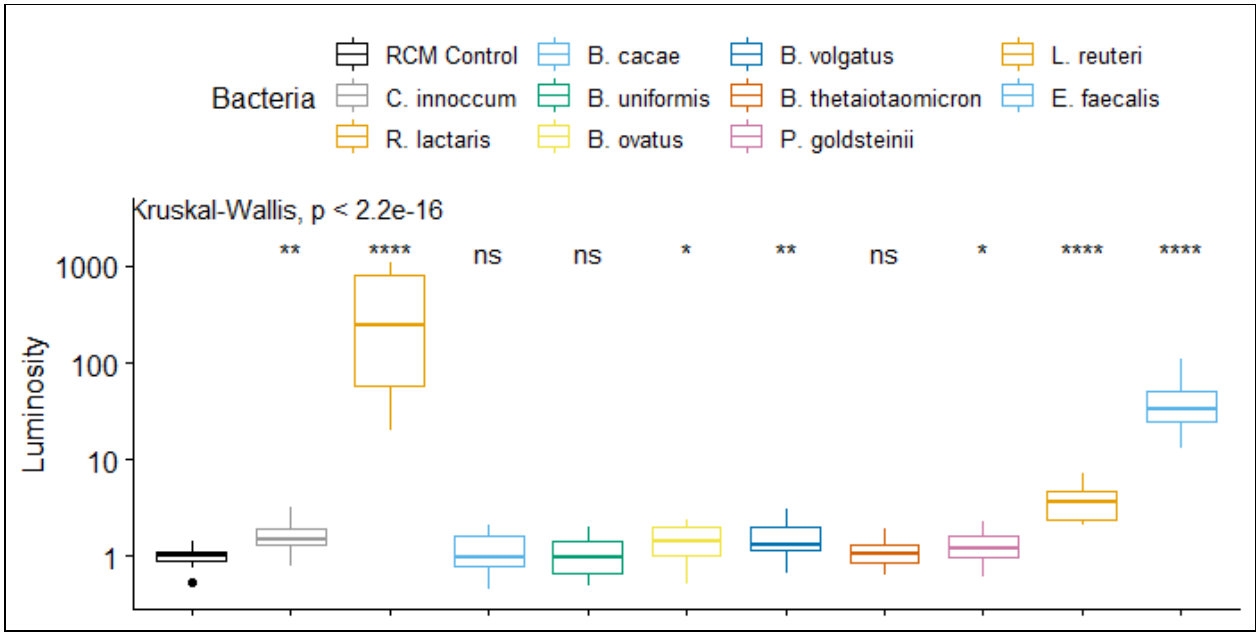

Figure 10(a) Bioluminescence induced by conditioned media selected gut microbes in *V.. harveyi.* Two biological replicates (conditioned media preparations) and 5 technical replicates (3 and 2 for each media preparation). Luminosity scaled, treatment/control, to luminosity induced by RCM media alone, "RCM Control". In order to compare induced luminosity, log10 of this ratio is reported. The Wilcoxon Pairwise Test compares conditioned media of various species to RCM alone, "RCM Control". p- values ≤ * (0.05), ** (0.005), *** (0.0005), and **** (5 e-5).

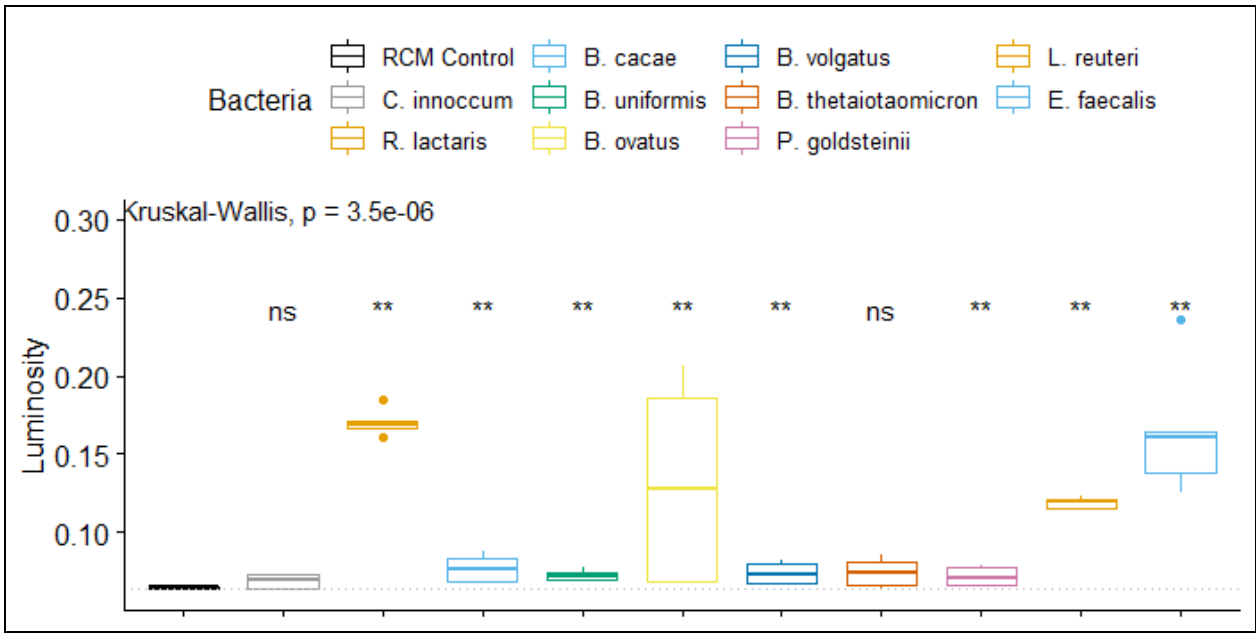

Figure 10(b) Final OD600 of gut bacteria from above after 6 hour incubation in RCM. Box plot is the average of two trials, measured in triplicate Dashed horizontal line marks the absorbance of RCM media alone at OD600. Wilcoxon Pairwise Test compares final OD600 to OD600 of RCM media alone, "RCM Control". p- values ≤ ** (0.005).

6.3.1 AI-2 production differential due to culture media and density of culture growth.

Diet is an important regulator of gut microbiota. To explore how AI-2 concentration varies relative to diet, a select group of gut bacteria were cultured in either Reinforced Clostridia Media (RCM) or Brain and Heart Infusion Media (BHI). Growth in BHI was 3-10X more dense compared to RCM for all cultured microbes. Although cultures in BHI media were denser, *R. lacteris* conditioned media induced luminosity 33.4 fold less than when grown in RCM media. This observation was specific to species, as *L. reuteri, B. eggarti* and *B. stercorsis* had more detectable AI-2 when grown in BHI (See Figure 11). Bioluminescence induction was not increased to the same magnitude as the observed growth. The primary differences between RCM and BHI are the presence of corn starch and 5 fold higher glucose concentration for RCM, where BHI is unique in its complexity of organ extracts. Fermentation of the starch and the presence of glucose in RCM could be reasons for the reduced AI-2 detection in this system for most of the species tested. Reduced media pH due to starch fermentation and residual glucose in the media are both known to inhibit AI-2 detection in *V. harveyi* (Turovskiy Y 2006).

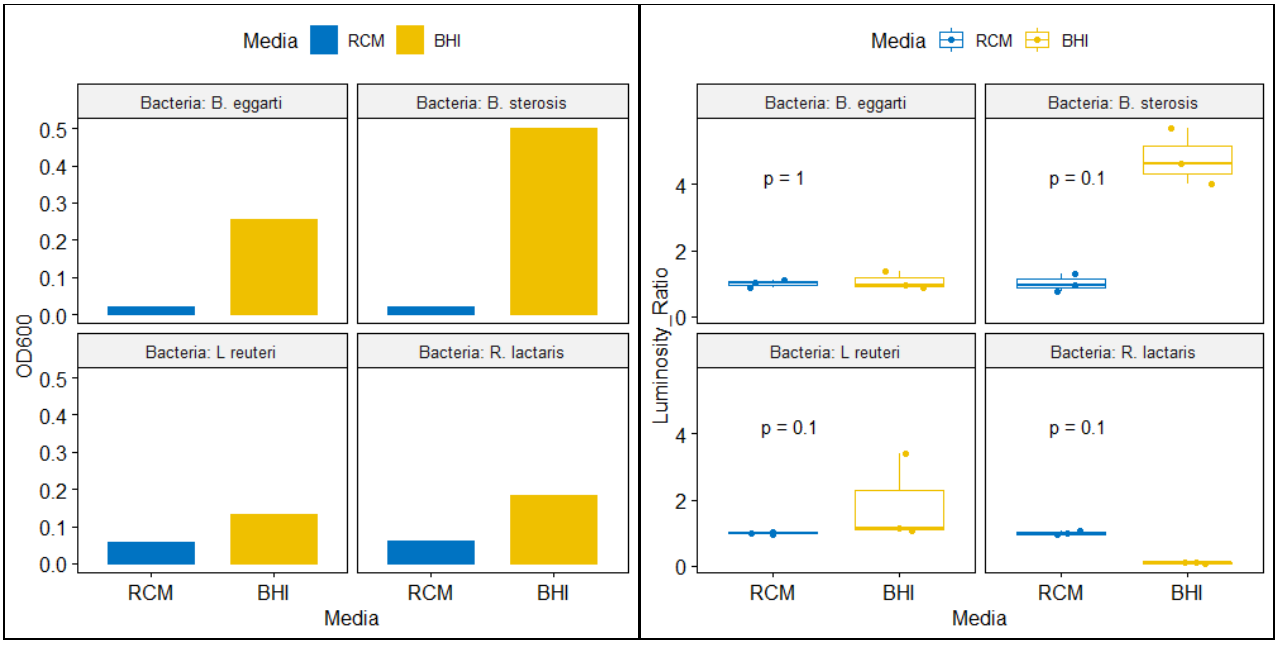

.

Figure 11. Barplot and box plot of gut bacterial density and bioluminescence induced by the same media in *V. harveyi*. Species averaged final growth for both conditioned media preparations taken at time of filter sterilization, left. Luminosity Score taken from normalizing Luminosity to biosensor growth. Luminosity_Ratio scores are scaled to the luminosity score of the respective fresh media and fresh media with *V. harveyi*, respectively. Reinforced Clostridia Media (RCM) and Brain and Heart Infusion Media (BHI)." p " is the p-value comparing the difference in luminosity induced by bacteria in RCM and BHI.

6.4 Differential Induction of Bioluminescence by Male and Female Fecal Samples

Since gut microbiota strains were shown to induce AI-2 regulated bioluminescence in *V. harveyi*, I hypothesized that AI-2 may be detectable in feces. Raut et. al 2013 found detectable AI-2 in stool, ileal washings, and saliva of IBD patients and healthy people's saliva, using bioluminescence in *V. harveyi* TL26 as a reporter. In my inquiry, I explored if healthy female and male feces had detectable AI-2. Samples from a healthy female volunteer were diluted in LM for dilution series for comparison. No induction of bioluminesce was observed without the exogenous addition of synthetic AI-2 from the female volunteer feces at either crest or trough of E2 cycling (data not shown). Enhanced bioluminescent signal when exogenous AI-2 was added was seen in samples collected at patient's crest E2 in her estrous cycle (P1). Interestingly, inhibition of bioluminescence was observed in all dilutions of samples taken at patient's estrogen trough (P2) and at 2.5% final well volume, from the estrogen crest (P1), see Figure 12(c).

The presence of AI-2 was also measured in a male volunteer fecal sample over 4 timepoints during fecal fermentation to compare the effect of 25uM BPA amendment on community composition and AI-2 production. AI-2 induction was determined as an increase in bioluminescence production in the presence of exogenous AI-2 relative to Basal Media (BM) L-cysteine was not controlled for in this experiment. The addition of AI-2 tests the ability of *V. harveyi* to detect AI-2 in the fecal sample matrix, as quorum sensing inhibitors could be present. In the male sample, significant induction was observed at T0 for both Control, unamended media (BM), and 25uM BPA amended media, p-value = Control (0.00076) and 25uM BPA (0.01094) compared to BM alone. Reduced bioluminescence in 25uM BPA was predicted due to treatment. At hour 4 of the incubation, no additional bioluminescence was measured from any of the fecal fermentations compared to BM. Interestingly, the fecal ferment treated with 25uM BPA profoundly induced bioluminescence at T16 and T24, p-value = 0.00021 and 9.7e-07, where no induction (T16/19) or less induction (T24) was observed in the Control ferment, see Figure 12(d). Inhibition of bioluminescence induction did not appear to occur in any of the male samples as was seen in the female fecal slurry. Growth of *V. harveyi* was inhibited at T16 and T24 in both Control and 25uM BPA treatment. Hence, the phenomenon of bioluminescence enhancement seen when samples are incubated with estrogen is not an expected explanation for increased AI-2 detection in the fecal ferment. This data suggested that incubation with BPA results in greater production of AI-2 in the human gut microbiome.

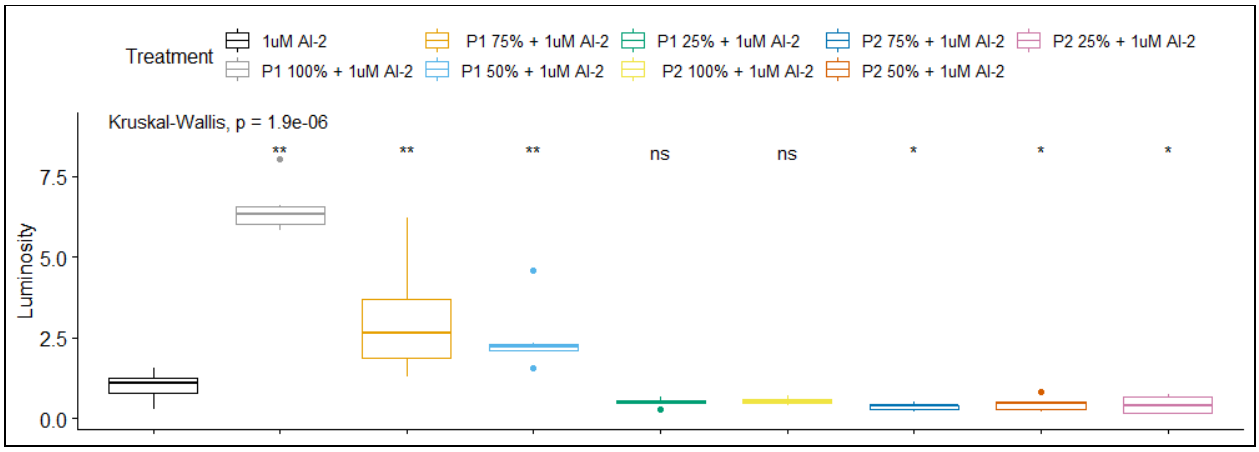

Figure 12(c) Bioluminescence induced by Female Fecal Extract in *V. harveyi*, 1uM AI-2 background. Serial dilution of fecal extract 100%, 75%, 50% and 25% relate to final well volumes of 10%, 7.5%, 5% and 2.5% respectively. Kruskal-Wallis Test was used to compare induced bioluminescence across all dilutions, p-value = 1.9 e-06. A pairwise Wilcoxon Test was used to compare individual samples to 1uM LM, p-values ≤ **(0.005), *≤(0.05). P-values for pairwise Wilcoxon were corrected with a Bonferroni Adjustment for multiple hypothesis testing. Box plots represent the standard deviation from the mean of 3 technical replicates and 2 biological replicates (*Vibrio*) for an n = 6.

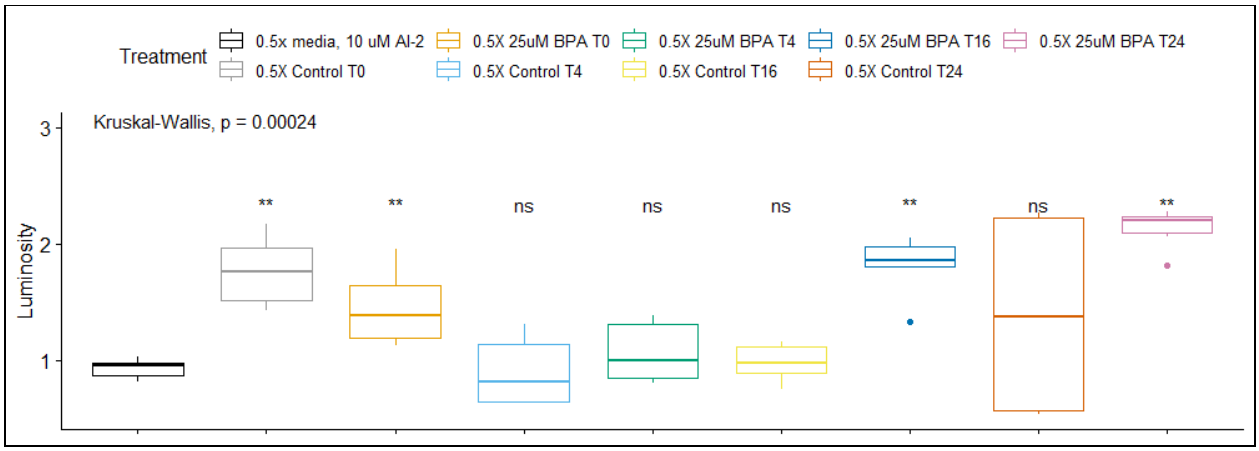

Figure 12(d) Bioluminescence induced by male fecal ferment overtime in *V. harveyi.* Note all samples induced by 10uM AI-2. Kruskal Wallis Test was used to compare induced bioluminescence across all time points, p-value = 0.00024, A pairwise pairwise Wilcoxon test was used to compare individual samples to 10uM AI-2 Basal Media, p-values ≤ **(0.005). P-values for pairwise pairwise Wilcoxon were corrected with a Bonferroni adjustment for multiple hypothesis testing. Box plots represent the standard deviation from the mean of 3 technical replicates and 2 biological replicates (*Vibrio*) for an n = 6.

6.5 Bisphenol A and Estradiol Quench Bioluminescence Induced by Synthetic and Metabolic AI-2.

6.5.1 Quenching of QS in *V. harveyi* by BPA solavated in DMSO and aqueous preparations.

V. harveyi TL26 was used as a model system to determine to what degree BPA influences quorum sensing through the measurement of bioluminescent output. Synthetic AI-2 was used to induce bioluminescence. Dosage-dependent quenching of quorum sensing was observed for both DMSO and aqueous preparations of BPA. For BPA solvated in DMSO, quenching was not significant at the highest dilution, 40uM BPA, a clear dose-dependent trend can be seen where higher concentrations of BPA vary with Luminosity inversely, see Figure 13(a). At concentrations lower than 10nM BPA solvated in DMSO, no significant difference was observed, see Figure 13(b). BPA appears to be a more potent QQ molecule when solvated in LM, as all concentrations (1uM - 100uM BPA) were observed to significantly quench bioluminescence, see Figure 13(c). Strength of the quenching signal was dependent on the concentration of AI-2 used to induce. When samples were induced by 25uM AI-2 the difference between control, 25uM AI-2 in LM, compared to 5uM BPA as was 57% ± 5.8, while induction with only 1uM AI-2 resulted in insignificant difference between control, 1uM AI-2 1% DMSO, and 5uM AI-2, 1% DMSO, 13% ± 39, see Figure 13(d) and 13(b) respectively. No enhancement of bioluminescence was observed at any concentration of the aqueous BPA preparation.

Figure 13(a-b) High (a) and low(b) levels of BPA solvated in DMSO. Luminosity is reported after normalization of lumens measured to cell density (Lumens/OD600) and expressed as a ratio between the treatment and control (Treatment/Control). Kruskal-Wallis Test was used to compare mean induced bioluminescence across all samples. The Wilcoxon Pairwise Test compares "Treatment", BPA solvated in and background AI-2, to "Control" (specified in each figure), background AI-2 and vehicle (1% DMSO). Bonferroni Adjustment was applied to all Wilcoxon Pairwise Test p-values to account for multiple hypothesis testing.

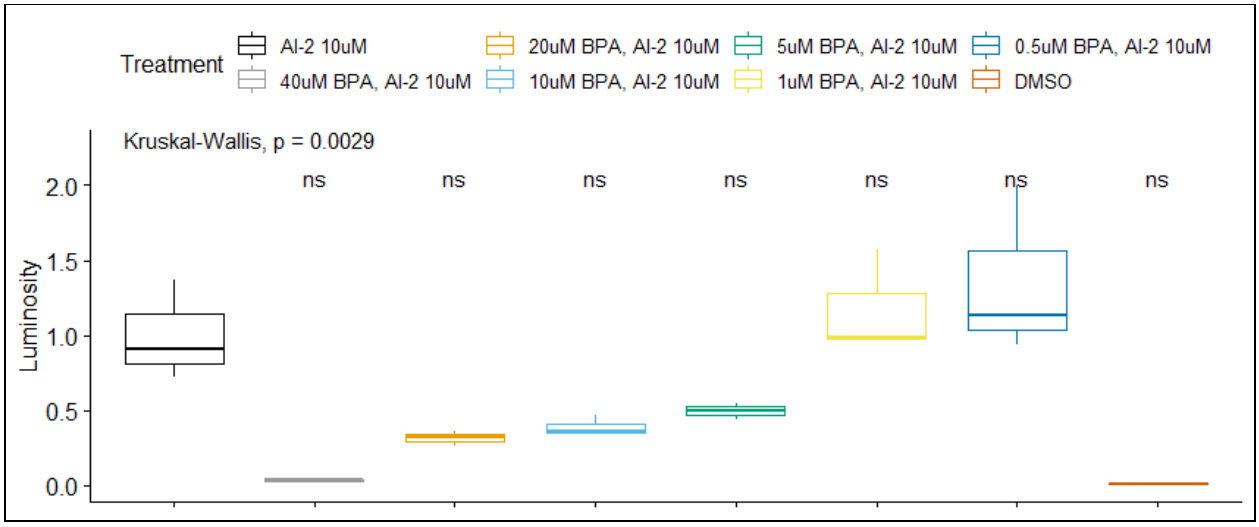

Figure 13(a) Bioluminescence of *V. harveyi* incubated with BPA (0.5uM-40uM) solvated in DMSO.. All samples tested have 1% DMSO. Box plots represent the standard deviation from the mean of 3 technical replicates, n = 3, where p-value > 0.05 (ns). The Wilcoxon Pairwise Test compares all treatments to luminosity induced by AI-2 10uM.

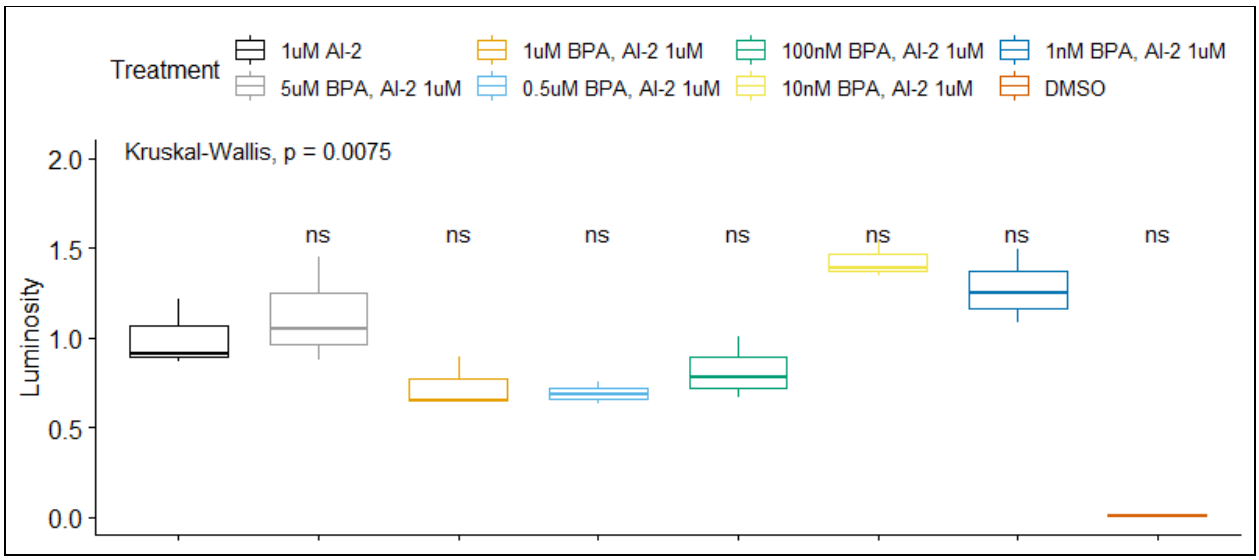

Figure 13(b) Bioluminescence of *V. harveyi* incubated with BPA (1nM-5uM) solvated in DMSO. All samples tested have 1% DMSO. Box plots represent the standard deviation from the mean of 3 technical replicates, n = 3, where p-value p-value > 0.05 (ns). Wilcoxon Pairwise Test compares all treatments to luminosity induced by 1 uM AI-2 amendment.

Figures 13(c-d) Aqueous BPA inhibition of bioluminescence. Graph (13(d)) is the growth curve of *V. harveyi* over the full 5.5 hours of incubation and graph (13(e)) highlights time point hour 5.5 where the greatest difference is seen between treatment groups. Luminosity is reported after normalization of lumens measured to cell density (Lumens/OD600) and expressed as a ratio between the treatment and control (Treatment/Control).

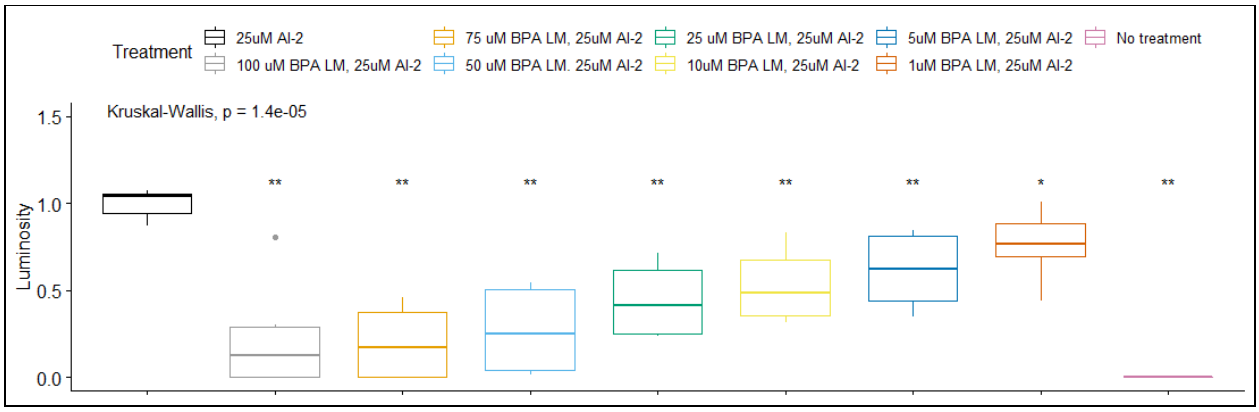

Figure 13(c) Bioluminescence of *V. harveyi* incubated with BPA (1uM-100uM) amended media. Box plots represent the standard deviation from the mean of 3 technical replicates, n = 3, where p-value ≤ *(0.05),**(0.005). “No Treatment” has no AI-2 or BPA amendment. The Wilcoxon Pairwise Test compares all treatments to luminosity induced by 25 uM AI-2.

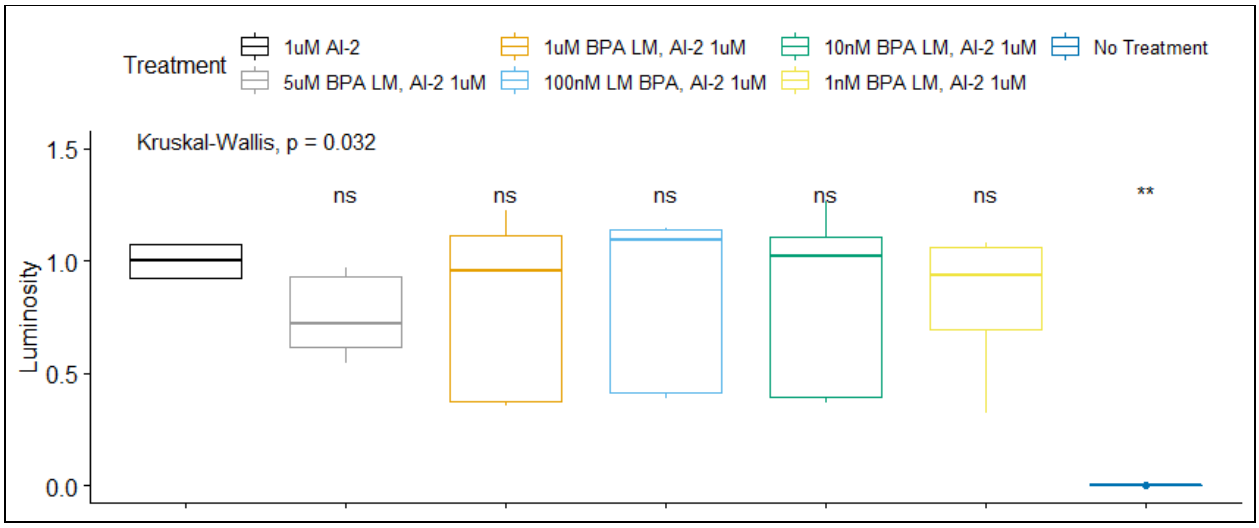

Figure 13(d) Bioluminescence of *V. harveyi* incubated with BPA (1nM-5uM) amended media. Box plots represent the standard deviation from the mean of 3 technical replicates, n = 3, where p-value = 5uM(0.041). This result indicates that more AI-2 background may be necessary to distinguish bioluminescence inhibition at lower concentrations, as significant inhibition was observed to1uM BPA. “No Treatment” has no AI-2 or BPA amendment. Wilcoxon Pairwise Test compares all treatment to luminosity induced by 1 uM AI-2 amendment. Box plots represent the standard deviation from the mean of 3 technical replicates, n = 3, where p-value = **(0.0079).

6.5.2 Quenching of QS by E2 at concentrations measured in feces.

V. harveyi TL26 was incubated with E2 in a 96-well plate, with each treatment replicated in triplicate. Due to the induction of growth by treatment, AI-2 signalling inhibition could not be detected at higher concentrations (>50nM); rather, bioluminescent enhancement was observed as in with low concentrations of BPA solvated in DMSO. Bioluminescent enhancement was observed at concentrations between 10nM and 100 nM, see Figure 14(a.1). While it appears that E2 induces bioluminescence in *V. harveyi*, in the absence of AI-2, no luminosity was observed. In a repeat experiment, a positive correlation of inhibition bioluminescence on increasing E2 concentrations was observed, with the greatest inhibition at 50nM (p-value = 0.0022), see Figure 14(b). It is important to note the difference between the two assays, Figures 14a and b. In the second trial, the divergence in induced growth was half as much as the first trial (27% vs 63% more growth for 50nM BPA treatment than 1uM AI-2 treatment without E2, for a reference see Figure 14(d).

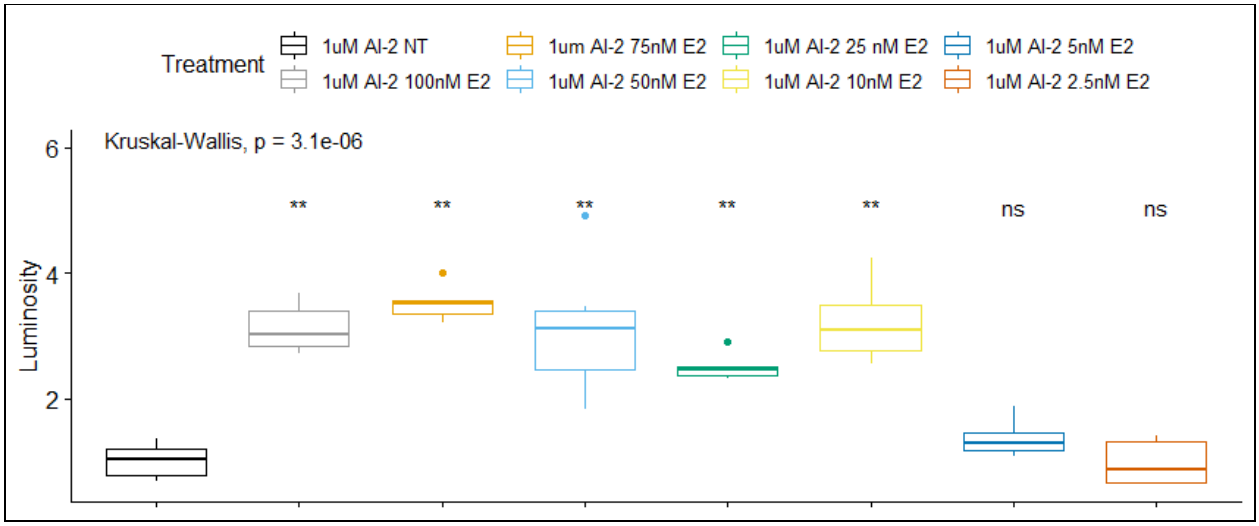

Figure 14(a). Bioluminescence of *V. harveyi* incubated with 5nM-100nM E2 and 1uM AI-2. All luminosity scores are normalized to the cell density of V. harveyi. Luminosity values are reported as a ratio of E2 Treatment/1uM AI-2 NT. Box plots represent the standard deviation from the mean of 6 technical replicates, n = 6, where p-value ≤ **0.05. The Wilcoxon Pairwise Test compares each condition to “1uM AI-2 NT” which has no E2 amendment.

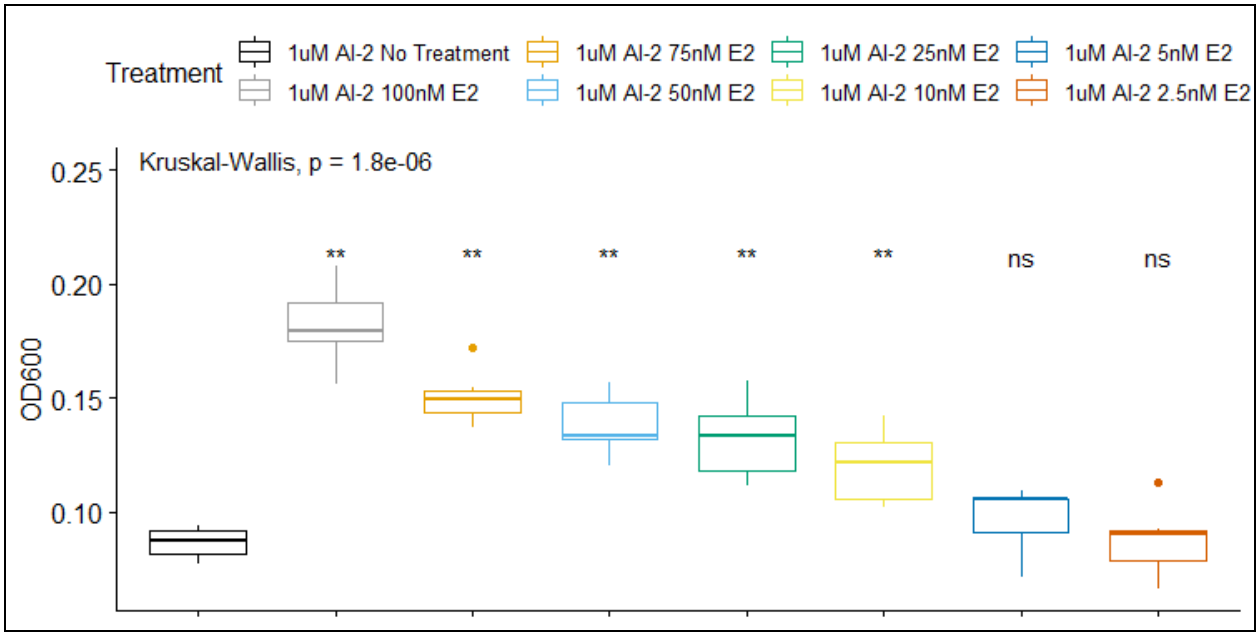

Figure 8(d). Final growth, OD600, *V. harveyi* incubated in 1% Ethanol and E2 (5nM-100nM). Box plots represent the standard deviation from the mean of 6 technical replicates. Wilcoxon Pairwise Test compares E2 amendment to "1uM AI-2 No Treatment". p-values≦ **(0.0022).

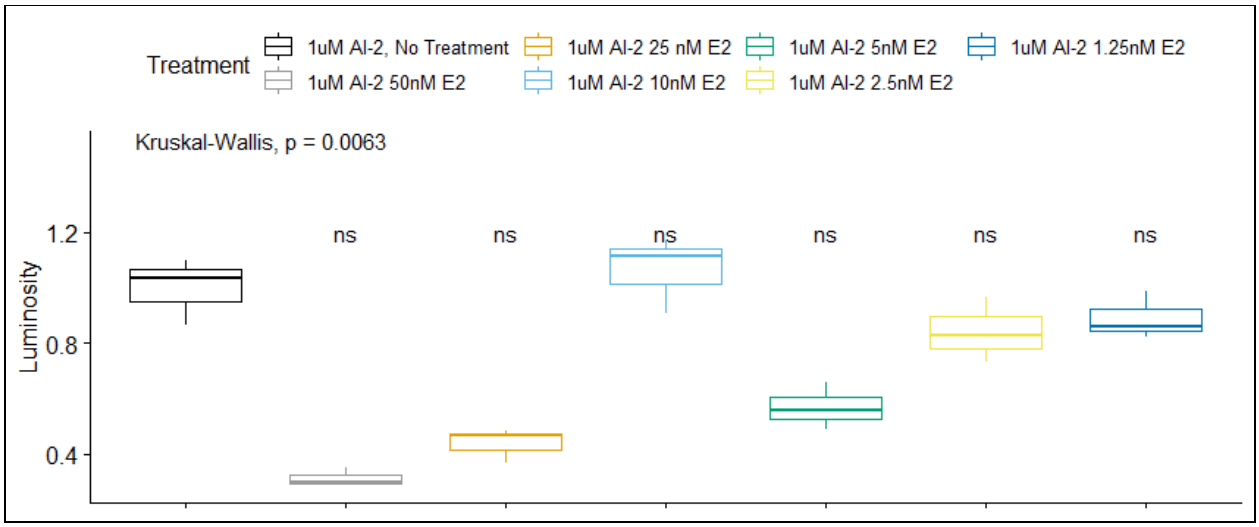

Figure 14(b) Bioluminescence of *V. harveyi* incubated with 1.25nM-50nM E2 and 1uM AI-2. Luminosity values are reported as a ratio of E2 Treatment/1uM AI-2 NT. Box plots represent the standard deviation from the mean of 3 technical replicates, n = 3. The Wilcoxon Pairwise Test compares each condition to "1uM AI-2 NT" which has vehicle control, where p-value≥ 0.1 (ns).

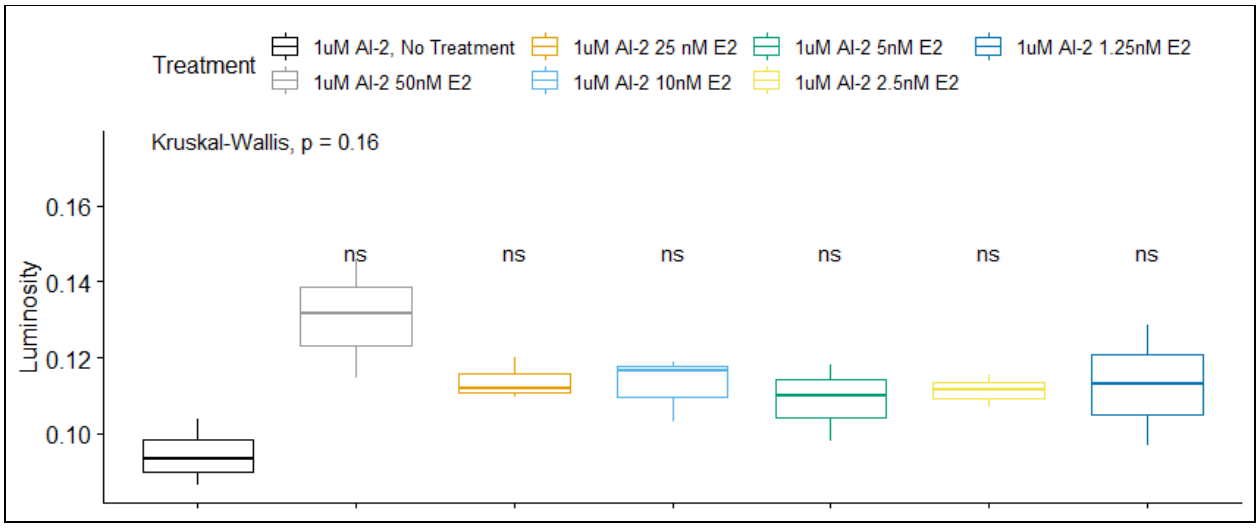

Figure 14(c). Final growth, OD600, *V. harveyi* incubated in 1% Ethanol with 1.25nM-50nM E2. Box plots represent the standard deviation from the mean of 6 technical replicates. The Wilcoxon Pairwise Test compares E2 amendment to "1uM AI-2 No Treatment", where p-values ≥ 0.05 (ns).

6.6 Diversity of Fecal Ferment Varied Significantly by Time, but not by Treatment.

6.2.1 Beta Diversity by Treatment and Incubation Time

Feces from a healthy male donor were fermented in rich Basal Media over a 24 hour period with 25uM BPA or none, Control. To investigate if phenotypic change in induced bioluminescence was reflected in a change in the fecal microbiota community, sequences were analyzed to compare Beta and Alpha diversity based on 16S ASV assignment. Unlike the Wang et al approach, fermenters were sampled at 4 time points over a short period, 24 hours, and the full time series was reported and analyzed. Two trials, Trial 1 and 2, were conducted using the same donor sample. Beta diversity compared the dissimilarity of each sample to all other samples. Differences between samples were attributed to specific taxa using Bray-Curtis distances of the ASV samples normalized to the shallowest sequencing depth. Samples were rarefied to read depth before Beta Diversity analysis. Beta diversity was compared across all 4 time points and both treatments using Principal Coordinates Analysis, PCoA, based on Bray-Curtis dissimilarities. Samples clustered primarily by Incubation Time, by PcoA1 accounting for 57.1% of the difference in the data. Permutational ANOVA (PERMANOVA) was applied to the Bray-Curtis dissimilarity; however, the p-value was not significant, R2= 0.05022, p-value = 0.557 when 25uM BPA communities were compared to Control communities. PERMANOVA does support a change in Beta diversity overtime, p-value = 0.009, for all samples. As T19 and T24 in Trial 2 diverged in the PCoA from all other samples, the data was subset by Trial, 1 or 2, and reanalyzed to test if differences within Trial 1 and Trial 2 were significant. Figure 15 (a and b) show the PCoAs of the Bray-Curtis dissimilarity subset by Trial. PERMANOVA was then used to evaluate the significance of the distribution. BPA treatment did not impact Bray-curtis dissimilarity compared to Control in either trial analyzed separately, p-value = 0.726 (Trial 1), and 0.594 (Trial2). PERMANOVA was used to compare if treatments, either Control of 25uM BPA treatment were significantly different between Trial 1 and 2; however, no significant differences was found by treatment between trials, p-value = 0.272 (Control) and p-value = 0.832. (25uM BPA). A heatmap at the rank of Genus was visualized to better understand the species that contributed by 5% or more difference in the samples. The taxa of the genus *Bacteroides*, *Escherichia/Shigella*, *Faecalibacterium*, *Lachnoclostriduim*, *Clostridium*, *Ersypelotrichaceae*, *Bifidobacterium, and Eubacterium*. Without careful inspection, a spatial pattern emerges in which the pattern of these taxa abundances correlate to time, rather than being distinguished from each other by treatment. This observation agrees with the distribution in the PCoA, see Figure 15.e and Figures 15 a and b).

Figure 15(a-b) PCoA of Control samples colored by Trial and labeled by the number of hours of incubation. d. is the PCoA of 25uM BPA samples colored by Trial and labeled by the number of hours of incubation, p-value = 0.557.

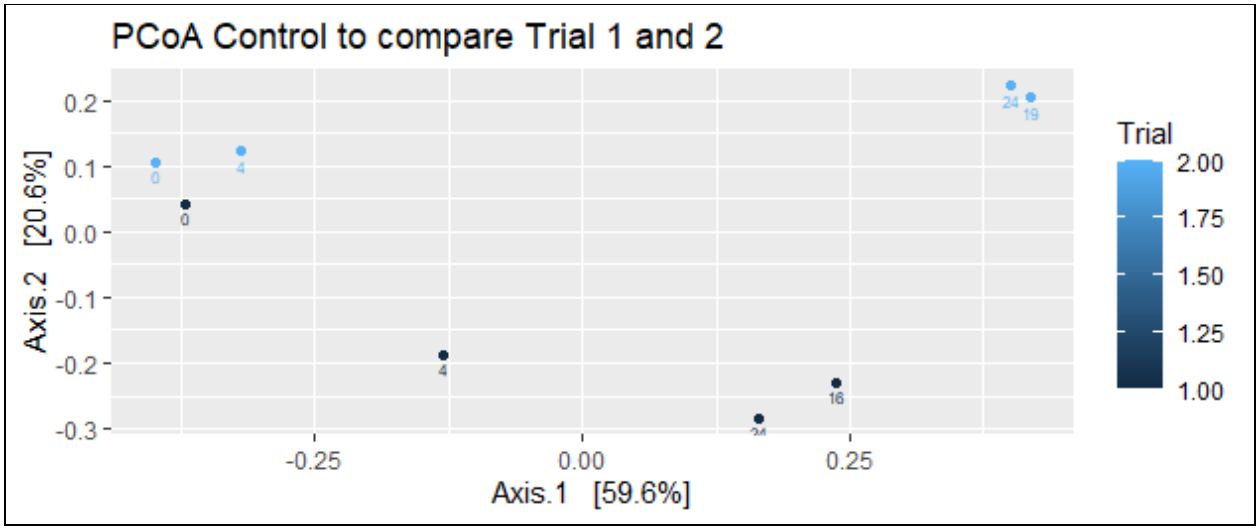

Figure 15 (a) PCoA of Bray-Curtis dissimilarity comparing Control samples from Trial 1 and 2. PERMANOVA confirms that there is no significant difference between trials, p-value = 0.272.

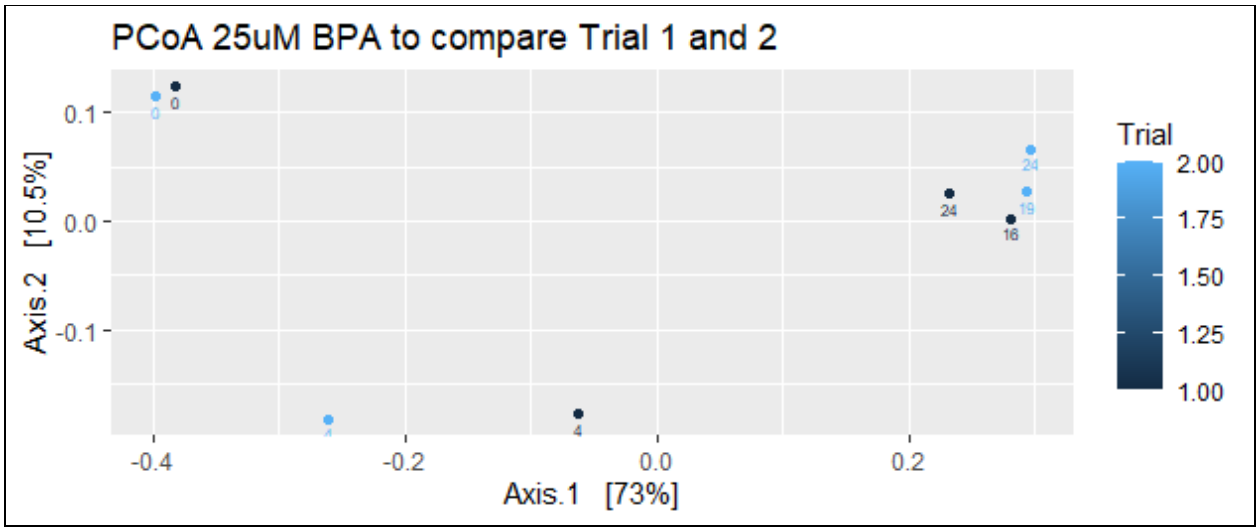

Figure 15 (b) PCoA of Bray-Curtis dissimilarity comparing Trial 1 and 2 of BPA treated samples. PERMANOVA confirms that there is no significant difference between trials, p-value = 0.832. Though this is notably more similar than control.

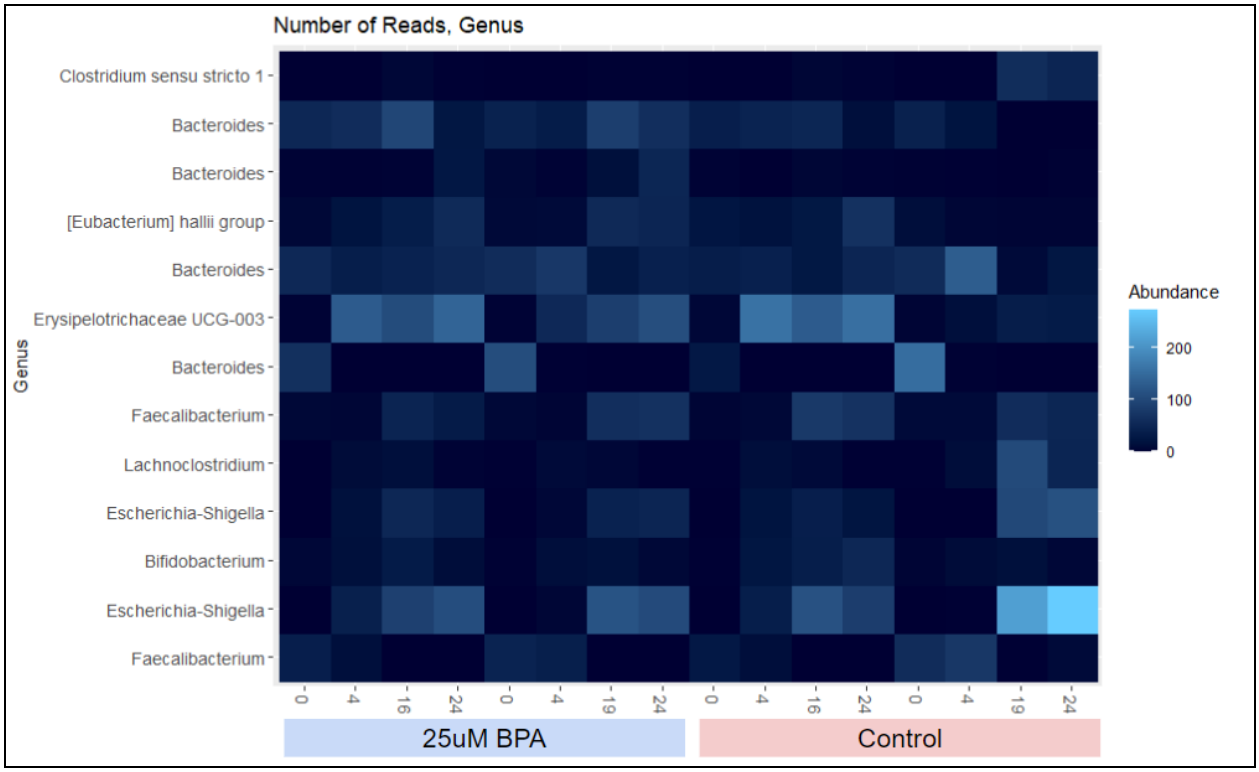

Figures 15 (e) Heatmap of major contributors to grouping of fecal ferment samples. The Heatmap was simplified by only including the top 5%. Samples are identified based on the last two digits of the sample code. Numbers 0-24 correspond to the incubation time at which the sample was drawn. Abundance refers to the number of reads for each genus listed on the right. Taxa were filtered by contribution to the Bray-Curtis dissimilarity seen between the samples.

6.2.2 Alpha diversity by treatment and incubation time

Alpha diversity is a measurement of ASV richness and evenness within a sample. When considering both richness and evenness within a sample, indexes such as Chao, Shannon and Inverse Simpson are used to mathematically combine these metrics into one numeric variable that can be passed to downstream analysis for comparisons between samples or groups of samples. Here I describe 4 metrics.To estimate richness, Observed Species and Chao1 index were calculated. Observed Species counts unique taxa in each sample and Chao1 estimates richness based on the abundance of each taxa. Shannon and Inverse Simpson indexes include evenness into consideration the alpha diversity calculation. Here, increased evenness of abundance across species in a sample results in a higher metric for Shannon and a lower metric for Inverse Simpson. The distribution of diversity was similar as diversity was lost by all samples overtime, see figure 16.a and b. Figure 16(a) shows the Observed Species and Chao1 Index, where higher scores are interpreted as higher richness and samples are grouped by treatment and colored by Incubation time. Kruskal-Wallis test was used to measure if the samples alpha diversity indices vary significantly by treatment, incubation time or by trial. Overall there was no significant difference in Shannon or Inverse Simpson metrics due to treatment, Kruskal-Wallis p-value = 0.2936 and p =.0.2076, respectively. The most divergent samples at time point T24, were compared using the same statistics by treatment, but it was not found to be significant, reporting Shannon, p-value = 0.33. Variations in alpha diversity by Incubation Time were significant, Kruskall-Wallis for both Shannon and InvSimpson index, p-value = 0.02 and p-value = 0.02 respectively; however, no significant difference was found in the pairwise comparisons of the samples by time point with Wilcoxon Pairwise Test, reporting Shannon, p-value ≥ 0.29 (after Bonferroni Adjustment). This difference agrees with the Bray-Curtis distribution, where samples cluster by Incubation Time rather than Treatment.

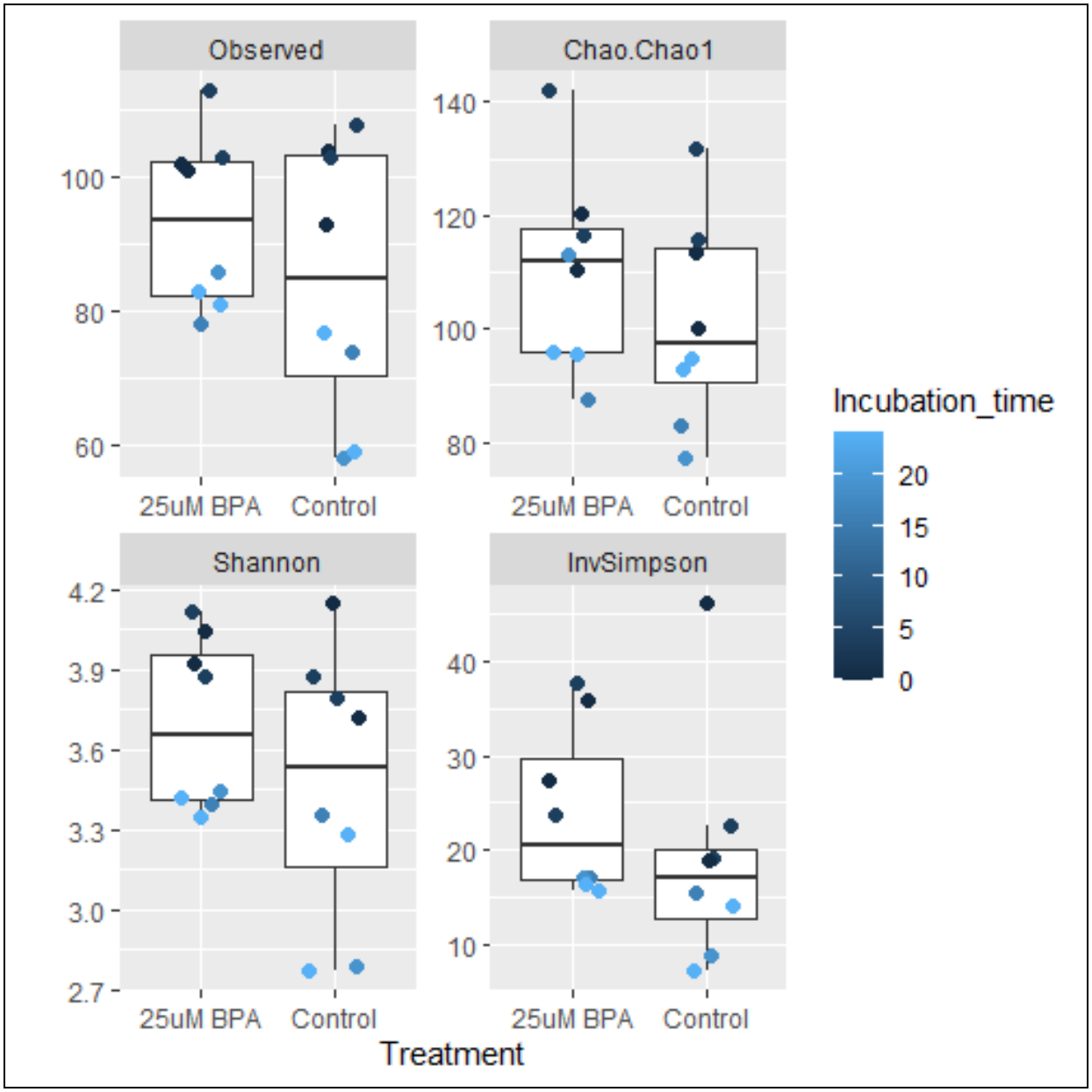

Figure 16(a.1). "Alpha.diversity.metrics.png" Alpha diversity metrics by treatment. On the left is the value of the diversity metric, The color or the dots refers to the number of hours of Incubation, where T0 is dark blue and T24 is light blue.

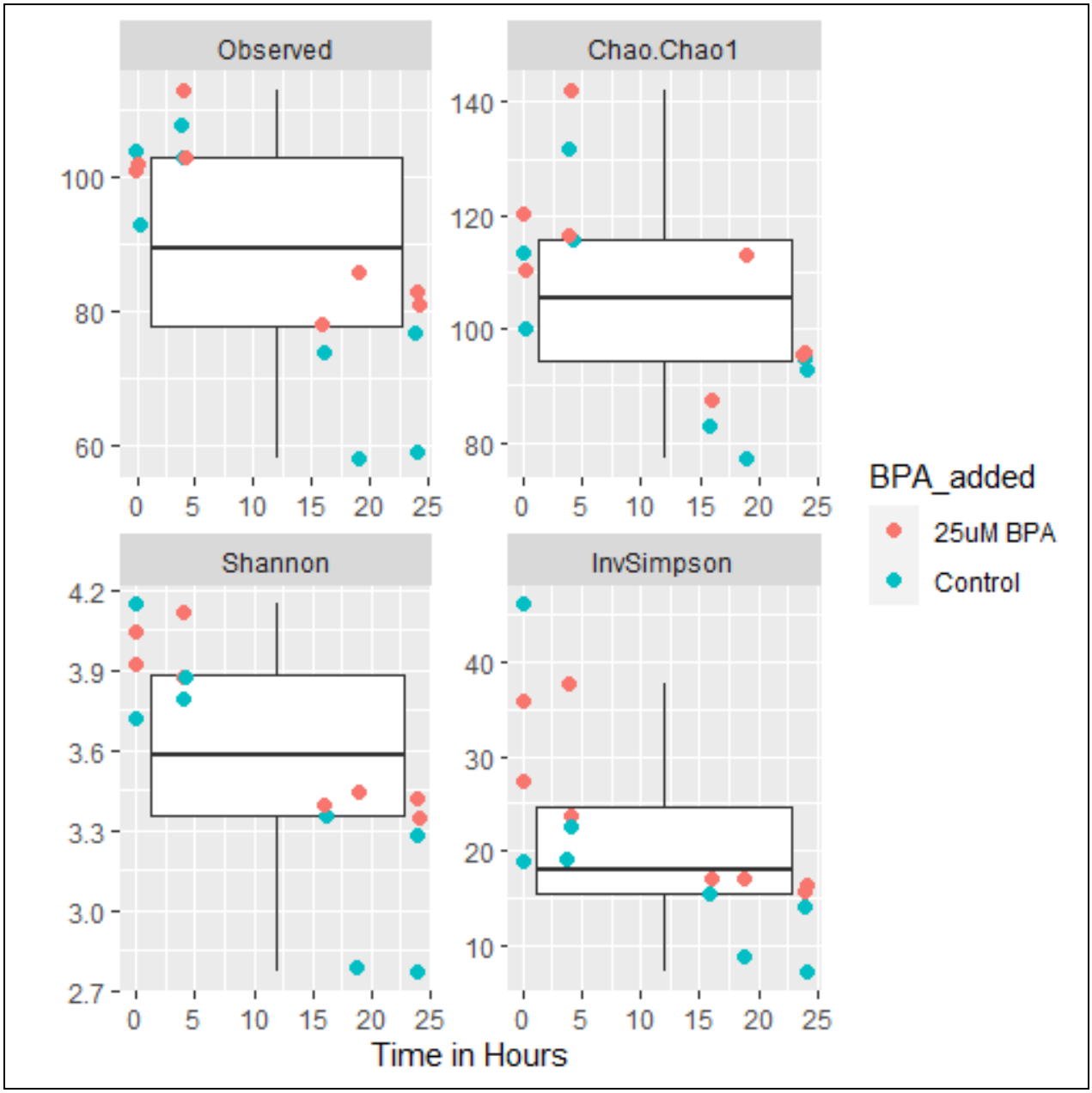

Figure 16(a.2) "Alpha.diversity.metrics.time.png". Alpha diversity metrics grouped by incubation timeSamples are color coded by treatment: blue, Control; and red 25uM BPA. Samples are in sequential order from left to right. Points are placed over the proper x- coordinate axis.

The data was parsed by treatment and the homogeneity of the samples by trial was evaluated. Shannon index did not vary significantly by trial within a treatment group, with intergroup differences evaluated with a non-parametric Kruskal-Wallis test: BPA treatment (p-value = 0.2119) and Control (p-value = 0.2472). The same statistics were used to analyze the Inverse Simpson Metric, as this metric is more sensitive to a dominance shift in relative taxa abundance. There was a significant difference in Inverse Simpson by Trial in the Control, Kruskal-Wallis p-value = 0.03569, but no significant difference between Trial 1 and 2 in the 25uM BPA treatment was observed, Kruskal-Wallis p-value = 0.8336. Since trial 1 and 2 control treatments appeared to have diverged, the data was parsed by Trial and the impact of BPA treatment was the compared again to Control; however no significant difference in Shannon Diversity due to BPA treatment was observed for either Trial 1, p-value = 0.69, or Trial 2, p-value =0.3

Figures 17 (a,b). Taxonomically assigned bar graph of absolute abundance(a) and relative abundance (b) after rarefaction to normalize read depth. Samples are labeled with a terminal numeric code 01-16, and increase in order over incubation time. Control is (01-04 and 09-12) and 25uM BPA (05-08 and 13-16).

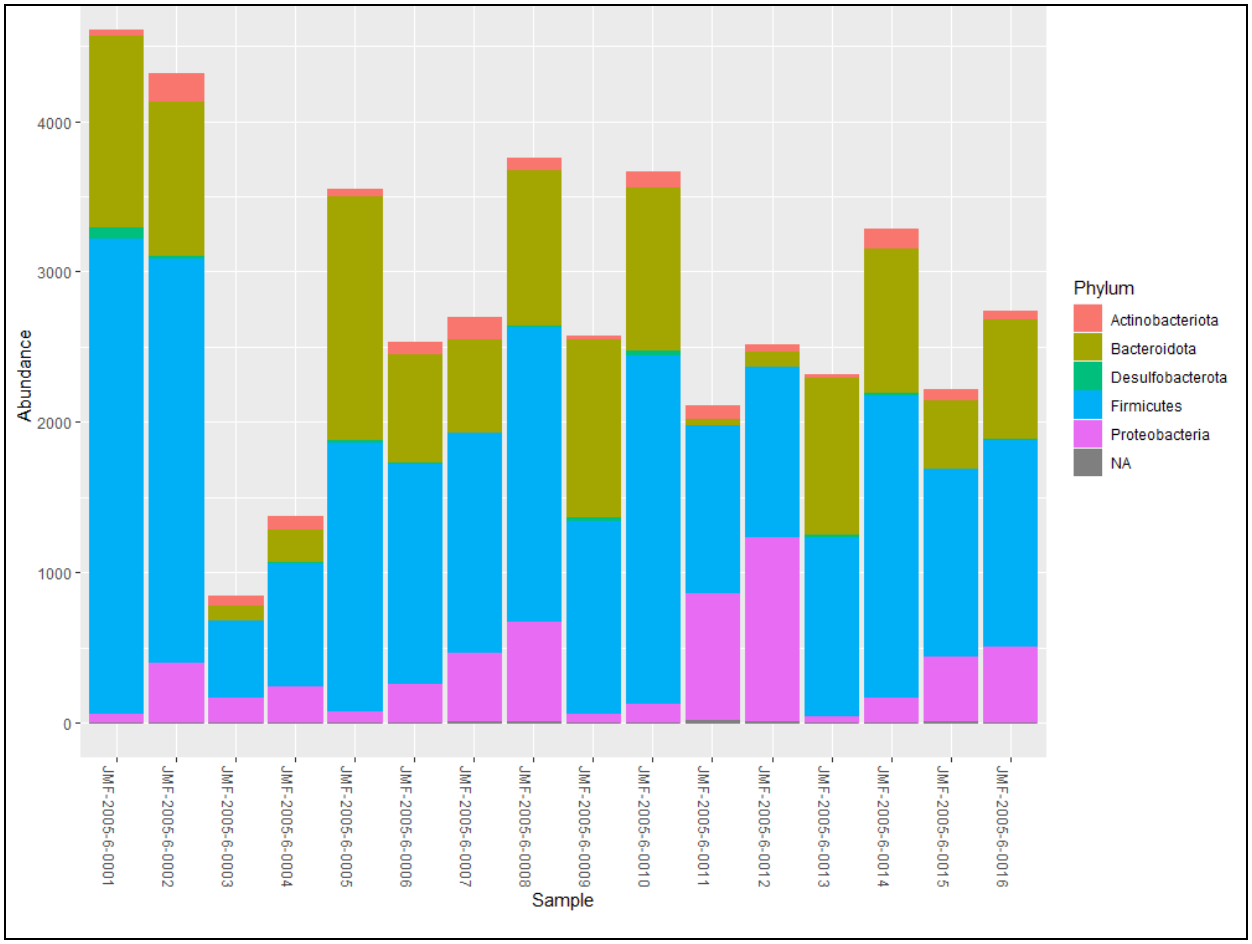

Figure 17 (**a).** Absolute abundance by taxonomic Phylum.

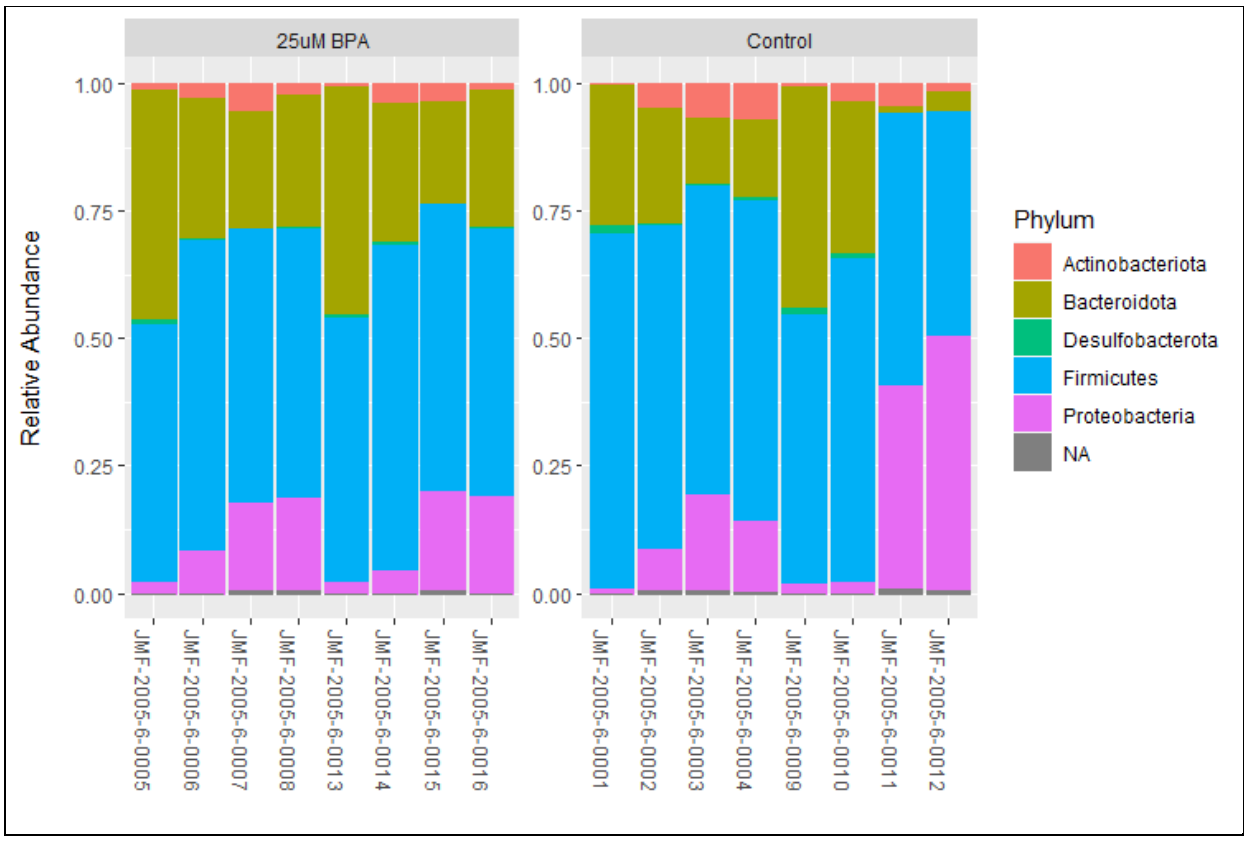

Figure 17 (b) Relative abundance by taxonomic Phylum.

.

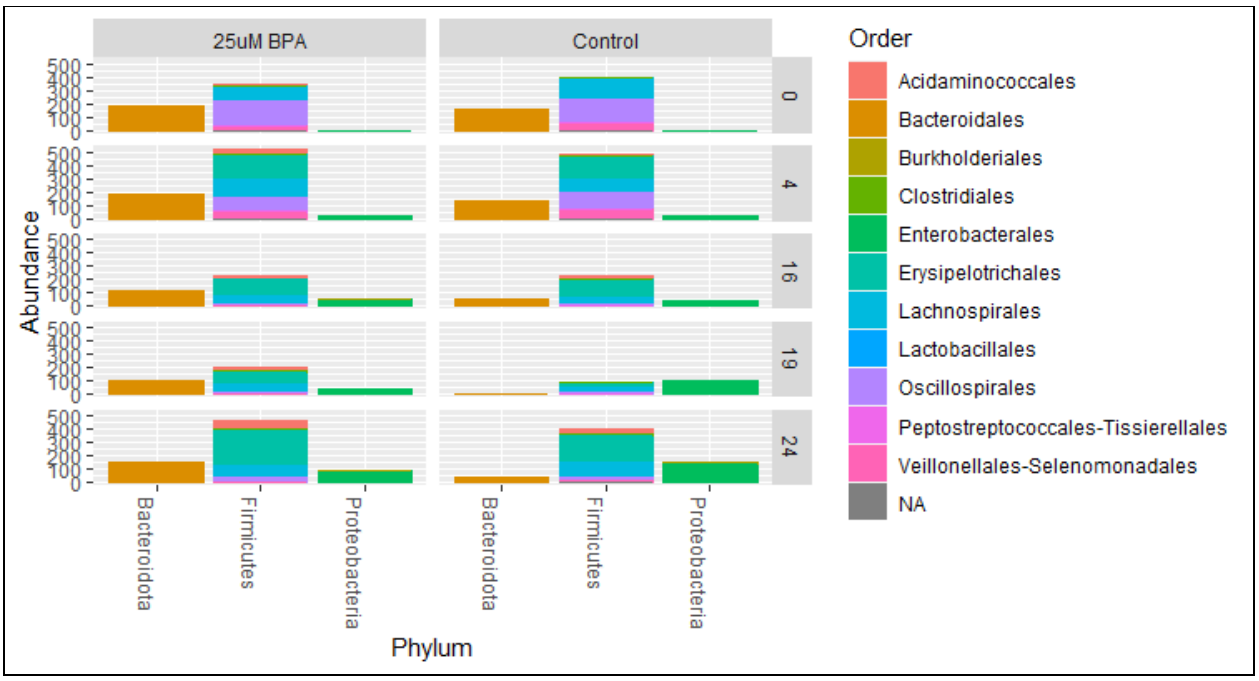

Figure 17(c). Relative abundance of taxa parsed by most abundant taxonomic Phylum, x-axis, and colored by taxonomic Order. Number on the right vertical axis refers to the time point in hours of the sample.

6.2.3 Taxa differentially abundant between treatments

Visualization of taxa by Phylum and Order, Figure 17(c), suggests that specific taxa may vary by treatment. To understand which taxonomic groups contributed to the change in alpha diversity overtime and resulted from BPA amendment, differential abundance of ASVs was analyzed by ranking each ASV using a Wilcoxon Sum Rank Test. Relative abundance based on ranking was resolved at the Genus level to compare variations in taxa due to 25uM BPA treatment. Changes in taxa due to the model system are assumed to be the taxon who change consistently between treatment groups and trials. *Bacteroides uniformis* (p-value = 0.05) and *Alistipes finegoldii/onderdonkii* (p-value = 0.03) were significantly enriched in the samples treated with 25uM BPA, see in Figure 18 a and b, respectively. A few other taxa also tended to vary with 25uM BPA treatment, including 2 taxa of the genus *Bacteroides* which were enriched in 25uM BPA (p-value =0.08) and a *Sutterela* sp. which was enriched in Control (p-value =0.08). Figure 18(c) shows the differential abundance of reads for Clostridium sensu strictu 1, p-value = 0.96, which is mentioned, as this species is under study as an indicator species of colon cancer. Interestingly, The difference in reads was found to be significantly different for *C. sensu strictu* 1 when the sample set was limited to T16/19 and T24, Wilcoxon Test p-value = 0.03, but not when sample set included all time points, Wilcoxon Test p-value 0.72.

Figures 18.a-d Graphs show number of reads, left, for both trials across time (right).Graph is fractured by treatment vertically (25uM BPA and Control) and by time horizontally which are sampling points across time, where 0, 4, 16, 19, 24 are hours after inoculation. Along the X-axis is the taxa by genus and when possible species.

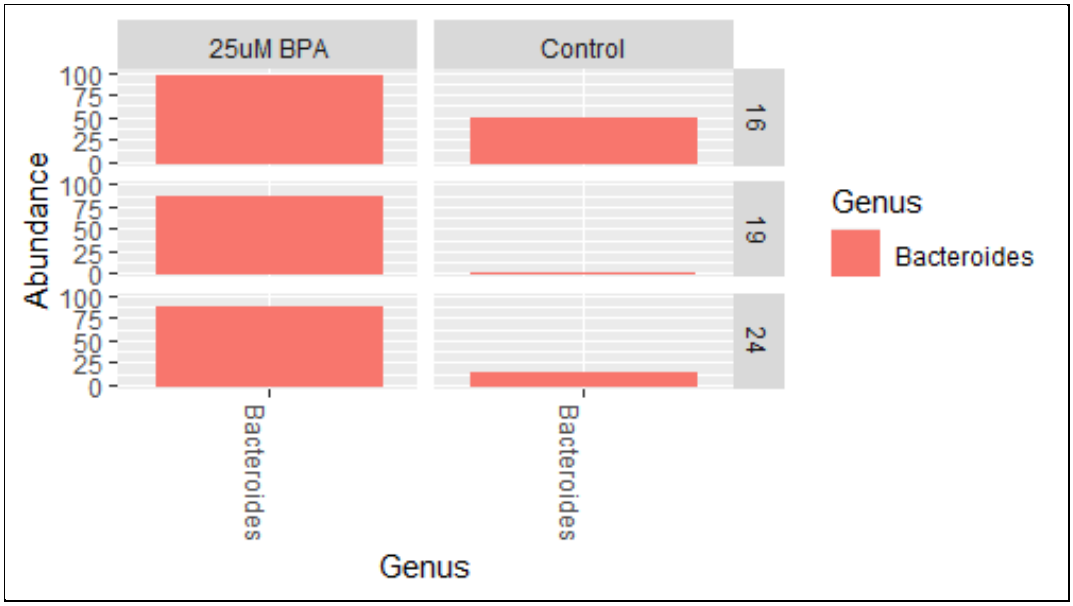

Figure 18(a). Abundance of *Bacteroides uniformis* enriched in BPA treatment. Where *Bacteroides uniformis,* "Bacteroides" significantly enriched in 25uM BPA, Wilcoxon Test p-value = 0.05. This bacteria species is not known to contain *luxS*. Bar graph of the distribution of Genuses in the Order Bacteroidales observed by treatment over time, both Trial 1 and 2.

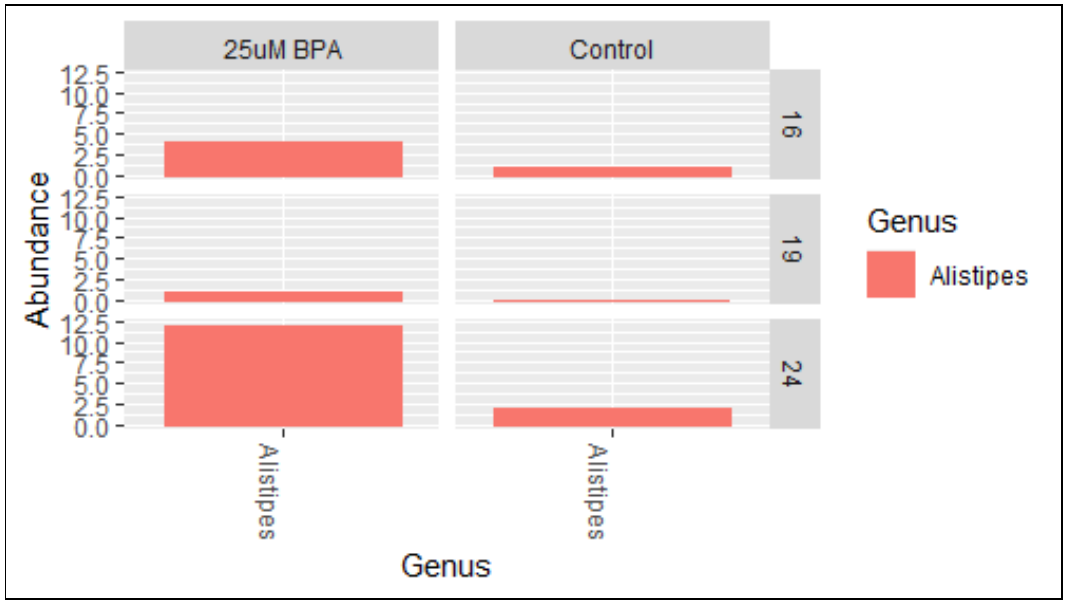

Figure 18(b). *Alistipes finegoldii/onderdonkii* is significantly depleted in the Control compared to 25uM BPA, Wilcoxon Test p-value = 0.03.The genus Alistipes is not known to contain an *luxS* orthologue in the genome.

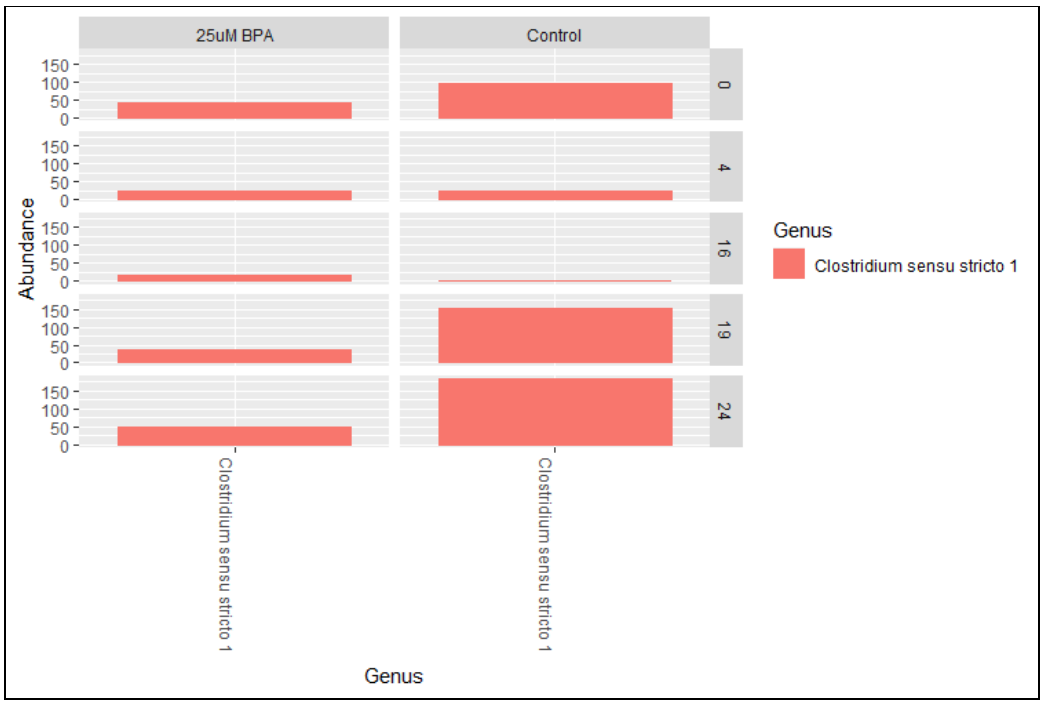

Figure 18 (c) Bar graph of the distribution of Genuses in the Order Clostridiales observed by treatment over time, both Trial 1 and 2. This species is not known to contain an *luxS* orthologue in the genome.

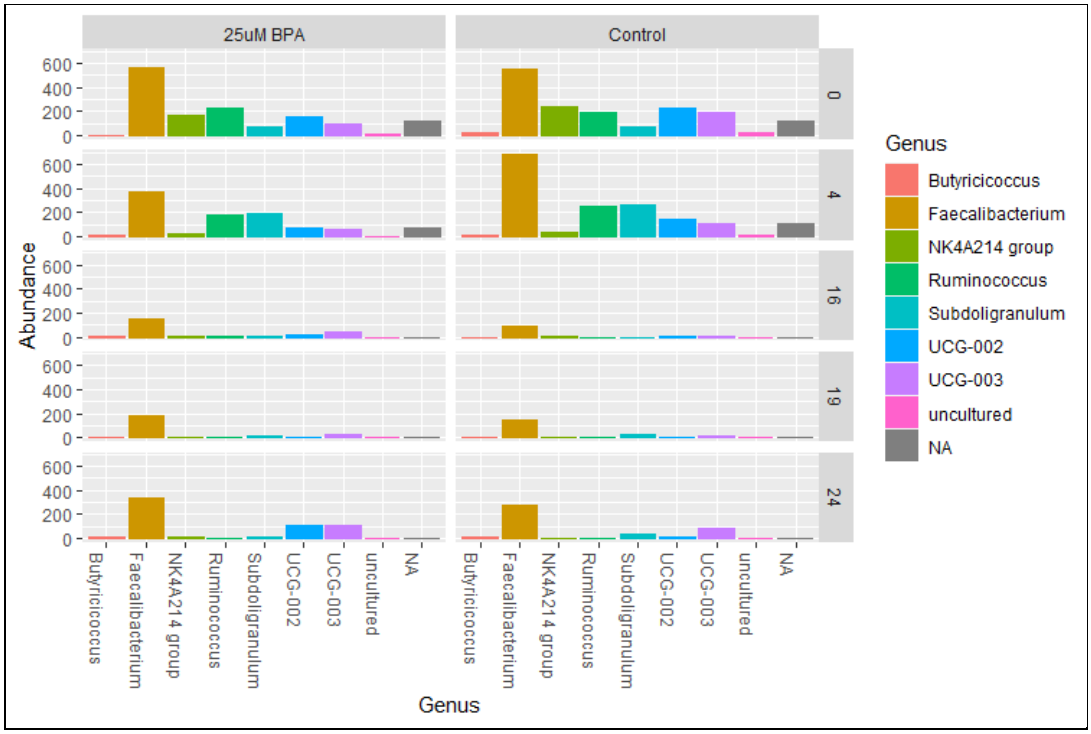

Figure 18 (d). Bar graph of the distribution of Genuses in the Order Enterobacterales observed by treatment over time, both Trial 1 and 2.

7. DISCUSSION:

In this thesis, I explored the impact of E2 and BPA on growth kinetics and AI-2 signaling in the human gut. Here it was demonstrated that aqueous BPA, at concentrations measured in canned foods (100nM), inhibits the induction of bioluminescence by AI-2 in *V. harveyi* for the first time. Gut microbiota have been shown to regulate growth in an AI-2 mediated mechanism (Thompson et. al 2015). In addition to demonstrating putative AI-2 production in the fecal microbiome of healthy people, the results of the fecal fermentation showed QS signalling varies overtime and that the presence of BPA is correlated with an upregulated AI-2 expression. Importantly, QS was induced from male but not female fecal samples. The absence of detection may indicate low production of AI-2 or efficient sequestration of AI-2 by resident microbiota, such as *B. subtilis* (Teasdale M 2009). In a study by Rickard et al 2006, AI-2 dose was found to be an important phenotype of community biofilm formation in saliva isolated microbes. Under detectable levels (0.08nM) exogenous AI-2, growth induction of the species was tested. 0.8nM induced biofilm formation and higher concentrations had little to no effect on behaviour, despite AI-2 being essential for biofilm formation. In this work I demonstrated that BPA exposure resulted in significantly higher AI-2 concentrations than untreated gut microbiota. In characterized QS systems, autoinducers are inducers for their own expression, such as with *V. harveyi* and *E. coli* (Guo M et. al. 2013). This implies that BPA may be an agonist for the AI-2 receptors and induces increased AI-2 production. In addition, BPA may select for bacterial species which have AI-2 signalling capability in an QS independent manner, such as differential growth induction or suppression as discussed. Alternatively, as an antagonist of the repressor of AI-2 regulon, increased production could be induced by a cell not transducing the signal that the AI-2 threshold has been met. An increase in AI-2 production could also be a response to BPA toxicity. For example in a chemostat incubation of *E. coli* K-12, AI-2 production generally increased overtime, and was induced by some stress conditions including anoxic fermentation (DeLisa MP et al. 2001).

If BPA prevents the message from being received or being transduced, AI-2 producers will have unregulated AI-2 synthesis and may miss coordinated behaviours that would be adaptive to the environment. Members of the microbiome that do not uilize AI-2 signaling would regulate per normal and have similar growth to unexposed microbiota. As AI-2 is detected and produced community wide, increased expression of AI-2 with BPA treatment could result in a shift of expression across various taxa rather than a shift in community composition. In this model, BPA/E2 would act as a QS buffer, increasing the threshold at which QS behaviour is turned on or off. Hence, the difference in between exposed and naive fecal communities may be due to interference of AI-2 signalling in Firmicutes or Proteobacteria, resulting in less competition for Bacteroidetes. Inhibition of AI-2 signaling in vivo with bromofurnone, a QQ molecule, resulted in the proliferation of several genera, including Lactobacillus, Sutterella, Allobaculum, and Adlercreutzia. Interestingly, the shift in the gut microbiome resulted in a change in secondary metabolism of glucocorticoids by the microbiota (He Z et al 2019).

Through interference ith AI-2 signalling, BPA amendment could be a driver of community difference, however, longer exposure times may be necessary to see this effect at a significant level, where metabolites of BPA and longer incubations could explain the differences between these results and Wang Y. et al. (2008). This work demonstrated that fecal communities may quench quorum sensing, as seen in P2 females fecal samples, and that this phenotype varies across individuals or by gender or time. This behavior may be a competitive advantage against community members that use AI-2 signaling to coordinate blooms. The differential expression and response to the later stressful conditions of the bioreactor suggest how short term incubation with BPA can result in a cascade of events that lead to a shift in the gut microbiome due to enhanced AI-2 signaling.

In addition, BPA differentially impacted the growth of *V. harveyi* and *E. coli*, where *E. coli* tolerated BPA at concentrations almost two orders of magnitude greater than *V. harveyi*, 10mM compared to 100uM. Detection of host metabolites could signal to possible pathogens or colonizers of arrival in the preferred niche. Here I show a differential growth induction between species of bacteria and between strains *(E. coli)*. This phenomenon was also observed in other *Vibrio* species. In agreement with the observations in this assay, researchers observed that E2 induced growth of *Vibrio sp.*, but this effect was not observed when *Vibrio sp.* was incubated in the presence of progesterone and estrogen. To be clear, growth induction was observed in the presence of progesterone, but not when progesterone concentrations were greater than that of estrogen (Walsh AF 1973). Hence a signal transduction pathway rather than utilization of E2 as a carbon substrate is hypothesized. Indeed, the presence of E2 or endogenous estrogen appears to confer resistance to possible growth inhibitors present in fecal extracts, as growth inhibition was observed in the female fecal extract from the E2 trough. The analysis on *E. coli* isolates also supports that E2 induces growth in some strains. In this analysis, I observed growth induction in *E. coli* BW25133_Δ*lsrR* but not other strains. This is remarkable since similar observations were observed with BPA treatment. *E. coli* BW25133_Δ*lsrR* behaviour changes in response to BPA and E2 show an important role of *lsrR* in regulating growth and mediating response to estrogenic chemicals. The chemical similarity of E2 and BPA and this shared phenotypic response may indicate a similar pharmacology of BPA and E2 on growth and other *V. harveyi* phenotypes. While *V. harveyi* AI-2 regulated genes are repressed by the presence of glucose, *E. coli* AI-2 production is stimulated by glucose and inhibited by CAP in a catabolite repression mechanism (Pereira CS 2013). This could enable *E. coli* kin to take advantage of labile carbon, such as glucose, through increasing cell numbers in anticipation of glucose availability prior to direct detection. Increased mutation rate was observed in one study of *E. coli* K-12 strains that was shown to be *luxS* dependent (Krašovec R 2014). Indeed mutation rate is attributed to colonization success of known enteric pathogens (Selber-Hnatiw S 2017) and *E. coli* K-12 strains are known to undergo global adaptive mutations during *in vivo* colonization (Barroso-Batista J 2014). This would be an interesting competitive advantage employed by members of this communication network and a compelling method of controlling the community which could be exploited by the host.

To translate the disruption observed in V. harveyi to the gut system, it is essential to understand how BPA inhibits bioluminesce induction in V. harveyi. First, BPA was observed to be toxic to V. harveyi above 100mM. Since bioluminescence is an ATP dependent activity, any stress that prevents ATP synthesis to the cell could compromise the reporter's response to AI-2 signaling (Zenno S and Saigo K 1994). BPA and E2 could inhibit the reaction mechanism, specifically, in several ways: i, by competitively binding to the protein conjugate for signal transduction, LuxP; ii, by competing with the endogenous substrate, AI-2;or iii, interfering with LuxR binding to the lux operon promoter. To explore the first possibility, Quantitative Reverse Transcription PCR , qRT-PCR, could be used to quantify how BPA or E2 affects the levels of mRNA transcripts for luxCDABEGH. Northern blot could reveal at which point in the signal transduction BPA and E2 have their impact. Loss of signal transduction at detection with LuxP would result in increased sRNA and decreased luxR transcripts. If luxR mRNA levels are not influenced, mechanism iii is implied. Electrophoretic Mobility shift assay could provide detect interference with DNA-binding of luxR to the lux operon promoter. Here, increased band migration in the presence of increased concentrations of BPA or E2 would indicate interference of these molecules in DNA-binding, which could be reversed by increased concentrations of LuxR. To address this mechanism, a reporter could be constructed in which the lux promoter is ligated to B-galactosidase or GFP expression plasmid and transformed in V. harveyi TL26. Here, variation in reporter gene expression could be linked to lux operon expression, rather than luciferase activity or physiological stress which may interfere with bioluminescence specifically. Nonetheless, autochthonous bacteria of the gut may respond differently due to differences in endogenous AI-2 receptor proteins (Waidmann MS 2011).

In general, false discovery rate increases with data set size. Gut microbiota sample data is by definition high due to the richness in these samples; therefore, differential abundance correlations, at the resolution of taxa should, be interpreted very conservatively (Thorsen J et al. 2016). As demonstrated in this work, human microbiota vary enough at the species level that species which vary significantly in one study are completely absent in another sample. This work highlights a phenotypic inquiry into the gut microbiome as an ecological whole, where genomic redundancy promotes robust functional output in the case of dynamic changes in individual membership in that niche. It is worth noting that Malaisé et. al (2016) findings support that significant changes in metabolite production by small community differences could result in negative clinical outcomes overtime for the host. AI-2 signaling presents a mechanism in which complex functional community dynamics can be regulated at a systems level. Possible interactions between the gut microbiota and the host as a holo-organism provides an additional mechanism of host-symbiota evolution through modulation of growth, colonization, and virulence through endogenous hormone signaling, AI-2 and E2. Disruption of this homeostasis could result due to the exposure to exogenous estrogenic compounds, such as BPA, where microbiota growth and AI-2 signaling were differentially impacted compared to E2 or no treatment at all. This work suggests a novel mechanism for endocrine disrupting chemicals via disruption of gut microbiota communication and possible grounds for heterogeneity seen in animal models of BPA as an endocrine disruptor.

8. CONCLUSIONS:

This work supports a possible role of E2 in regulating gut microbiota activity and composition through AI-2 signaling. Several studies have linked microbiome composition to levels of estrogens and impaired estrogen-mediated phenotypes (Garcia-Reyero N et al. 2018, Shimizu K et al. 1998, Kwa M et al. 2016, Eriksson H et al. 1969, Flores R et al. 2012). The microbiome is capable of metabolizing conjugated (Garcia-Reyero N 2018, Baker JM, 2017 , Shimizu K, 1998, Kwa M 2016, Eriksson H,1969, Ginsberg G 2009, McIntosh FM 2012, Flores, R 2012) and unconjugated estrogen (Järvenpää P et al. 1980). This activity is carried out by several families of enzymes that are broadly expressed in the gut bacteria: Hydroxysteroid dehydrogenases (HSDs), β-glucuronidase, β-glucosidase and sulfatases (Kisiela M 2012, Baker JM, 2017, Kwa M 2016, Ginsberg G 2009, McIntosh FM 2012, 19 Flores, R 2012, Velmurugan 2017). Both metabolism of estrogens and modification of estrogens change the affinity of these hormones for their cognate receptor. HSDs are widely expressed in the kingdom bacteria and function in the metabolism of steroid molecules. Once conjugated, estrogens are again more hydrophobic and reenter enterohepatic cycling (Kwa M et al. 2016 , Raftogianis R et al. 2000, Gruber, C M.D 2002).

Comparisons of serum estrogens and their metabolites in men, women and postmenopasual women to gut microbiota composition and β-glucuronidase activity, demonstrated that serum estrogens correlated negatively with bacterial diversity and positively with β-glucuronidase activity; however, no trend could be determine in premenopausal women as samples were taken across the menstrual cycle (Flores R et. al 2012). Both increased protein and fat consumption increase β-glucuronidase activity (Reddy BS 1980), consumption of fiber decreases β-glucuronidase activity (Reddy BS 1992). Fecal ß-glucuronidase activity has been linked to serum estrogen levels in healthy women consuming diets high in fat, protein or fiber (Goldin BR et al. 1982). Vegetarians had triple the estrogens in feces and reduced fecal ß-glucuronidase and 15% to 20% lower serum estrogen levels, than women who reported a high fat, low fiber diet (Goldin BR 1982). In addition, administration of antibiotics in humans has been shown to increase in steroid hormone excretion in the feces (Martin F et al. 1975) and lower serum estrogen levels (Adlercreutz et al. 1984). In a study comparing steroid hormones in the feces of germ-free and conventional rats, the proportion of unconjugated steroids were significantly less than the concentration found in the feces of conventional rats (Eriksson H 1969). Germ-free mice gavaged with *Bacteroides distasonis* and *Clostridium perfringens* conferred normal fecundity in male and female mice, while mono-association *Bacteroides subtilis* maintained aberrant estrous cycle and implantation rates of common germ-free mice (Shimizu K 1998). A shift in gut microbiome composition alone, is correlated to diseases associated with dysregulation of estrogen homeostasis in humans. These include but are not limited to obesity, cancer, polycystic fibrosis ovarian syndrome, Type 2 diabetes, metabolic syndromes, inflammation (Maruvada P 2017, Baker JM 2017, Kwa M 2016, Plottel C 2004,

Malaisé Y 2017, Abbassi-Ghanavati M 2009, Velmurugan G 2017, Neuman H 2015). Therefore, understanding the relationship between estrogens, pseudoestrogens and gut microbiota could reveal important pathways that could lead to better clinical outcomes and treatments of these intractable syndromes.

Implications at a Systems Level: Gut, Endocrine, Liver Axis.

Systemic regulation of BPA and estrogen by the liver can be negatively impacted by metabolites of the gut microbiota correlated with dysbiosis. Changes in bacterial metabolites lipopolysaccharides and decreased output of short chain fatty acids, are correlated with liver inflammation and decreased liver functionality (Malaisé Y 2017, Reddivari L 2017). Liver damage reduces activity of the UDP-glucuronosyltransferase, which regulates both estrogen and BPA bioactivity through conjugation of chemical moieties (Lee C.S. 1992, Baker JM 2017). Furthermore, rodent models have shown than the combination of BPA exposure and a change in microbial metabolites result in liver dysfunction (Malaisé Y 2017, Reddivari L 2017). This suggests the microbiome may contribute to liver homeostasis and functioning. Together these studies suggests that a positive feedback loop exists between gut microbiota, the liver, and hormone homeostasis. In this model, a community shift in the gut microbiome, caused by BPA, would result in a cascade of further dysregulation. Here, BPA and estrogen metabolism would become dysregulated due to changes in microbiome deconjugation activity. This loop could also interfere with the conjugation activity of the liver brought on by functional output change of the gut microbiota. Data presented in this thesis suggests a possible mechanism of AI-2 mediated microbiome disruption by BPA and elucidates on how BPA exposure may lead to disease. Hence, this thesis supports further research into opportunities for applications of AI-2 mediated therapies for liver and hormone homeostasis the clinic.

9. LIST OF ABBREVIATIONS:

S-adenosyl-L-methionine (SAM)
ATP-binding cassette (ABC)
Autoinducer 2, (AI-2)
Quorum Sensing, (QS)
Bisphenol A (BPA)
17β- Estradiol (E2)
4,5-dihydroxy-2,3-pentadione (DPD)
Dextran sulfate sodium (DSS)
Short Chain Fatty Acids (SCFA)
Irritable Bowel Syndrome (IBS)
Body Mass Index (BMI)
High Fat Diet (HFD)
Peyer's Patches (PP)
Hydroxysteroid dehydrogenases (HSDs)
Basal Media, BM
Dimethyl sulfoxide (DMSO)
Permutational ANOVA (PERMANOVA)
Principal Components Analysis, (PCoA)
borated tetrahydrofurane, (S-THMF-borate)
lipopolysaccharide (LPS)
Basal media (BM)
Luria Marine Media (LM)
LB Luria Berotelli Media (LB)
Brain and Heart Infusion (BHI)
Reinforced Clostridia Media (RCM)
Estrogen Receptor Alpha(ER**α**)
Estrogen Receptor Beta(ER***β***)

10. REFERENCES:

Abisado R, Benomar S, Klaus JR, Dandekar AA, Chandler JR. Bacterial Quorum Sensing and Microbial Community Interactions. *mBio.* May 2018, 9 (3) e02331-17; **DOI:** 10.1128/mBio.02331-17

Adlercreutz H, Pulkkinen MO, Hämäläinen EK, Korpela JT. Studies on the role of intestinal bacteria in metabolism of synthetic and natural steroid hormones. *J Steroid Biochem*. 1984;20(1):217-229. doi:10.1016/0022-4731(84)90208-5

Adlercreutz H, Pulkkinen MO, Hamalainen EK, et al. Studies on the role of intestinal bacteria in metabolism of synthetic and natural steroid hormones. *J Steroid Biochem.* 1984;20:217–29.

Almeida, S., Raposo, A., Almeida‐González, M. and Carrascosa, C. Bisphenol A: Food Exposure and Impact on Human Health. *Comprehensive Reviews in Food Science and Food Safety*, 2018;17: 1503-1517. doi:10.1111/1541-4337.12388

Anderson GD. Children versus adults: pharmacokinetic and adverse-effect differences. *Epilepsia*. 2002;43 Suppl 3:53-9. doi: 10.1046/j.1528-1157.43.s.3.5.x. PMID: 12060006.

Arumugam M, Raes J, Pelletier E, Le Paslier D, Yamada T, Mende DR, Fernandes GR, Tap J, Bruls T, Batto JM, Bertalan M, Borruel N, Casellas F, Fernandez L, Gautier L, Hansen T, Hattori M, Hayashi T, Kleerebezem M, Kurokawa K, Leclerc M, Levenez F, Manichanh C, Nielsen HB, Nielsen T, Pons N, Poulain J, Qin J, Sicheritz-Ponten T, Tims S, Torrents D, Ugarte E, Zoetendal EG, Wang J, Guarner F, Pedersen O, de Vos WM, Brunak S, Doré J, MetaHIT Consortium., Antolín M, Artiguenave F, Blottiere HM, Almeida M, Brechot C, Cara C, Chervaux C, Cultrone A, Delorme C, Denariaz G, Dervyn R, Foerstner KU, Friss C, van de Guchte M, Guedon E, Haimet F, Huber W, van Hylckama-Vlieg J, Jamet A, Juste C, Kaci G, Knol J, Lakhdari O, Layec S, Le Roux K, Maguin E, Mérieux A, Melo Minardi R, M'rini C, Muller J, Oozeer R, Parkhill J, Renault P, Rescigno M, Sanchez N, Sunagawa S, Torrejon A, Turner K, Vandemeulebrouck G, Varela E, Winogradsky Y, Zeller G, Weissenbach J, Ehrlich SD, Bork P. Enterotypes of the human gut microbiome. *Nature. 2011 May 12; 473(7346):174-80.*

Baker JM, Al-Nakkash L, Herbst-Kralovetz MM. Estrogen-gut microbiome axis: *Physiological and clinical implications*. Maturitas. 2017 Sep;103:45-53. doi: 10.1016/j.maturitas.2017.06.025.

Barakat R, Oakley O, Kim H, Jin J, Ko CJ. Extra-gonadal sites of estrogen biosynthesis and function. *BMB Rep*. 2016;49(9):488–496. doi:10.5483/bmbrep.2016.49.9.141.

Bansal, T., Jesudhasan, P., Pillai, S., Wood, T. K., & Jayaraman, A. Temporal regulation of enterohemorrhagic Escherichia coli virulence mediated by autoinducer-2. Applied Microbiology and Biotechnology. 2008;78(5), 811–819. doi:10.1007/s00253-008-1359-8

Barroso-Batista J, Sousa A, Lourenço M, et al. The first steps of adaptation of Escherichia coli to the gut are dominated by soft sweeps. *PLoS Genet*. 2014;10(3):e1004182. Published 2014 Mar 6. doi:10.1371/journal.pgen.1004182

Bassler BL, Wright M, Showalter RE, Silverman MR. Intercellular signalling in Vibrio harveyi: sequence and function of genes regulating expression of luminescence. *Mol Microbiol.* 1993 Aug;9(4):773-86. doi: 10.1111/j.1365-2958.1993.tb01737.x. PMID: 8231809.

Beury-Cirou A, Tannières M, Minard C, Soulère L, Rasamiravaka T, Dodd RH, et al. At a Supra-Physiological Concentration, Human Sexual Hormones Act as Quorum-Sensing Inhibitors. *PLoS ONE*. 2013;8(12): e83564.

Berridge, M.J. Cell Signalling Biology. Portland Press. 2012;6 csb0001012. doi:10.1042/csb0001012

Bertoli S, Leone A, Battezzati A. Human Bisphenol A Exposure and the "Diabesity Phenotype". *Dose Response*. 2015;13(3):1559325815599173. doi:10.1177/1559325815599173

Blasco-Baque V, Serino M, Vergnes JN, Riant E, Loubieres P, et al. Correction: High-Fat Diet Induces Periodontitis in Mice through Lipopolysaccharides (LPS) Receptor Signaling: Protective Action of Estrogens. *PLOS ONE.* 2013; 8(5).

Braniste V, Jouault A, Gaultier E, et al. Impact of oral bisphenol A at reference doses on intestinal barrier function and sex differences after perinatal exposure in rats. *Proc Natl Acad Sci U S A.* 2010;107(1):448-453. doi:10.1073/pnas.0907697107

Brüssow H. Problems with the concept of gut microbiota dysbiosis. *Microbial Biotechnology* (2020) 13(2), 423– 434.

Bose JL, Rosenberg CS, Stabb EV. Effects of luxCDABEG induction in Vibrio fischeri: enhancement of symbiotic colonization and conditional attenuation of growth in culture. *Arch Microbiol*. 2008;190(2):169-183. doi:10.1007/s00203-008-0387-1

Buck BL, Azcarate-Peril MA, Klaenhammer TR. Role of autoinducer-2 on the adhesion ability of Lactobacillus acidophilus. *J Appl Microbiol.* 2009;107(1):269-279. doi:10.1111/j.1365-2672.2009.04204.x

Buffie, C. G. & Pamer, E. G. Microbiota-mediated colonization resistance against intestinal pathogens. *Nat. Rev. Immunol*. 2013;13, 790–801.

Carbonell X, Corchero JL, Cubarsí R, Vila P, Villaverde A. Control of Escherichia coli growth rate through cell density. *Microbiol Res*. 2002;157(4):257-265. doi:10.1078/0944-5013-00167

Carding S, Verbeke K, Vipond DT, Corfe BM, Owen LJ. Dysbiosis of the gut microbiota in disease. *Microb Ecol Health Dis*. 2015;26:26191. doi:10.3402/mehd.v26.26191.

Chen, X., Schauder, S., Potier, N. *et al.* Structural identification of a bacterial quorum-sensing signal containing boron. *Nature* 415, 545–549 (2002). https://doi.org/10.1038/415545a

Christiaen SE, O'Connell Motherway M, Bottacini F, et al. Autoinducer-2 plays a crucial role in gut colonization and probiotic functionality of Bifidobacterium breve UCC2003. *PLoS One*. 2014;9(5):e98111. Published 2014 May 28. doi:10.1371/journal.pone.0098111

Choi, J., Shin, D., & Ryu, S. Implication of Quorum Sensing in Salmonella enterica Serovar Typhimurium Virulence: the luxS Gene Is Necessary for Expression of Genes in Pathogenicity Island 1. *Infection and Immunity*, 2007; 75(10), 4885–4890. doi:10.1128/iai.01942-06

Chong, J., & Xia, J. Computational Approaches for Integrative Analysis of the Metabolome and Microbiome. *Metabolites.* 2017;7(4), 62.doi:10.3390/metabo7040062

Claus S, Guillou H, Ellero-Simatos S. The gut microbiota: a major player in the toxicity of environmental pollutants? *npj Biofilms and Microbiomes*. 2016;2:16003.

Collado MC, Isolauri E, Laitinen K, Salminen S. Distinct composition of gut microbiota during pregnancy in overweight and normal-weight women. *Am J Clin Nutr. 2008 Oct; 88(4):894-9.*

Corrales, J. Global Assessment of Bisphenol A in the Environment. *Dose Response*. 2015 Jul-Sep; 13(3): 1559325815598308.

Dabek M, McCrae SI, Stevens VJ, Duncan SH, Louis P: Distribution of beta-glucosidase and beta-glucuronidase activity and of beta-glucuronidase gene gus in human colonic bacteria. *FEMS Microbiol Ecol*. 2008 Dec;66(3):487-95

Das A, Srinivasan M, Ghosh TS, Mande SS. Xenobiotic Metabolism and Gut Microbiomes. *PLoS One*. 2016;11(10):e0163099. Published 2016 Oct 3. doi:10.1371/journal.pone.0163099.

Defois C, et al. Food Chemicals Disrupt Human Gut Microbiota Activity And Impact Intestinal Homeostasis As Revealed By In Vitro Systems. *Scientific Reports*. 2018;8, Article number: 11006.

DeKeersmaecker SC, Vanderleyden J. Constraints on detection of autoinducer-2 (AI-2) signalling molecules using Vibrio harveyi as a reporter. *Microbiology*. 1 Aug 2003; Volume 149, 8.

de la Cuesta-Zuluaga J, Kelley ST, Chen Y, et al. Age- and Sex-Dependent Patterns of Gut Microbial Diversity in Human Adults. *Msystems*. 2019 Jul-Aug;4(4). DOI: 10.1128/msystems.00261-19.

DeLisa MP, Valdes JJ, Bentley WE. Mapping stress-induced changes in autoinducer AI-2 production in chemostat-cultivated Escherichia coli K-12. *J Bacteriol*. 2001 May;183(9):2918-28. doi: 10.1128/JB.183.9.2918-2928.2001. PMID: 11292813; PMCID: PMC99510.

DeLuca, J. A., Allred, K. F., Menon, R., Riordan, R., Weeks, B. R., Jayaraman, A., & Allred, C. D. (2018). Bisphenol-A alters microbiota metabolites derived from aromatic amino acids and worsens disease activity during colitis. *Experimental Biology and Medicine*, 243(10), 864–875. doi:10.1177/1535370218782139

DiGiulio DB, Callahan BJ, McMurdie PJ, Costello EK, Lyell DJ, Robaczewska A, Sun CL, Goltsman DS, Wong RJ, Shaw G, Stevenson DK, Holmes SP, Relman DA. Temporal and spatial variation of the human microbiota during pregnancy. *Proc Natl Acad Sci U S A. 2015 Sep 1; 112(35):11060-5.*

Diebel M, Diebel LN, Manke CW, Liberati DM: Estrogen modulates intestinal mucus physiochemical properties and protects against oxidant injury. J Trauma Acute Care Surg. 2015 Jan;78(1):94-9.

Donaldson GP, Ladinsky MS, Yu KB, Sanders JG, Yoo BB, Chou WC, Conner ME, Earl AM, Knight R, Bjorkman PJ, Mazmanian S. Gut microbiota utilize immunoglobulin A for mucosal colonization. *Science*. 18 May 2018 : 795-800

Ducarmon Q, Zwittink R, Hornung V, van Schaik W, Young VB, Kuijper EJ.Gut Microbiota and Colonization Resistance against Bacterial Enteric Infection. *Microbiology and Molecular Biology Reviews*. Jun 2019, 83 (3) e00007-19; DOI: 10.1128/MMBR.00007-19

Edwards SM, Cunningham SA, Dunlop AL, Corwin EJ. The Maternal Gut Microbiome During Pregnancy. *MCN Am J Matern Child Nurs.* 2017;42(6):310-317. doi:10.1097/NMC.0000000000000372

EFSA Panel on Food Contact Materials, Enzymes, Flavourings and Processing Aids (CEF). A statement on the developmental immunotoxicity of bisphenol A (BPA): answer to the question

from the Dutch Ministry of Health, Welfare and Sport. *EFSA Journal*: 2016 October. Volume 14, Issue 10. E04580.

Elkins CA, Mullis LB. Mammalian steroid hormones are substrates for the major RND- and MFS-type tripartite multidrug efflux pumps of Escherichia coli. *J Bacteriol.* 2006;188(3):1191-1195. doi:10.1128/JB.188.3.1191-1195.2006

Eriksson H, Gustafsson JA, Sjovall J. Steroids in germfree and conventional rats. Free steroids in faeces from conventional rats. *Eur J Biochem*.1969 Jul;9(4):550-4

Evans JM, Morris LS, and Marchesi JR. The gut microbiome: the role of a virtual organ in the endocrinology of the host. *Journal of Endocrinology*. 2013;Volume 218: Issue 3:R37–R47

Eyster KM. The Estrogen Receptors: An Overview from Different Perspectives. *Methods Mol Biol.* 2016;1366:1-10. doi:10.1007/978-1-4939-3127-9_1

Fadlallah J, El Kafsi H, Sterlin D, Juste C, Parizot C, Dorgham K, Autaa G, Gouas D, Almeida M, Lepage P, Pons N, Le Chatelier E, Levenez F, Kennedy S, Galleron N, de Barros JP, Malphettes M, Galicier L, Boutboul D, Mathian A, Miyara M, Oksenhendler E, Amoura Z, Doré J, Fieschi C, Ehrlich SD, Larsen M, Gorochov G. Microbial ecology perturbation in human IgA deficiency. Sci Transl Med. 2018 May 2;10(439):eaan1217. doi: 10.1126/scitranslmed.aan1217. PMID: 29720448.

Fagerberg L et al., Analysis of the human tissue-specific expression by genome-wide integration of transcriptomics and antibody-based proteomics. *Mol Cell Proteomics*, 2014 Feb;13(2):397-406

Foo JL, Ling H, Lee YS, Chang MW. Microbiome engineering: Current applications and its future. *Biotechnol J*. 2017 Mar;12(3). doi: 10.1002/biot.201600099. Epub 2017 Jan 30. PMID: 28133942.

Fteita D, Könönen E, Söderling E, Gürsoy UK. Effect of estradiol on planktonic growth, coaggregation, and biofilm formation of the Prevotella intermedia group bacteria. *Anaerobe.* 2014;27:7-13. doi:10.1016/j.anaerobe.2014.02.003

Fteita D, Könönen E, Gürsoy M, Ma X, Sintim HO, Gürsoy UK. Quorum sensing molecules regulate epithelial cytokine response and biofilm-related virulence of three Prevotella species. *Anaerobe*. 2018;54:128-135. doi:10.1016/j.anaerobe.2018.09.001

Flores R, Shi J, Fuhrman B, et al. Fecal microbial determinants of fecal and systemic estrogens and estrogen metabolites: a cross-sectional study. *J Transl Med*. 2012;10:253. doi:10.1186/1479-5876-10-253.

Fox JE, Starcevic M, Jones PE, Burow ME, McLachlan JA. Phytoestrogen signaling and symbiotic gene activation are disrupted by endocrine-disrupting chemicals. *Environ Health Perspect*. 2004;112(6):672-677. doi:10.1289/ehp.6456

Fuhrman BJ, et al. Associations of the fecal microbiome with urinary estrogens and estrogen metabolites in postmenopausal women. *J Clin Endocrinol Metab*. 2014;99(12):4632-4640

Gao Z., Yin J., Zhang J., Ward R. E., Martin R. J., Lefevre M., et al. Butyrate improves insulin sensitivity and increases energy expenditure in mice. *Diabetes* 2009;58, 1509–1517. 10.2337/db08-1637

Garcia-Reyero, N: The clandestine organs of the immune system. *General and Comparative Endocrinology*. February 2018;257,1, Pages 264-271

Genuis S 2012, Beesoon S, Birkholz D, Lobo R. Human excretion of bisphenol A: blood, urine, and sweat (BUS) study. *J. Environ. Publ. Health* 201; 10.1155/2012/185731

Gironi B, Kahveci Z, McGill B, Lechner B, Pagliara S, Metz J, Morresi A, Palombo F, Sassi P, Petrov P. Effect of DMSO on the Mechanical and Structural Properties of Model and Biological Membranes. *Biophysical Journal*. 2020;Volume 119, Issue 2, Pages 274-286.

Ginsberg G, Rice DC. Does rapid metabolism ensure negligible risk from bisphenol A? *Environ Health Perspect*. 2009 Nov;117(11):1639-43.

Goldin BR, Gorbach SL. Alterations of the intestinal microflora by diet, oral antibiotics, and Lactobacillus: decreased production of free amines from aromatic nitro compounds, azo dyes, and glucuronides. *J Natl Cancer Inst*. 1984;73(3):689–695.

Grandclément C, Tannières M, Moréra S, Dessaux Y,Faure D, Quorum quenching: role in nature and applied developments, *FEMS Microbiology Reviews*, 2016 January 1;Volume 40, Issue 1, Pages 86–116, https://doi.org/10.1093/femsre/fuv038

Gruber, C M.D., Tschugguel, W M.D, Schneeberger, C Ph.D, Huber, J M.D., Ph.D. Production and Actions of Estrogens. *N Engl J Med* 2002; 346:340-352 DOI: 10.1056/NEJMra000471

Guo M, Gamby S, Zheng Y, Sintim HO. Small molecule inhibitors of AI-2 signaling in bacteria: state-of-the-art and future perspectives for anti-quorum sensing agents. *Int J Mol Sci*. 2013;14(9):17694-17728. Published 2013 Aug 29. doi:10.3390/ijms140917694

Guo Y, Qi Y, Yang X, Zhao L, Wen S, Liu Y, Tang L: Association between Polycystic Ovary Syndrome and Gut Microbiota. *PloS one* 201;11(4):e0153196.

Györgypal Z, Kondorosi A. Homology of the ligand-binding regions of Rhizobium symbiotic regulatory protein NodD and vertebrate nuclear receptors. *Mol Gen Genet.* 1991;226(1-2):337-340. doi:10.1007/BF00273624

Hammarström L, Vorechovsky I, Webster D. Selective IgA deficiency (SIgAD) and common variable immunodeficiency (CVID). *Clin Exp Immunol.* 2000;120(2):225–231. doi:10.1046/j.1365-2249.2000.01131.x

He G. et al. Determination of the sulfate and glucuronide conjugates of levornidazole in human plasma and urine, and levornidazole and its five metabolites in human feces by high performance liquid chromatography-tandem mass spectrometry. *J Chromatogr B Analyt Technol Biomed Life Sci*. 2018 Apr 1;1081-1082:87-100. doi: 10.1016/j.jchromb.2018.02.025

He Z, Kong X, Shao T, Zhang Y, Wen C. Alterations of the Gut Microbiota Associated With Promoting Efficacy of Prednisone by Bromofuranone in MRL/lpr Mice. *Front Microbiol*. 2019 May 1;10:978. doi: 10.3389/fmicb.2019.00978. PMID: 31118928; PMCID: PMC6504707.

d'Hennezel E, Abubucker S, Murphy LO, Cullen TW. Total Lipopolysaccharide from the Human Gut Microbiome Silences Toll-Like Receptor Signaling. *mSystems*. 2017;2(6):e00046-17. Published 2017 Nov 14. doi:10.1128/mSystems.00046-17.

Higgins, D. A., Pomianek, M. E., Kraml, C. M., Taylor, R. K., Semmelhack, M. F., & Bassler, B. L. The major Vibrio cholerae autoinducer and its role in virulence factor production. *Nature*, 2007;450(7171), 883–886. doi:10.1038/nature06284

Hopkins M, Englyst H, Macfarlane S, Furrie E, Macfarlane G, McBain A. Degradation of Cross-Linked and Non-Cross-Linked Arabinoxylans by the Intestinal Microbiota in Children. *Appl. Environ. Microbiol..* Nov 2003, 69 (11) 6354-6360; DOI: 10.1128/AEM.69.11.6354-6360.2003

Hsiao, A., Ahmed, A., Subramanian, S. *et al.* Members of the human gut microbiota involved in recovery from *Vibrio cholerae* infection. *Nature.* 2014;515, 423–426. https://doi-org.uaccess.univie.ac.at/10.1038/nature13738

Huang YF, Wang PW, Huang LW, Lai CH, Yang W, Wu KY, Lu CA, Chen CH, and Chen ML. Prenatal Nonylphenol and Bisphenol A Exposures and Inflammation Are Determinants of Oxidative/Nitrative Stress: A Taiwanese Cohort Study. *Environ. Sci. Technol*., 2017; 51 (11), pp 6422–6429. doi:10.1021/acs.est.7b00801

Hug L., Sharrow D, and You, D. UN Inter-agency Group for Child Mortality Estimation. Levels and Trends in Childhood Mortality, Report 2019.

Huo X, Chen D, He Y, Zhu W, Zhou W, Zhang J. Bisphenol-A and Female Infertility: A Possible Role of Gene-Environment Interactions. *Int J Environ Res Public Health.* 2015;12(9):11101-16. doi:10.3390/ijerph120911101.

Human Microbiome Project Consortium. Structure, function and diversity of the healthy human microbiome. *Nature*. 2012;486(7402):207-214. Published 2012 Jun 13. doi:10.1038/nature11234

Husain A, Khan SA, Iram F, Iqbal MA, Asif M. Insights into the chemistry and therapeutic potential of furanones: A versatile pharmacophore. *Eur J Med Chem*. 2019;171:66-92. doi:10.1016/j.ejmech.2019.03.021

Hwang N, Eom T, Gupta SK, et al. Genes and Gut Bacteria Involved in Luminal Butyrate Reduction Caused by Diet and Loperamide. *Genes (Basel)*. 2017;8(12):350. Published 2017 Nov 28. doi:10.3390/genes8120350

Ilina P, Ma X, Sintim HO, Tammela P. Miniaturized whole-cell bacterial bioreporter assay for identification of quorum sensing interfering compounds. *J Microbiol Methods*. 2018 Nov;154:40-45. doi: 10.1016/j.mimet.2018.10.005. Epub 2018 Oct 6. PMID: 30300658.

Ismail A, et al. Host-Produced Autoinducer-2 Mimic Activates Bacterial Quorum Sensing. *Cell Host & Microbe*. 17 March 2016; 19(4): 470 - 480.

Järvenpää P, Kosunen T, Fotsis T, Adlercreutz H. In vitro metabolism of estrogens by isolated intestinal micro-organisms and by human faecal microflora. *J Steroid Biochem*. 1980 Mar; 13(3):345-9.

Javurek AB, Spollen WG, Johnson SA, et al. Effects of exposure to bisphenol A and ethinyl estradiol on the gut microbiota of parents and their offspring in a rodent model. *Gut Microbes*. 2016;7(6):471-485.

Johansson MEV, Jakobsson HE, Holmén-Larsson J, Schütte A, Ermund A, Rodríguez-Piñeiro A, Arike L, Wising C, Svensson F, Bäckhed F, Gunnar C. Normalization of Host Intestinal Mucus Layers Requires Long-Term Microbial Colonization. *Cell & Microbe.* 2015 Nov. 11; 18(5): 582-592.

Jun Li, Can Attila, Liang Wang, Thomas K. Wood, James J. Valdes, William E. Bentley. Quorum Sensing in *Escherichia coli* Is Signaled by AI-2/LsrR: Effects on Small RNA and Biofilm Architecture. *Journal of Bacteriology.* Aug 2007, 189 (16) 6011-6020; **DOI:** 10.1128/JB.00014-07

Kaliannan K, Robertson RC, Murphy K, et al. Estrogen-mediated gut microbiome alterations influence sexual dimorphism in metabolic syndrome in mice. *Microbiome*. 2018;6(1):205. Published 2018 Nov 13. doi:10.1186/s40168-018-0587-0

Kamrin MA. Bisphenol A: a scientific evaluation. *MedGenMed*. 2004 Sep ;6(3):7.

Kane M, Case L, Kopaskie K, Kozlova A, MacDearmid C, Chervonsky A, Golovkina T. Successful Transmission of a Retrovirus Depends on the Commensal Microbiota. *Science*.2011 October 14: 245-249

Kemis JH, Linke V, Barrett KL, Boehm FJ, Traeger LL, Keller MP, et al..Genetic determinants of gut microbiota composition and bile acid profiles in mice. *PLoS Genet.* 2019 15(8): e1008073. https://doi.org/10.1371/journal.pgen.1008073

Kettle, Helen & Holtrop, Grietje & Louis, Petra & Flint, Harry. microPop: Modelling microbial populations and communities in R. *Methods in Ecology and Evolution*. 2017. doi: 10.1111/2041-210X.12873.

Kim Y., Oh, S., Park, S., Seo, J. B., & Kim, S.-H. (2008). Lactobacillus acidophilus reduces expression of enterohemorrhagic Escherichia coli O157:H7 virulence factors by inhibiting autoinducer-2-like activity. *Food Control*, 19(11), 1042–1050. doi:10.1016/j.foodcont.2007.10.014

Kisiela M, Skarka A, Ebert B, Maser E. Hydroxysteroid dehydrogenases (HSDs) in bacteria: a bioinformatic perspective. *J Steroid Biochem Mol Biol*. 2012;129(1-2):31-46. doi:10.1016/j.jsbmb.2011.08.002

Koestel, Z. L., Backus, R. C., Tsuruta, K., Spollen, W. G., Johnson, S. A.,Javurek, A. B., et al.. Bisphenol A (BPA) in the serum of pet dogs following short-term consumption of canned dog food and potential health consequences of exposure to BPA. *Sci. Total Environ*. 2017; 579, 1804–1814. doi: 10.1016/j.scitotenv.2016.11.162

Konieczna A, et al. Health risk of exposure to Bisphenol A (BPA). *Rocz Panstw Zakl Hig*. 2015;66(1):5-11.

Koren O, Goodrich JK, Cullender TC, et al. Host remodeling of the gut microbiome and metabolic changes during pregnancy. *Cell*. 2012;150(3):470-480. doi:10.1016/j.cell.2012.07.008

Kornman KS, Loesche WJ. Effects of estradiol and progesterone on Bacteroides melaninogenicus and Bacteroides gingivalis. *Infect Immun*. 1982;35(1):256-263.

Kostic, A.D.; Gevers, D.; Siljander, H.; Vatanen, T.; Hyötyläinen, T.; Hämäläinen, A.-M.; Peet, A.; Tillmann, V.; Pöhö, P.; Mattila, I.; et al. The dynamics of the human infant gut microbiome in development and in progression toward type 1 diabetes. *Cell Host Microbe.* 2015, 17, 260–273

Krašovec R, Belavkin RV, Aston JA, et al. Mutation rate plasticity in rifampicin resistance depends on Escherichia coli cell-cell interactions. *Nat Commun*. 2014;5:3742. Published 2014 Apr 29. doi:10.1038/ncomms4742

Krishan AV, et al. Bisphenol-A: an estrogenic substance is released from polycarbonate flasks during autoclaving. *Endocrinology.* 1993 Jun;132(6):2279-86.

Krzyżek P. Challenges and Limitations of Anti-quorum Sensing Therapies. *Front Microbiol*. 2019;10:2473. Published 2019 Oct 31. doi:10.3389/fmicb.2019.02473

Kwa M, Plottel CS, Blaser MJ, Adams S:The Intestinal Microbiome and Estrogen Receptor–Positive Female Breast Cancer. 2016 Apr 22;108(8).

Lai KP, Chung YT, Li R, Wan HT, Wong CK. Bisphenol A alters gut microbiome: Comparative metagenomics analysis. *Environ Pollut.* 2016 Nov;218:923-930. doi: 10.1016/j.envpol.2016.08.039.

Lang IA, Galloway TS, Scarlett A, et al. Association of Urinary Bisphenol A Concentration With Medical Disorders and Laboratory Abnormalities in Adults. *JAMA*. 2008;300(11):1303–1310. doi:10.1001/jama.300.11.1303

Laitinen K, Mokkala K. Overall Dietary Quality Relates to Gut Microbiota Diversity and Abundance. *Int J Mol Sci*. 2019;20(8):1835. Published 2019 Apr 13. doi:10.3390/ijms20081835

Lawley, T. D. and Walker, A. W. (2013), Intestinal colonization resistance. *Immunology*, 2013;138: 1-11. doi:10.1111/j.1365-2567.2012.03616.x

Laukens, D. Heterogeneity of the gut microbiome in mice: guidelines for optimizing experimental design. *FEMS Microbiol Rev*. 2016 Jan;40(1):117-32

LeBlanc JG, Milani C, de Giori GS, Sesma F, van Sinderen D, Ventura M. Bacteria as vitamin suppliers to their host: a gut microbiota perspective. *Curr Opin Biotechnol*. 2013 Apr;24(2):160-8. doi: 10.1016/j.copbio.2012.08.005. Epub 2012 Aug 30. PMID: 22940212.

Lecomte V, Kaakoush NO, Maloney CA, Raipuria M, Huinao KD, Mitchell HM, et al. Changes in Gut Microbiota in Rats Fed a High Fat Diet Correlate with Obesity-Associated Metabolic Parameters. *PLoS ONE*. 2015;10(5): e0126931. https://doi.org/10.1371/journal.pone.0126931

Lee CS, et al. Human liver injuries and the effects on udp glucuronosyltransferase. *Pathology.* 1992; Volume 24, Supplement 1, Page 2. https://doi.org/10.1016/S0031-3025(16)35955-4.

Lee, A. S. Y., & Song, K. P. 2005. LuxS/autoinducer-2 quorum sensing molecule regulates transcriptional virulence gene expression in Clostridium difficile. *Biochemical and Biophysical Research Communications*, 2005; 335(3), 659–666. doi:10.1016/j.bbrc.2005.07.131

Lebeer S, Vanderleyden J, De Keersmaecker SC. Genes and molecules of lactobacilli supporting probiotic action. *Microbiol Mol Biol Rev*. 2008;72(4):728-764. doi:10.1128/MMBR.00017-08

Lerner A, Jeremias P, Matthias T. The World Incidence and Prevalence of Autoimmune Diseases is Increasing. *International Journal of Celiac Disease.* 2015;3(4):151-155. doi: 10.12691/ijcd-3-4-8.

Ley RE, Bäckhed F, Turnbaugh P, Lozupone CA, Knight RD, Gordon JI. Obesity alters gut microbial ecology. *Proc Natl Acad Sci U S A*. 2005;102: 11070–11075. 10.1073/pnas.0504978102.

Liang H, Xu W, Chen J, Shi H, Zhu J,4 Liu X,5 Wang J, Miao M, Yuan W. The Association between Exposure to Environmental Bisphenol A and Gonadotropic Hormone Levels among Men. *PLoS One*. 2017; 12(1): e0169217.

Liang JQ, Li T, Nakatsu G*, et al*A novel faecal *Lachnoclostridium* marker for the non-invasive diagnosis of colorectal adenoma and cancer. *Gut.* 2020;**69:**1248-1257

Li C, Wang Z, Yang J, Liu J, Mao X, and Zhang Y. Transformation of Bisphenol A in Water Distribution Systems, A Pilot-scale Study. *CHEMOSPHERE*. 2015;125:86-93.

Li J, Zhao F, Wang Y, Chen J, Tao J, Tian G, Wu S, Liu W, Cui Q, Geng B et al: Gut microbiota dysbiosis contributes to the development of hypertension. *Microbiome* 2017, 5(1):14.

Li M, Ni N, Chou HT, Lu CD, Tai PC, Wang B. Structure-based discovery and experimental verification of novel AI-2 quorum sensing inhibitors against Vibrio harveyi. *ChemMedChem*. 2008;3(8):1242-1249. doi:10.1002/cmdc.200800076

Li X, Watanabe K, Kimura I. Gut Microbiota Dysbiosis Drives and Implies Novel Therapeutic Strategies for Diabetes Mellitus and Related Metabolic Diseases. *Front Immunol*. 2017;8:1882. Published 2017 Dec 20. doi:10.3389/fimmu.2017.01882

Ling Z, Li Z, Liu X, Cheng Y, Luo Y, Tong X, Yuan L, Wang Y, Sun J, Li L, Xiang C. Altered Fecal Microbiota Composition Associated with Food Allergy in Infants. *Applied and Environmental Microbiology.* 2014 March;80 (8) 2546-2554; **DOI:** 10.1128/AEM.00003-14.

Liou AP, Paziuk M, Luevano JM, Machineni S, Turnbaugh PJ, Kaplan LM., Conserved shifts in the gut microbiota due to gastric bypass reduce host weight and adiposity. *Sci. Transl. Med.* 2013; 5: 178ra41

Liu Y, Yao Y, Li H, Qiao F, Wu J, Du Z-y, et al. Influence of Endogenous and Exogenous Estrogenic Endocrine on Intestinal Microbiota in Zebrafish. *PLoS ONE.* 2016;11(10): e0163895. https://doi.org/10.1371/journal.pone.0163895

Lombardía E, Rovetto A , Arabolaza A, Grau R. A LuxS-Dependent Cell-to-Cell Language Regulates Social Behavior and Development in *Bacillus subtilis. Journal of Bacteriology Jun 2006, 188 (12) 4442-4452;* ***DOI:*** *10.1128/JB.00165-06*

Lu L, Hume ME, Pillai SD. Autoinducer-2-like activity associated with foods and its interaction with food additives. *J Food Prot.* 2004 Jul;67(7):1457-62. doi: 10.4315/0362-028x-67.7.1457. PMID: 15270501.

Lukás F, Gorenc G, Kopecný J. Detection of possible AI-2-mediated quorum sensing system in commensal intestinal bacteria. *Folia Microbiol* (Praha). 2008;53(3):221-224. doi:10.1007/s12223-008-0030-1

Ma B, McComb E, Gajer P, et al. Microbial Biomarkers of Intestinal Barrier Maturation in Preterm Infants. *Front Microbiol*. 2018;9:2755. doi:10.3389/fmicb.2018.02755.

Malaisé Y, et al. Gut dysbiosis and impairment of immune system homeostasis in perinatally-exposed mice to Bisphenol A precede obese phenotype development. *Scientific Reports*. 2017;7: 14472.

Martin F, Peltonen J, Laatikainen T, Pulkkinen M, Adlercreutz H. Excretion of progesterone metabolites and estriol in faeces from pregnant women during ampicillin administration. *J Steroid Biochem*. 1975; 6:1339–1346. [PubMed: 1181489]

Martín-Rodríguez AJ, and Fernández, JJ. A Bioassay Protocol for Quorum Sensing Studies Using Vibrio campbellii. *Bio-protocol*. 2016; 6(14): e1866. DOI: 10.21769/BioProtoc.1866.

Maruvada, P et al. The Human Microbiome and Obesity: Moving beyond Associations. *Cell Host & Microbiome*. 2017 Nov;Vol. 22(5): 589-599.

Maurice CF, Haiser HJ, Turnbaugh PJ. Xenobiotics shape the physiology and gene expression of the active human gut microbiome. *Cell*. 2013;152(1-2):39-50

Mayes JS, Watson GH: Direct effects of sex steroid hormones on adipose tissues and obesity. *Obes Rev*. 2004 Nov;5(4):197-216.

Mayer EA, Savidge T, Shulman RJ. Brain-gut microbiome interactions and functional bowel disorders. *Gastroenterology*. 2014 May; 146(6):1500-12.

Mayneris-Perxachs, J., Arnoriaga-Rodríguez, M., Luque-Córdoba, D. et al. Gut microbiota steroid sexual dimorphism and its impact on gonadal steroids: influences of obesity and menopausal status. *Microbiome*. 2020;136. https://doi.org/10.1186/s40168-020-00913-x

Mazel-Sanchez, B., Yildiz, S., & Schmolke, M. (2019). Ménage à trois: Virus, Host, and Microbiota in Experimental Infection Models. *Trends in Microbiology*. doi:10.1016/j.tim.2018.12.004

McIntosh FM, Maison N, Holtrop G, et al. Phylogenetic distribution of genes encoding beta-glucuronidase activity in human colonic bacteria and the impact of diet on faecal glycosidase activities. *Environ Microbiol*. 2012;14(8): 1876–1887

McMurdie PJ , Holmes S (2013) phyloseq: An R Package for Reproducible Interactive Analysis and Graphics of Microbiome Census Data. *PLoS ONE* 8(4): e61217. https://doi.org/10.1371/journal.pone.0061217

McNulty NP, Yatsunenko T, Hsiao A, et al. The impact of a consortium of fermented milk strains on the gut microbiome of gnotobiotic mice and monozygotic twins. *Sci Transl Med.* 2011;3(106):106ra106.

Menon R, Sara E. Watson, Laura N. Thomas, Clinton D. Allred, Alan Dabney, M. Andrea Azcarate-Peril, Joseph M. Sturino. Diet complexity and estrogen receptor beta status affect the composition of the murine intestinal microbiota. *Applied and Environmental Microbiology*. 2017; 79 (18) 5763-5773; DOI: 10.1128/AEM.01182-13

Merkel SM, Alexander S, Zufall E, Oliver JD, Huet-Hudson YM. Essential role for estrogen in protection against Vibrio vulnificus induced endotoxic shock. *Infect Immun.* 2001;69(10):6119–6122.

Merritt JH, Kadouri DE, O'Toole GA. Growing and analyzing static biofilms. *Curr Protoc Microbiol*. 2005;Chapter 1:Unit 1B.1.

Miao M, et al. Associations between Bisphenol A Exposure and Reproductive Hormones among Female Workers. *Int J Environ Res Public Health*. 2015 Oct 22;12(10):13240-50.

Miller MB, Bassler BL. Quorum sensing in bacteria. *Annu Rev Microbiol*. 2001;55:165-99. doi: 10.1146/annurev.micro.55.1.165. PMID: 11544353.

Mok KC, Wingreen NS, Bassler BL. Vibrio harveyi quorum sensing: a coincidence detector for two autoinducers controls gene expression. *EMBO J*. 2003;22(4):870-81.

Morita T, Aiba H. Mechanism and physiological significance of autoregulation of the *Escherichia coli hfq* gene. *RNA*. 2019;25(2):264-276. doi:10.1261/rna.068106.118

Mueller S, Saunier K, Hanisch C, et al. Differences in fecal microbiota in different European study populations in relation to age, gender, and country: a cross-sectional study. *Appl Environ Microbiol.* 2006;72(2):1027–1033. doi:10.1128/AEM.72.2.1027-1033.2006 (s)

Nakatsu, C. High-Fat Diet Induces Periodontitis in Mice through Lipopolysaccharides (LPS) Receptor Signaling: Protective Action of Estrogens. *PLoS One*. 2014; 9(10): e108924.

Nakajima A, Vogelzang A, Maruya M, et al. IgA regulates the composition and metabolic function of gut microbiota by promoting symbiosis between bacteria. *J Exp Med*. 2018;215(8):2019–2034. doi:10.1084/jem.20180427

National Academies of Sciences, Engineering, and Medicine; Division on Earth and Life Studies; Board on Life Sciences; Board on Environmental Studies and Toxicology; Committee on Advancing Understanding of the Implications of Environmental-Chemical Interactions with the Human Microbiome. Washington (DC): National Academies Press (US); 2017 Dec 29.

Nealson K, Platt T, Hastings J. Cellular Control of the Synthesis and Activity of the Bacterial Luminescent System. *JOURNAL OF BACtERIOLOGY*, October 1970, p. 313-322.

Neuman H, Debelius JW, Knight R, Koren O. Microbial endocrinology: the interplay between the microbiota and the endocrine system. *FEMS Microbiol Rev*. 2015 Jul;39(4):509-21.

Newbold RR, Teng CT, Beckman WC Jr, Jefferson WN, Hanson RB, Miller JV, McLachlan JA. Fluctuations of lactoferrin protein and messenger ribonucleic acid in the reproductive tract of the mouse during the estrous cycle. *Biol Reprod.* 1992 Nov;47(5):903-15. doi: 10.1095/biolreprod47.5.903. PMID: 1477216.

Nuriel-Ohayon M, Neuman H, Koren O. Microbial Changes during Pregnancy, Birth, and Infancy. *Front Microbiol*. 2016;7:1031. Published 2016 Jul 14. doi:10.3389/fmicb.2016.01031

Oakley OR, Kim KJ, Lin PC, et al. Estradiol Synthesis in Gut-Associated Lymphoid Tissue: Leukocyte Regulation by a Sexually Monomorphic System. *Endocrinology.* 2016;157(12):4579-4587. doi:10.1210/en.2016-1391

Oishi K, Sato T, Yokoi W, Yoshida Y, Ito M, Sawada H. Effect of probiotics, Bifidobacterium breve and Lactobacillus casei, on bisphenol A exposure in rats. *Biosci Biotechnol Biochem*. 2008;72(6):1409-1415. doi:10.1271/bbb.70672

Org E, Mehrabian M, Parks BW, et al. Sex differences and hormonal effects on gut microbiota composition in mice. *Gut Microbes*. 2016;7(4):313-322. doi:10.1080/19490976.2016.1203502

Pereira CS, Santos AJ, Bejerano-Sagie M, Correia PB, Marques JC, Xavier KB. Phosphoenolpyruvate phosphotransferase system regulates detection and processing of the quorum sensing signal autoinducer-2. *Mol Microbiol*. 2012;84(1):93-104. doi:10.1111/j.1365-2958.2012.08010.x

Pereira CS, Thompson JA, Xavier KB. AI-2-mediated signalling in bacteria. *FEMS Microbiol Rev*. 2013;37(2):156-181. doi:10.1111/j.1574-6976.2012.00345.x

Petersen C, Round JL. Defining dysbiosis and its influence on host immunity and disease. *Cell Microbiol*. 2014;16(7):1024-1033. doi:10.1111/cmi.12308

Plottel C, Blaser M. Microbiome and Malignancy. *Cell Host Microbe*. 2011 Oct 20; 10(4): 324–335

Pollet, R. M., D'Agostino, E. H., Walton, W. G., Xu, Y., Little, M. S., Biernat, K. A., … Redinbo, M. R.. An Atlas of β-Glucuronidases in the Human Intestinal Microbiome. *Structure,* 2017;25(7), 967–977.e5.doi:10.1016/j.str.2017.05.003

Praneenararat T, Palmer AG, Blackwell HE. Chemical methods to interrogate bacterial quorum sensing pathways. *Org Biomol Chem*. 2012;10(41):8189-8199. doi:10.1039/c2ob26353j

Prossnitz ER, Barton M:The G-protein-coupled estrogen receptor GPER in health and disease. *Nat Rev Endocrinol.* 2011 Aug 16;7(12):715-26.

Qin X-Y, Sone H, Kojima Y, Mizuno K, Ueoka K, Muroya K, et al.. Individual Variation of the Genetic Response to Bisphenol A in Human Foreskin Fibroblast Cells Derived from Cryptorchidism and Hypospadias Patients. *PLoS ONE*. 2012;7(12): e52756. https://doi.org/10.1371/journal.pone.0052756.

Quan Y, Meng F, Ma X, et al. Regulation of bacteria population behaviors by AI-2 "consumer cells" and "supplier cells". *BMC Microbiol*. 2017;17(1):198. Published 2017 Sep 19. doi:10.1186/s12866-017-1107-2

Raftogianis R, Creveling C, Weinshilboum R, Weisz J; Chapter 6: Estrogen Metabolism by Conjugation. *JNCI Monographs*, 2000 July; 2000(27):113–124.

Rao RM, Pasha SN, Sowdhamini R. Genome-wide survey and phylogeny of S-Ribosylhomocysteinase (LuxS) enzyme in bacterial genomes. *BMC Genomics.* 2016;17(1):742. Published 2016 Sep 20. doi:10.1186/s12864-016-3002-x

Rasheed A, Kola RK, Yalavarthy PD. Assessment of Antibacterial Activity of Bisphenol A (4,4'-Isopropylidenebisphenol). International Journal of Innovative *Research in Science, Engineering and Technology*. 2013 November;2(11).

Rajamani S., Sayre R.. Biosensors for the Detection and Quantification of AI-2 Class Quorum-Sensing Compounds. In: Leoni L., Rampioni G. (eds) Quorum Sensing. Methods in Molecular Biology. 2018;1673. Humana Press, New York, NY. https://doi.org/10.1007/978-1-4939-7309-5_6

Raut N, Pasini P, and Daunert S. Deciphering Bacterial Universal Language by Detecting the Quorum Sensing Signal, Autoinducer-2, with a Whole-Cell Sensing System. *Anal. Chem.* 2013;85, 20, 9604–9609.

Rezzonico, F., Duffy, B. Lack of genomic evidence of AI-2 receptors suggests a non-quorum sensing role for luxS in most bacteria. *BMC Microbiol.* 2008 August; 154. https://doi.org/10.1186/1471-2180-8-154.

Redanz, Sylvio & Standar, Kerstin & Podbielski, Andreas & Kreikemeyer, Bernd. Heterologous Expression of sahH Reveals That Biofilm Formation Is Autoinducer-2-independent in Streptococcus sanguinis but Is Associated with an Intact Activated Methionine Cycle. *The Journal of Biological Chemistry*. 2012;287. 36111-22.

Reddivari L, Veeramachaneni DNR, Walters WA, et al. Perinatal Bisphenol A Exposure Induces Chronic Inflammation in Rabbit Offspring via Modulation of Gut Bacteria and Their Metabolites. *mSystems*. 2017;2(5):e00093-17. doi:10.1128/mSystems.00093-17.

Ren D, Sims JJ, Wood TK. Inhibition of biofilm formation and swarming of Escherichia coli by (5Z)-4-bromo-5-(bromomethylene)-3-butyl-2(5H)-furanone. *Environ Microbiol.* 2001;3(11):731-736. doi:10.1046/j.1462-2920.2001.00249.x

Rickard AH, Palmer RJ Jr, Blehert DS, et al. Autoinducer 2: a concentration-dependent signal for mutualistic bacterial biofilm growth. *Mol Microbiol*. 2006;60(6):1446-1456. doi:10.1111/j.1365-2958.2006.05202.x

Ridaura VK, Faith JJ, Rey FE, et al. Gut microbiota from twins discordant for obesity modulate metabolism in mice. *Science.* 2013;341:1241214.

Rinninella E, Raoul P, Cintoni M, et al. What is the Healthy Gut Microbiota Composition? A Changing Ecosystem across Age, Environment, Diet, and Diseases. *Microorganisms.* 2019;7(1):14. Published 2019 Jan 10. doi:10.3390/microorganisms7010014

Ríos-Covián David, Ruas-Madiedo Patricia, Margolles Abelardo, Gueimonde Miguel, de los Reyes-Gavilán Clara G., Salazar Nuria. Intestinal Short Chain Fatty Acids and their Link with Diet and Human Health. *Frontiers in Microbiology*. 2016 July:185. DOI=10.3389/fmicb.2016.00185

Rodríguez JM, Murphy K, Stanton C, et al. The composition of the gut microbiota throughout life, with an emphasis on early life. *Microb Ecol Health Dis*. 2015 Feb 2;26:26050. doi:10.3402/mehd.v26.26050.

Thayer KA, Doerge DR, Hunt D, et al. Pharmacokinetics of bisphenol A in humans following a single oral administration. *Environ Int*. 2015;83:107-15.

Roen EL, Wang Y, Calafat AM, et al. Bisphenol A exposure and behavioral problems among inner city children at 7-9 years of age. *Environ Res*. 2015;142:739-45.

Rolhion N, Chassaing B. When pathogenic bacteria meet the intestinal microbiota. *Philos Trans R Soc Lond B Biol Sci*. 2016;371(1707):20150504. doi:10.1098/rstb.2015.0504

Rosenfeld CS. Gut Dysbiosis in Animals Due to Environmental Chemical Exposures. *Front Cell Infect Microbiol*. 2017;7:396. Published 2017 Sep 8. doi:10.3389/fcimb.2017.00396)

Savage DC. Associations and physiological interactions of indigenous microorganisms and gastrointestinal epithelia. *Am J Clin Nutr.* 1972;25: 1372–1379.

Schuijt TJ, Lankelma JM, Scicluna BP, et al The gut microbiota plays a protective role in the host defence against pneumococcal pneumonia. *Gut.* 2016;65:575-583.

Schulster M, Bernie AM, Ramasamy R. The role of estradiol in male reproductive function. *Asian J Androl*. 2016 May-Jun;18(3):435-40.

Selber-Hnatiw S, Rukundo B, Ahmadi M, et al. Human Gut Microbiota: Toward an Ecology of Disease. *Front Microbiol*. 2017;8:1265. Published 2017 Jul 17. doi:10.3389/fmicb.2017.01265

Sharon K. Kuss, Gavin T. Best, Chris A. Etheredge, Andrea J. Pruijssers, Johnna M. Frierson, Lora V. Hooper, Terence S. Dermody, Julie K. Pfeiffer. Intestinal Microbiota Promote Enteric Virus Replication and Systemic Pathogenesis. *Science.* 2011 October 14: 249-252

Seachrist DD, Bonk KW, Ho SM, Prins GS, Soto AM, Keri RA. A review of the carcinogenic potential of bisphenol A. *Reprod Toxicol.* 2015;59:167-82.

Seedorf H, Griffin NW, Ridaura VK, Reyes A, Cheng J, Rey FE, Smith MI, Simon GM, Scheffrahn RH, Woebken D, Spormann AM, Van Treuren W, Ursell LK, Pirrung M, Robbins-Pianka A, Cantarel BL, Lombard V, Henrissat B, Knight R, Gordon JI. . Bacteria from diverse habitats colonize and compete in the mouse gut. *Cell.* 2014;159:253–266

Secky L, Svoboda M, Klameth L, et al. The sulfatase pathway for estrogen formation: targets for the treatment and diagnosis of hormone-associated tumors. *J Drug Deliv*. 2013;2013:957605. doi:10.1155/2013/957605

Sharma, R. P., Schuhmacher, M., & Kumar, V. (2017). Review on crosstalk and common mechanisms of endocrine disruptors: Scaffolding to improve PBPK/PD model of EDC mixture. *Environment International.* 2017;99, 1–14.

Shimizu K, Muranaka Y, Fujimura R, Ishida H, Tazume S, Shimamura T. Normalization of reproductive function in germfree mice following bacterial contamination. *Exp Anim.* 1998;47(3):151–158.

Shin JH, Park YH, Sim M, Kim SA, Joung H, Shin DM. Serum level of sex steroid hormone is associated with diversity and profiles of human gut microbiome. *Res Microbiol.* 2019 Jun-Aug;170(4-5):192-201. doi: 10.1016/j.resmic.2019.03.003. Epub 2019 Mar 30. PMID: 30940469.

Shin, N.-R., Whon, T. W., & Bae, J.-W. Proteobacteria: microbial signature of dysbiosis in gut microbiota. *Trends in Biotechnology*. 2015:33(9), 496–503. doi:10.1016/j.tibtech.2015.06.011

Sprockett,D, Fukami T, Relman DA. Role of priority effects in the early-life assembly of the gut microbiota. *Nature Reviews Gastroenterology & Hepatology*. 2018;15(4), 197–205. doi:10.1038/nrgastro.2017.173

Stocco C. Tissue physiology and pathology of aromatase. *Steroids*. 2012;77(1-2):27-35. doi:10.1016/j.steroids.2011.10.013

Straub RH.The complex role of estrogens in inflammation. *Endocr Rev.* 2007 Aug;28(5):521-74.

Sun, J, Daniel R, Wagner-Döbler I, Zeng A. Is autoinducer-2 a universal

signal for interspecies communication: a comparative genomic and phylogenetic analysis of the synthesis and signal transduction pathways. *BMC Evolutionary Biology*, 2004; 4 (36).

Swearingen MC, Sabag-Daigle A, Ahmer BM. Are there acyl-homoserine lactones within mammalian intestines?. *J Bacteriol*. 2013;195(2):173-179. doi:10.1128/JB.01341-12

Tal T, Betancourt D, Hunter D, Espenschied S, Rawls J, Charla S, Dean T, and Wood C. Microbiota colonization status influences developmental toxicity of bisphenol A in embryonic zebrafish. Society of Toxicology, New Orleans, LA, March 13 - 17, 2016.

Teasdale M, Liu J, Wallace J, Akhlaghi F, Rowley D . Secondary Metabolites Produced by the Marine Bacterium *Halobacillus salinus* That Inhibit Quorum Sensing-Controlled Phenotypes in Gram-Negative Bacteria. *Applied and Environmental Microbiology.* 2009 January;75 (3) 567-572; **DOI:** 10.1128/AEM.00632-08.
.
Thompson J, et al. Manipulation of the Quorum Sensing Signal AI-2 Affects the Antibiotic-Treated Gut Microbiota. *Cell Rep*. 2015 Mar; 10(11): p1861–1871.

Thompson J, Oliveira R, Xavier K. Chemical conversations in the gut microbiota. *Gut Microbes*. 2016;7:2, 163-170, DOI: 10.1080/19490976.2016.1145374

Thorsen, J., Brejnrod, A., Mortensen, M. *et al.* Large-scale benchmarking reveals false discoveries and count transformation sensitivity in 16S rRNA gene amplicon data analysis methods used in microbiome studies. *Microbiome.* 2016 April;62. . https://doi.org/10.1186/s40168-016-0208-8

Tremellen K, Pearce K. Dysbiosis of Gut Microbiota (DOGMA)--a novel theory for the development of Polycystic Ovarian Syndrome. *Med Hypotheses.* 2012;79(1):104-112. doi:10.1016/j.mehy.2012.04.016

Toranallerand CD, Miranda RC, Bentham WDL, Sohrabji F, Brown TJ, Hochberg RB, Maclusky NJ: Estrogen-Receptors Colocalize with Low Affinity Nerve Growth-Factor Receptors in Cholinergic Neurons of the Basal Forebrain. *P Natl Acad Sci USA.* 1992, 89(10):4668-4672.

Torcato IM, Kasal MR, Brito PH, Miller ST, Xavier KB. Identification of novel autoinducer-2 receptors in Clostridia reveals plasticity in the binding site of the LsrB receptor family. *J Biol Chem*. 2019;294(12):4450-4463. doi:10.1074/jbc.RA118.006938

Turovskiy, Y., & Chikindas, M. L. (2006). Autoinducer-2 bioassay is a qualitative, not quantitative method influenced by glucose. *Journal of Microbiological Methods,* 66(3), 497–503. doi:10.1016/j.mimet.2006.02.001

U.S. Environmental Protection Agency. Bisphenol A Action Plan CASRN 80-05-7. 9 March 2010. https://www.epa.gov/sites/production/files/2015-09/documents/bpa_action_plan.pdf

Udayappan, S., Manneras-Holm, L., Chaplin-Scott, A. *et al.* Oral treatment with *Eubacterium hallii* improves insulin sensitivity in *db/db* mice. *npj Biofilms Microbiomes.* 2016 February; 16009

Vandenberg LN, Maffini MV, Sonnenschein C, Rubin BS, Soto AM. Bisphenol-A and the Great Divide: A Review of Controversies in the Field of Endocrine Disruption. *Endocrine Reviews.* 2009 Feb;30(1): 75–95. https://doi.org/10.1210/er.2008-0021

van der Giessen J, van der Woude CJ, Peppelenbosch MP, Fuhler GM. A Direct Effect of Sex Hormones on Epithelial Barrier Function in Inflammatory Bowel Disease Models. *Cells*. 2019;8(3):261. Published 2019 Mar 19. doi:10.3390/cells8030261

Van Herreweghen F, De Paepe K, Roume H, Kerckhof FM, Van de Wiele T. Mucin degradation niche as a driver of microbiome composition and Akkermansia muciniphila abundance in a dynamic gut model is donor independent. *FEMS Microbiology Ecology*. 2018 Dec;94(12) 186. doi: 10.1093/femsec/fiy186.

Vayssier-Taussat M, Albina E, Citti C, Cosson JF, Jacques MA, Lebrun MH, Le Loir Y, Ogliastro M, Petit MA, Roumagnac P, Candresse T. Shifting the paradigm from pathogens to pathobiome: new concepts in the light of meta-omics. *Front Cell Infect Microbiol.* 2014; 4():29.

Vaughn AC, Cooper EM, DiLorenzo PM, et al. Energy-dense diet triggers changes in gut microbiota, reorganization of gut-brain vagal communication and increases body fat accumulation. *Acta Neurobiol Exp (Wars)*. 2017;77(1):18-30. doi:10.21307/ane-2017-033

Velmurugan G, et al.:Gut Microbiota, Endocrine Disrupting Chemicals, and the Diabetes Epidemic. *Trends Endocrinol Metab*. 2017 Aug;28(8):612-625.

Venturelli, O. S. A. Deciphering microbial interactions in synthetic human gut microbiome communities. *Molecular Systems Biology*. 2018;14(6), e8157.doi:10.15252/msb.20178157

Verbeke F, De Craemer S, Debunne N, et al. Peptides as Quorum Sensing Molecules: Measurement Techniques and Obtained Levels *In vitro* and *In vivo*. *Front Neurosci*. 2017;11:183. Published 2017 Apr 12. doi:10.3389/fnins.2017.00183

Vernocchi P, Del Chierico F, Putignani L. Gut Microbiota Profiling: Metabolomics Based Approach to Unravel Compounds Affecting Human Health. *Front Microbiol*. 2016;7:1144. Published 2016 Jul 26. doi:10.3389/fmicb.2016.01144

Vilchez R, Lemme A, Thiel V, Schulz S, Sztajer H, Wagner-Döbler I. Analysing traces of autoinducer-2 requires standardization of the Vibrio harveyi bioassay. *Anal Bioanal Chem.* 2007 Jan;387(2):489-96. doi: 10.1007/s00216-006-0824-4. Epub 2006 Dec 2. PMID: 17143597.

vom Saal FS, Welshons WV. Evidence that bisphenol A (BPA) can be accurately measured without contamination in human serum and urine, and that BPA causes numerous hazards from multiple routes of exposure. *Mol Cell Endocrinol*. 2014;398(1-2):101-13.

Vrieze A, Van Nood E, Holleman F, Salojarvi J, Kootte RS, Bartelsman JF, et al. Transfer of intestinal microbiota from lean donors increases insulin sensitivity in individuals with metabolic syndrome. *Gastroenterology.* 2012;143:913–16, e7

Waidmann, M. S., Bleichrodt, F. S., Laslo, T., & Riedel, C. U. Bacterial luciferase reporters: The Swiss army knife of molecular biology. *Bioengineered Bugs*. 2011;2(1), 8–16. doi:10.4161/bbug.2.1.13566

Walsh AF, White F, and Warnick A. The Effects Of Erythritol, Fsh And Female Gonadal Hormones On The Growth In Vitro Of Vibrio Fetus Var. Venerealis. *Reproduction*. 1973 March;. 32(3):465–471.

Wang, J.The environmental obesogen bisphenol A promotes adipogenesis by increasing the amount of 11b-hydroxysteroid dehydrogenase type 1 in the adipose tissue of children. *Int J Obes* (Lond). 2013 Jul;37(7):999-1005.

Wang Jingjing, Lang Tao, Shen Jian, Dai Juanjuan, Tian Ling, Wang Xingpeng. Core Gut Bacteria Analysis of Healthy Mice. *Frontiers in Microbiology*. 2016 ;10:887.

Wang X, Reisberg S, Serradji N, Anquetin G, Pham MC, WU W, Dong CZ, Piro B. E-Assay Concept: Detection of Bisphenol A with a Label-free Electrochemical Competitive Immunoassay. *Biosensors and Bioelectronics*. 2014; 52: 214–219.

Wang Y, Rui M, Nie Y, Lu G. Influence of gastrointestinal tract on metabolism of bisphenol A as determined by in vitro simulated system. *Journal of Hazardous Materials*. 2018;355:111-118.

Wang Y, Gao X, Zhang X, Xiao Y, Huang J, Yu D, Li X, Hu H, Ge T, Li D, Zhang T. Gut Microbiota Dysbiosis Is Associated with Altered Bile Acid Metabolism in Infantile Cholestasis. *mSystems.* 2019 December;4 (6) e00463-19; **DOI:** 10.1128/mSystems.00463-19

Welch JLM, Hasegawa Y, McNulty NP, Gordon JI, Borisy GG. Spatial organization of the gut microbiota. *Proceedings of the National Academy of Sciences*. 2017 October;114 (43) E9105-E9114; DOI:10.1073/pnas.1711596114.

Widmer, K., Soni, K.A., Hume, M., Beier, R., Jesudhasan, P. and Pillai, S. Identification of Poultry Meat-Derived Fatty Acids Functioning as Quorum Sensing Signal Inhibitors to Autoinducer-2 (AI-2). J*ournal of Food Science*, 2007;72: M363-M368. https://doi.org/10.1111/j.1750-3841.2007.00527.x

Wynendaele E, Bronselaer A, Nielandt J, D'Hondt M, Stalmans S, Bracke N, Verbeke F, Van De Wiele C, De Tré G, De Spiegeleer B. Quorumpeps database: chemical space, microbial origin and functionality of quorum sensing peptides. *Nucleic Acids Res. 2013 Jan; 41(Database issue):D655-9.*

Wolfgang Völkel, Thomas Colnot, György A. Csanády, Johannes G. Filser, and Wolfgang Dekant. Metabolism and Kinetics of Bisphenol A in Humans at Low Doses Following Oral Administration. *Chem. Res. Toxicol*. 2002, 15 (10), pp 1281–1287. doi: 10.1021/tx025548t.

Xavier KB, Bassler BL. Regulation of uptake and processing of the quorum-sensing autoinducer AI-2 in Escherichia coli. *J Bacteriol*. 2005;187(1):238-248. doi:10.1128/JB.187.1.238-248.2005

Xavier KB, Bassler BL. Interference with AI-2-mediated bacterial cell-cell communication. *Nature*. 2005;437(7059):750-753. doi:10.1038/nature03960

Yang, Y. et al. Estrogen inhibits the overgrowth of Escherichia coli in the rat intestine under simulated microgravity. *Molecular Medicine Reports.* 2018;17: 2313-2320.

Yatsunenko T, Rey FE, Manary MJ, et al. Human gut microbiome viewed across age and geography. *Nature*. 2012;486(7402):222-227. Published 2012 May 9. doi:10.1038/nature11053

You, D. et al. Global, regional, and national levels and trends in under-5 mortality between 1990 and 2015, with scenario-based projections to 2030: a systematic analysis by the UN Inter-agency Group for Child Mortality Estimation. *The Lancet*. 2015; 386: 2275–2286.

Zaborowska M, Wyszkowska J, Borowik A. Soil Microbiome Response to Contamination with Bisphenol A, Bisphenol F and Bisphenol S. *Int J Mol Sci*. 2020;21(10):3529. Published 2020 May 16. doi:10.3390/ijms21103529

Zang T, Lee BW, Cannon LM, et al. A naturally occurring brominated furanone covalently modifies and inactivates LuxS. *Bioorg Med Chem Lett*. 2009;19(21):6200-4.

Zheng, D., Liwinski, T. & Elinav, E. Interaction between microbiota and immunity in health and disease. *Cell Res.* 2020;30, 492–506 (2020). https://doi.org/10.1038/s41422-020-0332-7

Zeng MY, Inohara N, Nuñez G. Mechanisms of inflammation-driven bacterial dysbiosis in the gut. *Mucosal Immunol*. 2017;10(1):18-26. doi:10.1038/mi.2016.75

Zenno S, Saigo K. Identification of the genes encoding NAD(P)H-flavin oxidoreductases that are similar in sequence to Escherichia coli Fre in four species of luminous bacteria: Photorhabdus luminescens, Vibrio fischeri, Vibrio harveyi, and Vibrio orientalis. *J Bacteriol. 1994 Jun; 176(12):3544-51*